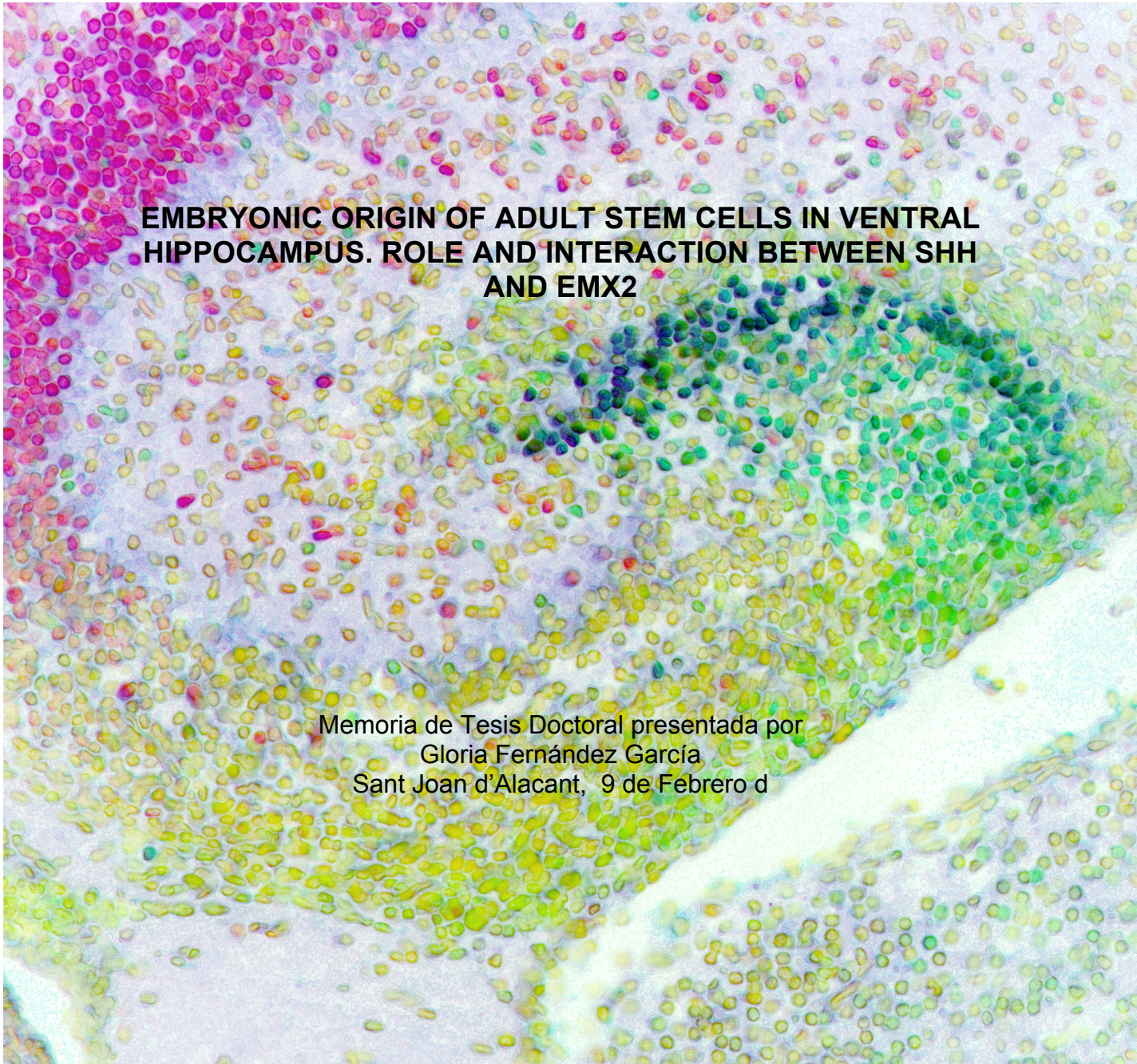INSTITUTO DE NEUROCIENCIAS

Universidad Miguel Hernández
Consejo Superior de Investigaciones Cientificas

EMBRYONIC ORIGIN OF ADULT STEM CELLS IN VENTRAL HIPPOCAMPUS. ROLE AND INTERACTION BETWEEN SHH AND EMX2

Memoria de Tesis Doctoral presentada por
Gloria Fernández García
Sant Joan d'Alacant, 9 de Febrero d

UNIVERSITAS
Miguel
Hernández

CSIC   UNIVERSITAS Miguel Hernández

INSTITUTO DE NEUROCIENCIAS

Comisión Académica del Programa
de Doctorado en Neurociencias
Universidad Miguel Hernández

Prof. Miguel Valdeolmillos
Coordinador

A QUIEN CORRESPONDA:

El Prof. Miguel Ángel Valdeolmillos López, Coordinador de la Comisión Académica del Programa de Doctorado en Neurociencias de la Universidad Miguel Hernández de Elche,

CERTIFICA:

Que la Tesis Doctoral titulada *"Embryonic Origin of adult stem cells in ventral hippocampus. Role and interaction between Shh and Emx2"* ha sido realizada por D.ª Gloria Fernández García (DNI 52960493A) bajo la dirección de los doctores Dr. Salvador Martínez y el Dr. Samuel J. Pleasure y da su conformidad para que sea presentada a la Comisión de Doctorado de la Universidad Miguel Hernández.

Para que así conste a los efectos oportunos, firma el presente certificado en San Juan de Alicante a 19 de Enero de 2017

Miguel Valdeolmillos
Coordinador

miguel.valdeolmillos@umhc.es
www.ina.umh.es

Tel: +34 965-919540
Fax: +34 965 919561

Av Ramón y Cajal s/n
Campus de San Juan
03550 SAN JUAN DE ALICANTE– ESPAÑA

Consejo Superior de Investigaciones Científicas
Universidad Miguel Hernández
Instituto de Neurociencias

Prof. Salvador Martínez
Director

INSTITUTO DE NEUROCIENCIAS

EXCELENCIA
SEVERO
OCHOA

Centro de Excelencia
«Severo Ochoa»
2014-2018

Prof. Salvador Martínez Pérez Catedrático de Anatomía y Embriología Humana en el departamento de Histología y Anatomía de la Universidad Miguel Hernandez de Elche,

CERTIFICA :

Que D.ª Gloria Fernández García (DNI 52960493A), ha realizado bajo su dirección, y co-dirección del Dr. Samuel J. Pleasure, el trabajo experimental que recoge la Tesis Doctoral titulada: *"Embryonic Origin of adult stem cells in ventral hippocampus. Role and interaction between Shh and Emx2"*, y que ha revisado los contenidos científicos y los aspectos formales del trabajo dando su conformidad para que la misma sea presentada a la Comisión de Doctorado d la Universidad Miguel Hernández.

Para que así conste a los efectos oportunos, firma el presente certificado en San Juan de Alicante a 19 de Enero de 2017

Salvador Martínez
Director

University of California
San Francisco

School of Medicine
Department of Neurology

Samuel J. Pleasure, M.D., Ph.D.
Professor and Vice Chair
Glenn W. Johnson, Jr. Memorial
Endowed Chair

Department of Neurology

Graduate Programs in
Neuroscience, Developmental and
Stem Cell Biology, Biomedical
Sciences

Eli and Edythe Broad Center of
Regeneration Medicine and Stem
Cell Research

Multiple Sclerosis Center

UCSF Mission Bay, Sandler
Neuroscience Center
Box 3206, Room 214
San Francisco, CA 94158

Office – 415/502-5683
Laboratory – 415/514-4949
Fax – 415/502-7168
Email – sam.pleasure@ucsf.edu

M.D. Samuel J. Pleasure, Professor and Vice Chair for Mission Bay Programs Glenn W. Johnson, Jr. Memorial Endowed Chair Department of Neurology School of Medicine of UCSF,

CERTIFIES:

Gloria Fernández García (DNI 52960493A), has carried out under my co-direction and the direction of Salvador Martínez Perez, the experimental work of this Doctoral Thesis entitled: *"Embryonic Origin of adult stem cells in ventral hippocampus. Role and interaction between Shh and Emx2"*, and I have reviewed the scientific and formal aspects of this work giving the approval to defend it under the doctorate´s committee of the University Miguel Hernandez of Elche.

San Juan de Alicante, 19th January 2017

Samuel J. Pleasure,
Codirector.

Agradecimientos

When I started to write the dissertation for my PhD I thought that this would be the easiest part. Not only because my first idea was to write it in Spanish, but also because it was something (I mean, to write) that was easy for me. It is not. And it will be part in English too.

We arrived to SF almost 6 years ago, and with two little girls everything was difficult, a fight. Everyday was a new fight. New country, new culture, new language, new work and two little girls that needed all the energy that I had (sorry, that WE had). But soon I realized that I was lucky.

This work would be impossible without the help and support of a lot of people. Firstly, to Sam Pleasure for give me the opportunity to join the lab and work with all them (Grant, Odessa, Laura, Trung….) that built the day by day work, showing me new things and having the patience to teach me not only the daily job, but the language (I am absolutely conscious that I am very bad speaking English and I was terrible when I arrived to the US). A special thank you to Odessa, who indeed now that I am in Spain is helping me each time I am bothering her with corrections and issues about this dissertation.

To all our friends in SF, from Rubenstein lab (old and new ones), for the parties, the diners… Because it was like a small family in US, thank you Andrew and Jasmine, for Christmas, Thank Giving and birthdays together, thank you for let us to be part of your lives.

To my friends from Andrea's school (I am sorry, Sabrina, you have to tell your mother to translate it, because it will be in Spanish). Pues eso, a Arancha, Jason, Sabrina, Pat, Daniela y Derek. Porque es difícil trabajar, escribir la tesis y además criar a dos niñas en una ciudad como SF. Por las veces que me habéis echado una mano y por los ratos que hemos pasado juntos. Ya sabéis que aquí tenéis vuestra casa. I miss you.

En realidad esto no tendría fin, puesto que llevo desde que terminé mi carrera trabajando en investigación, y en cada sitio que he estado he aprendido, no solo científicamente, también personalmente. A cada uno de los laboratorios donde he estado les agradezco todo lo que me han aportado. Especialmente a Salvador Martínez, que me da la oportunidad de terminar esto que empecé hace una eternidad y que parece que llega a su fin. También a Beatriz Rico, con la que aprendí a valorar el trabajo que hacen no solo los investigadores sino también, el personal de apoyo.

A mis amigos, a los españoles, a los que no tengo la suerte de poder ver a menudo ni siquiera ahora que estoy en España. Todo cambia, pero no dejo de echar de menos los cafés en el IN con Trini, María, Virtu, Carolina, Mariola o Mónica. No sigo, que sois muchos. No solo del instituto, sino también de fuera. Pero todos habéis aportado cosas importantes a mi vida y habéis estado conmigo en un montón de momentos especiales. Espero que siga siendo así, aunque estemos lejos. A todos los que me habéis ayudado con este trabajo, tanto científica como moralmente, sin vuestro apoyo no hubiera podido hacerlo.

Y por ultimo, a mi familia. Bueno, a la mía y a la de Ramón, porque vosotros habéis sufrido (a veces incluso más que nosotros) esta Aventura Americana, que además ni entendíais (tampoco yo lo entiendo a veces). Tanto al principio, cuidando de las niñas mientras nosotros organizábamos nuestra vida allí, como al final. Por vuestra paciencia, sobre todo en estos últimos meses que están siendo para mi casi tan duros como cuando estaba en USA.

A Ramón, que esto también es tuyo, que gracias por tu apoyo… bla, bla, bla…. La verdad es que no lo hubiera hecho. Me hubiera rendido hace tanto tiempo que quizá ni siquiera hubiera empezado. Me hubiera rendido el día que puse el pie por primera vez en San Francisco. Porque no es verdad lo que me decían. Yo no soy valiente. Ni tenía necesidad de aventuras. Era una etapa de nuestra vida y formación que había que hacer y eso hicimos, pero la hubiera preferido hacer aquí, cerca de los nuestros (también es cierto que me volvería a ir…). Gracias, no solo por esto, por todo. Por nuestra vida, por el apoyo constante e incansable en el día a día, por esas dos pequeñas y maravillosas fieras que nos hacen gritar desde por la mañana temprano. ¿He dicho algo que no sepas?

A mis padres, a Lupe

Para Andrea e Isabel,

Todo en la vida conlleva un esfuerzo, pero merece la pena llegar y saber que se siente cuando lo has conseguido. *Mamá*

INDEX

Table of Contents

ABSTRACT

Abstract

Adult neurogenesis represents a unique form of plasticity in the dentate gyrus that requires the presence of long-lived neural stem cells (LL-NSCs). However, the embryonic origin of these LL-NSCs remains unclear. The prevailing model assumes that the dentate neuroepithelium throughout the longitudinal axis of the hippocampus generates both the LL-NSCs and embryonically produced granule neurons. Here we show that the NSCs initially originate from the ventral hippocampus during late gestation and from there they migrate to colonize the dorsal hippocampus. The descendants of these cells are the source for the LL-NSCs in the subgranular zone (SGZ). We show the origin of NSCs and their maintenance are controlled by distinct sources of Sonic Hedgehog (Shh). Furthermore we found *Emx2* gene is essential for the survival of the Shh producing cells in the Amygdala, therefore controlling indirectly the generation and migration of NSCs from the ventral hippocampus. In contrast *Emx2$^{-/-}$* mutant mice show an increase of proliferation in the dorsal region of the dorsal hippocampus related with a higher number of Shh responsive cells. These results reveal the complexity of the embryonic origin of hippocampal LL-NSCs and the importance of *Emx2* gene on their generation.

Resumen

La neurogénesis en el adulto representa una forma única de plasticidad en el giro dentado que requiere la presencia de células madre neurales de larga vida (LL-NSCs). Sin embargo, el origen embrionario de estas LL-NSCs no está claro. El modelo prevalente supone que el neuroepitelio del dentado a lo largo del eje longitudinal del hipocampo genera tanto las células que van a dar lugar a las LL-NSCs en el adulto, como embrionariamente las neuronas de los granos. Aquí mostramos que las NSC se originan inicialmente en el hipocampo ventral durante la gestación tardía y desde allí migran para colonizar el hipocampo dorsal. Las descendientes de estas células son la fuente de las LL-NSCs en la zona subgranular (SGZ). Nosotros mostramos que el origen de las NSCs y su mantenimiento están

controlados por distintas fuentes de Sonic Hedgehog (Shh). Además encontramos que el gen *Emx2* es esencial para la supervivencia de las células productoras de Shh en la Amígdala, así pues controla indirectamente la generación y migración de las NSCs desde el hipocampo ventral. Por otro lado los ratones mutantes para el gen *Emx2* muestran un aumento de la proliferación en la región dorsal del hipocampo dorsal relacionado con un mayor número de células sensibles a Shh. Estos resultados revelan la complejidad del origen embrionario de las LL-NSCs en el hipocampo y la importancia del gen *Emx2* en su generación.

INTRODUCTION

1. The Hippocampus

The hippocampal formation is an important region of the mammalian brain that attracted the interest of researchers since the beginning of the study of the nervous system. In fact, much of the available information on the cellular organization and intrinsic connectivity of the hippocampal formation dates from the classical Golgi studies of Ramon y Cajal and Lorente de Nó in rat brain (Lorente de Nó 1933; Lorente de Nó 1934). In rodents, the hippocampal formation is located in the medial-temporal edge of the neocortex and harbors the neural circuitry essential for cognitive functions such as learning and memory (Lisman 1999).

A
           B
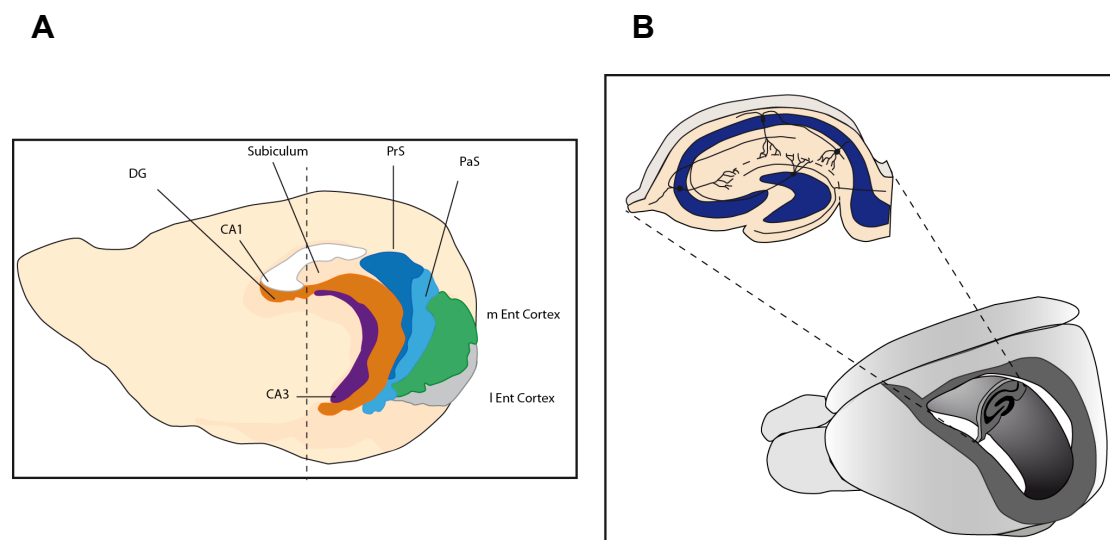
Figure 1: The hippocampal formation: (A) Schematic view of the hippocampal formation including the Dentate Gyrus (DG), Hippocampus (CA1 and CA3), Subiculum, Presubiculum (PrS), Parasubiculum (PaS), Medial Entorhinal Cortex (m Ent Cortex) and Lateral Entorhinal Cortex (l Ent Cortex) (B) Localization of the hippocampal complex in the adult brain: The hippocampal complex is located in the mid-wall of the telencephalon and it has a longitudinal axis bending in C shape from the septum to the temporal lobe.

1.1. Anatomic organization of the hippocampal formation

The hippocampal formation is composed of the dentate gyrus, the hippocampus, the subiculum complex (including presubiculum, subiculum and parasubiculum) and the entorhinal cortex (lateral and medial) (Figure 1, A). The three-dimensional shape of the rodent hippocampal complex (hippocampus itself plus the dentate gyrus) is intricate due to its longitudinal axis bending in a C-shaped manner from the septum (dorso-rostral) to the temporal lobe (ventro-caudal) (Amaral & Witter 1989) (Figure 1 B).

1.2. The Hippocampus proper

The hippocampus proper is a stratified structure with the following layers (*stratum*) from inner to outer.

• The *alveus*, the most internal layer rich in fibers (white matter).

• The *stratum oriens* (SO) mainly composed of basal dendrites of the pyramidal neurons, septal and commissural fibers and cell bodies of inhibitory basket cells and horizontal trilaminar cells.

• The *stratum pyramidale* (SP) contains the cell bodies of pyramidal neurons, (glutamatergic pyramidal cells), which are the principal excitatory neurons of the hippocampus. The Py also contain cell bodies of several types of interneurons.

• The *stratum radiatum* (SR) is composed of apical dendrites from the pyramidal cells and, as in the *SO*, contains septal and commissural axons and Schaffer collateral fibers coming from CA3 to CA1 as well as some interneurons.

• *The stratum lacunosum moleculare* (SLM), located close to the hippocampal fissure, contains the most distal part of apical dendrites from pyramidal cells.

• *The Stratum Lucidum* (SL), placed between the *SP* and *SR,* and located only in the CA3 territory is where the apical dendrites from pyramidal cells in CA3 establish connections with mossy fibers from the dentate (Figure 2).

•
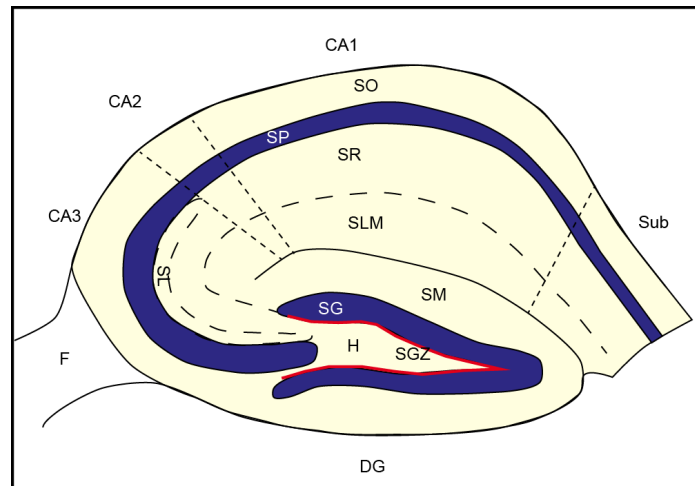
Figure 2: Schematic view of the Hippocampus: (CA1, CA2, CA3, *Cornus Ammonis 1,2 and 3)* and Dentate Gyrus (DG) showing their trilaminar structure. In the hippocampus we observe the *Stratum Oriens* (SO), Stratum *Pyramidale* (SP), *Stratum Radiatum* (SR), *Stratum Lucidum* (SL) and the *Stratum Lacunosum Moleculare* (SLM). The DG has these three layers: *Stratum Moleculare* (SM), *Stratum Granulosum* (SG) and the Hilus or *Polymorphic cell layer* (H). *Sub, Subiculum;* F, Fimbria.

1.3. Dentate Gyrus

The dentate gyrus (DG) is a cortical region that is an integral portion of the hippocampal formation (Amaral et al. 2007). The DG has a very organized structure in layers, which includes the molecular layer (ML), the granular cell layer (GCL) and polymorphic layer or hilus. Classically in Neurobiology, the DG is a model to study the central nervous system (CNS). Its well-organized structure with well-described cell types and connections are the perfect structure to study CNS neurophysiology, morphology and neurogenesis. Moreover, the later is particularly interesting in the DG since is one of the few regions of the brain that have adult neurogenesis.

1.3.1. Granule cell layer

The principal cell layer of the DG is called the *stratum granulosum* or GCL, and is composed mainly by granule cells (GCs). GCs have elliptical cell bodies tightly packed together with no glial sheath interposed between them. They have a characteristic cone shaped tree of spiny apical dendrites. The branches extend throughout the molecular layer and the distal tips of the dendritic tree end either at the hippocampal fissure or at the ventricular surface.

1.3.2. Molecular layer

The *stratum moleculare* or the ML is superficial to the GCL and mainly free of cells. Thus, the molecular layer is occupied primarily by dendrites of the GCs, the pyramidal-shaped basket cells and polymorphic layer cells as well as axons and terminal axonal arbors from the entorhinal cortex and other sources.

There are at least two types of GABAergic cells within the molecular layer. The first one, molecular layer perforant path-associated cells (MOPP, Han et al. 1993) are located deep in the molecular layer. These cells have a multipolar or triangular cell body with an axon that ends in a terminal plexus limited to the outer two thirds of the molecular layer. The second GABAergic cell type is an axo-axonic or chandelier cell-like, (Soriano & Frotscher 1989), generally located immediately adjacent or even within the superficial portion of the GCL.

1.3.3. Polymorphic cell layer (hilus)

The GCL encloses the third layer of the DG, a cellular region called the polymorphic cell layer or *hilus*. The mossy cells are the most prominent cell type in this layer (Amaral 1978). These cells are probably what Ramón y Cajal called as the ¨*stellate* or *triangular*¨ cells and are what Lorente de Nó referred to as ¨*modified pyramids*¨. They have triangular or multipolar cell bodies with

16

three or more thick dendrites that extend for long distances within the polymorphic layer and sometimes into the GCL or molecular layer, but never enter into the adjacent CA3 field. They are immunoreactive for glutamate (Soriano & Frotscher 1994) and project from both, ipsilateral and contralateral sides of the DG being part of the associational/commissural projection.

Other types of neurons, mainly inhibitory, that has been described in the polymorphic layer, mainly inhibitory, are the pyramidal-shaped basket cells (Ribak & Seress 1983). They are located along the interface between the GCL and the hilus and have pyramidal shaped bodies larger than GC.

Diverse types of interneurons have been described mainly in the hilus (Freund and Buzsáki 1996) as the hilar perforant path-associated cell (HIPP) (Han et al. 1993), which are interneurons that innervates GC dendrites with an axon that enter into the outer two thirds of the molecular layer (Han et al. 1993). Also, the hilar commissural-associational pathway related cells (HICAP), predominantly innervate the inner molecular layer and usually have the cell bodies located at the hilar border with GCL (Han et al. 1993; Soriano & Frotscher 1993).

1.4. **Wiring the Hippocampal formation**

The hippocampal formation is involved in functions as spatial memory and short and long term memories (Burgess et al. 2002; Deacon et al. 2002; Broadbent et al. 2004; Lieberwirth et al. 2016). However, since it is connected to other parts of the brain such as the septum or the amygdala complex (Kishi et al. 2006) it seems to be related to emotional behavior.

The two interlocking sheets that conform the hippocampus (the hippocampus itself and the DG) are interconnected and connect to the hippocampal formation in a unidirectional manner. They establish a trisynaptic loop from the entorhinal cortex following the laminar structure in a well-defined pathway. This route of information processing in this highly structured tissue with a small number of well-known cell types makes the hippocampus a very

popular target for the study of synaptic function. Basically, the fibers coming from the entorhinal cortex arrives mainly to the DG but also to the subiculum, CA1 and CA3 (perforant path). Thus, mossy fibers from the GC of the DG connects with pyramidal cells in CA3 (Mossy fibers path), and axons from CA3 to CA1, in an ipsilaterally or contralaterally way (the Schaffer collateral/associational commissural pathway). Finally, fibers from CA1 travel through the Subiculum and go out to the entorhinal cortex closing the network of the hippocampal formation (Figure 3).
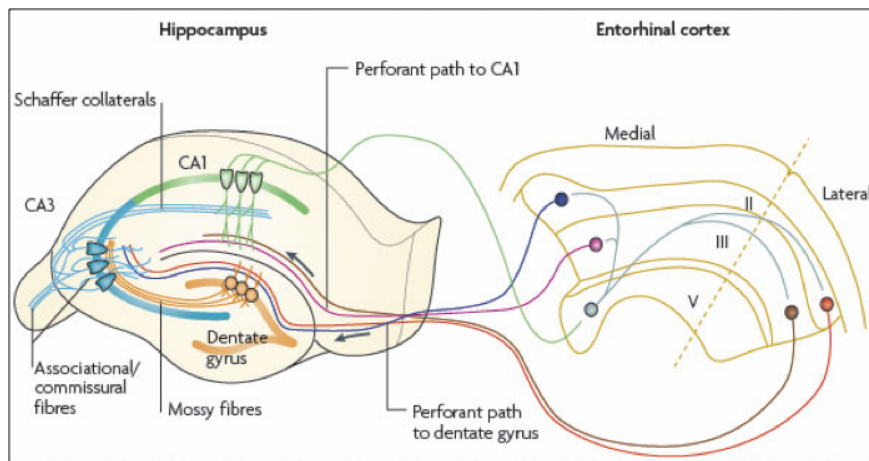
Figure 3: Wiring the hippocampus: Schematic representation of the hippocampal traditionally trisynaptic loop. The major input is carried by axons of the perforant path, from neurons in layer II and III of the entorhinal cortex to the dentate gyrus. Perforant path axons establish excitatory synapses with the dendrites of granule cells: axons from the lateral and medial entorhinal cortices innervate the outer and middle third of the dendritic tree, respectively. Granule cells in the DG, project, through their axons, the mossy fibers, to the proximal apical dendrites of CA3 pyramidal cells which, in turn, project to the ipsilateral CA1 pyramidal cells through Schaffer collaterals and to the contralateral CA3 and CA1 pyramidal cells through commissural connections. Finally, axons from CA1 close the loop connecting to the Subiculum and the Entorhinal cortex. (Adapted from Neves et al. 2008).

2. Hippocampal Development

The hippocampus develops from the medial wall of the telencephalon and it is strongly influenced by the organization and regionalization of this area. The establishment of rostro-caudal and dorso-ventral axis is orchestrated by diverse kinds of molecules released by organizer centers all along the neural tube. And this is one of the most critical events in the developing nervous system including the hippocampus.

The telencephalon originates as an outgrowth of the most rostral segments of the developing nervous system. After the bending of the neural plate into the neural groove and its closure to form the neural tube, the anterior portion will undergo drastic changes to form the three primary vesicles: forebrain (prosencephalon), midbrain (mesencephalon) and hindbrain (rhombencephalon). Subsequently, the prosencephalon subdivides into the anterior, called secondary prosencephalon (telencephalon and hypothalamus) and the more caudal, the diencephalon proper (Puelles & Rubenstein 2003; Puelles & Rubenstein 2015).

As the medial wall of the dorsal telencephalon, also named *pallium*, develops, it gives rise to a series of archipallial structures (archicortex) including (1) non-neuronal, secretory epithelium of the choroid plexus, adjacent to the roof; (2) the cortical hem, later in development called the fimbria when it is filled with projection fibers; (3) the hippocampal complex composed of the DG and CA fields; and (4) the subiculum, which is the transitional structure between the hippocampal complex and the medial limbic system composed by the cingulate and retrosplenial cortex (Li & Pleasure 2014). Also, the pallium will generate the paleocortex (olfactory, piriform and entorhinal cortex) and the neocortex. The ventral telencephalon or *subpallium* will mainly generate the basal ganglia and a part of the amygdala (Figure 4) (Moreno et al. 2009; Wang et al. 2011).
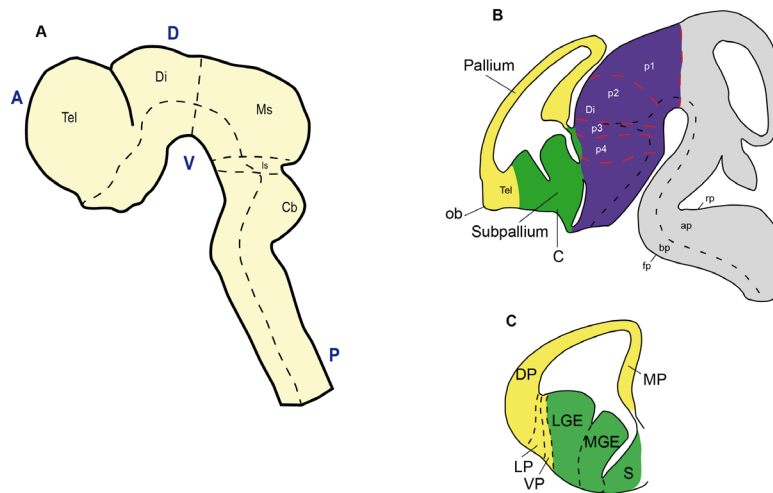
Figure 4: Prosencephalon organization. (A) Representation of the neural tube with Antero-Posterior and Dorso-Ventral axis (A-P; D-V, respectively) and main divisions: (Tel, Telencephalon, Di, Diencephalon, Ms, Mesencephalon, Cb, Cerebellum). (B) Schematic representation of a sagittal section from the neural tube; the telencephalon is already subdivided in pallium and subpalliun and the Diencephalon the prosomers 4 to 1 (from rostral to caudal). (Ob, Olfactory bulb, Di, Diencephalon rp, roof plate; ap, alar plate; bp, basal plate and fp, floor plate). (C) Drawing of a coronal section of the telencephalon with the main subdivision of the pallium (MP, medial pallium, which give rise the hippocampus, DP, dorsal pallium, LP, lateral pallium, VP, ventral pallium) and the subpallium (S), where at this level we find the MGE (medial ganglionic eminence) and LGE (lateral ganglionic eminence).

2.1. Morphogen molecules involved in the Hippocampal development

The initial development of the hippocampus shares features with the development of the cortex since the hippocampus originates from the caudo-medial portion of the embryonic cortex. Therefore the chain of events that regulates cortical development affects hippocampal development too. Gradients of different families of morphogenic molecules and transcription factors released by signaling centers or organizers are critical in the specification of the four compartments of the pallium including the hippocampal formation (Figure 5 and 6) (Wilson & Rubenstein 2000; Sur & Rubenstein 2005). The cortical hem, adjacent to the neuroepithelium from which the DG will arise, is the main organizer center that regulates the

development of the hippocampus and the DG (Grove et al. 1998; Tole & Grove 2001; Shimogori et al. 2004; Mangale et al. 2008). Studies where the cortical hem was deleted early in development, lead to the dramatic reduction of the neocortex and a total absence of the hippocampus, suggesting that the cortical hem is the source of molecules that lead the expansion of the cortex and the initial development of the hippocampus (Yoshida et al. 1996; Monuki & Walsh 2001; Caronia-Brown et al. 2014). Among the signaling molecules released by the hem are proteins from the Wnt and BMP families.

2.1.1.   Wnt proteins

Wnt proteins play an important role during the hippocampus development. Wnt signaling constitute a very complex pathway, and most of the hippocampal phenotypes caused by mutations in these genes are related to the Wnt ''canonical'' pathway through the low density lipoprotein receptor proteins (LRP) family and *Tcf/Lef* transcription factor (Galceran et al. 2000). For example, *Wnt3a* is the first Wnt ligand that appears in the cortical hem at E9.5 and mutations in this gene results in the failure of hippocampal morphogenesis since the neural precursors of the medial pallium are enable to expand (Lee et al. 2000). Downstream of Wnt3a, mutations in the transcription factor *Lef1*, which is expressed in the medial pallium, will produce a hippocampus that lacks dentate GCs (Galceran et al. 2000; Zhou et al. 2004).

2.1.2.   Bone morphogenetic proteins (BMP)

The cortical hem produces as well BMP family proteins, but they are also produced by the choroid plexus epithelium, adjacent to the hem (Furuta et al. 1997). Ectopic or reduction expression of BMP signals, alters the development and patterning of the dorsal pallium, dorsal midline and paramedial structures, as choroid plexus (Galceran et al. 2000; Hébert & Fishell 2008). Also, the loss of BMPR1a and BMPR1b receptors has a marked effect on the development of the hem. Double mutants for those genes will produced a normal hippocampus but a reduction of the DG (Caronia et al. 2010).

2.2. Transcription Factors involved in hippocampal patterning

The establishment of the cortical hem starts early in the development with the expression and tightly regulation of a group of transcription factors. Those factors are involved in the general patterning of the cortex and also in the establishment of the hem and the hippocampus. More specifically, *Emx2*, *Pax6*, *Coup-Tfl* and *Sp8* in the cortex, and *Lhx2*, *Lhx5* or *FoxG1* in hippocampus (Figure 5). They are characterized by a strong level of expression in medial or caudo-medial pallial regions or, as *Lhx2*, absent from the dorsal midline (Zhao 1999; Muzio & Mallamaci 2005; Mangale et al. 2008).
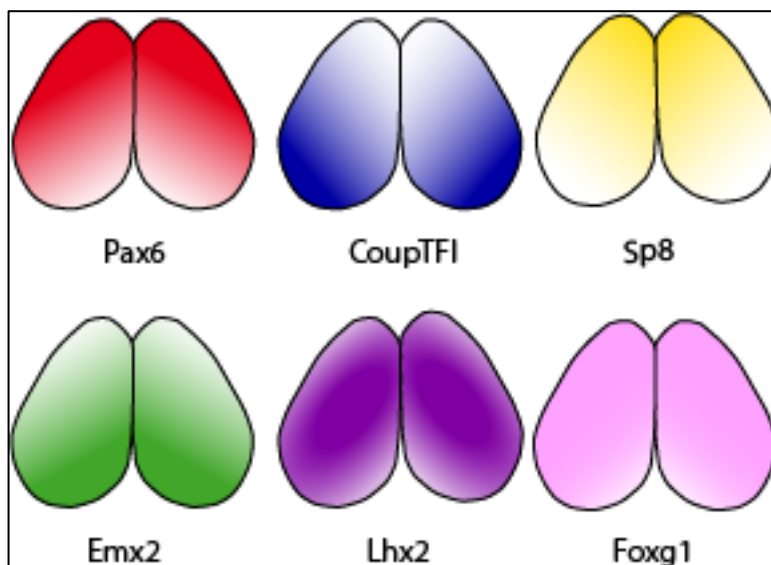
Figure 5: Expression pattern of genes involved in area patterning and cortical hem: Schematic drawings of the dorsal view of the telencephalon showing the expression pattern of *Pax6*, *CoupTFI*, *Sp8*, *Emx2*, *Lhx2* and *Foxg1* related to the patterning of the cortex. Pax6 is highly expressed in rostral and lateral regions and weakly in medial and caudal (opposite to *Emx2*), *CoupTFI*, shows a strong expression in caudal and lateral and weak in rostral and medial. *Sp8* is highly express in rostral and medial and weakly in caudal and lateral. *Lhx2*, absent from the dorsal midline and weaker in most anterior regions and

Foxg1, also absent from the hem.

2.2.1.   *Lhx2* and *FoxG1*

The expression of the LIM homeobox gene *Lhx2* starts in the forebrain early in the development but it is absent from the midline. This absence could allow the expression of Wnt proteins and establish the cortical hem. *Lhx2* has been postulated as a selector gene that can specify cortical identity and suppress alternative fates as hem or anti-hem in a spatially dependent manner (Mangale et al. 2008). Thus, in experiments with mutant embryonic stem cell (ESC) from a chimeric mouse for *Lhx2*, cells non-expressing *Lhx2* laterally in the cortex will adopt an anti-hem identity whereas medially, they will become cortical hem cells and induce ectopic hippocampal fields, establishing a ¨hem competent zone¨ that comprised the medial telencephalic wall and extended some distance laterally but did not include the entire pallium (Mangale et al. 2008).

FoxG1 has a role in the patterning of neocortex, regulating the expression of proteins that specify the dorso-medial identity. Thus, in *FoxG1$^{-/-}$* mutant mice, the neocortical tissue acquires hippocampal features and markers (such as bone morphogenetic protein 4 (BMP4) expression) usually confined to the dorsal midline, will appear expanded beyond their normal domain (Muzio & Mallamaci 2005).
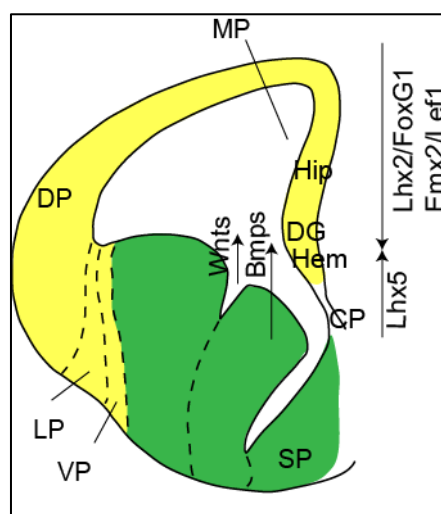
Figure 6: The cortical hem and the induction of the hippocampus.
Schematic diagram showing some of the genes involved in the dentate gyrus
morphogenesis. The development of the cortical hem (Hem), and the dentate
neuroepithelium (DG) are both regulated by Wnts. The hem and choroid plexus
(CP) are also regulated by BMPs. The expression domains for Wnts and BMPs
are shown with arrows to the left of the neuroepithelium. The dentate and
hippocampal neuroepithelium (Hip) are regulated by several transcription
factors (*FoxG1*, *Lhx2*, *Emx2*, and *Lef1*), while the hem development is
controlled by Lhx5. (Adapted from Li & Pleasure 2007).

2.2.2. *Emx2* and *Lhx5*

The homeobox gene *Emx2*, expressed in a high caudo-medial to low
antero-lateral gradient is one of the main players of the hippocampal
development and more concretely for the DG. Mutant mice for *Emx2* gene
show a reduction in caudal structures as visual and auditory cortex that is
compensated by a bigger motor and somatosensory cortex (Bishop et al.
2000; Muzio & Mallamaci 2005). As a caudo-medial structure the
hippocampus is strongly affected by a reduction in size, almost a lack of DG
and a reduction in the production of Cajal-Retzius cells from the cortical hem
(Pellegrini et al. 1996; Yoshida et al. 1997; Mallamaci et al. 2000; Shinozaki et
al. 2004). Another gene involved in hippocampal patterning is *Lhx5*, which is
expressed in the cortical hem and in Cajal-Retzius cells derived from the hem.
Lhx5^{-/-} mutant mouse lacks cortical hem development and as consequence of
this, the hippocampus shows defects derived from the loss of patterning
signals coming from the hem (Zhao 1999).

2.3. Types of cell migration in the developing telencephalon

Cell migration is one of the fundamental mechanisms during the brain
development. The size and complexity of the brain, as in other organs, create
the necessity to build a strategy to position each cell in a very specific place to
generate the proper local and long-range connections.

Not all cell types that will populate the cortex are generated in the cortex itself. It has been shown that projection glutamatergic neurons belonging to the layers II-VI, astrocytes and a subset of oligodendrocytes are generated in the dorsal pallium (*Emx1* expression domain) (Gorski et al. 2002; Kessaris et al. 2006). On the other hand, glutamatergic Cajal-Retzius cells, interneurons, and a subset of oligodendrocytes are generated outside the pallium (Bielle et al. 2005; Flames & Marín 2005; Kessaris et al. 2006; Colasante & Sessa 2010). This second group of cell types has to migrate long distances to reach their final destination. Thus, focusing on the timing of newly born neurons, we can distinguish two main types of migration in the developing telencephalon: Radial migration and Tangential migration (Figure 7).

2.3.1. Radial migration

At the end of XIX century, studies from Ramón y Cajal described that most of the neurons have to move radially to reach their final position in the brain. Also, it was described by Pasko Rakic in 1972 that during their radial migration, neurons were aligned with radial glial fibers suggesting the idea that those radial glia fibers act as scaffold providing support to those migrating neurons (Rakic 1972). Those studies were later confirmed by in vitro and in vivo experiments (Noctor et al. 2001; Noctor et al. 2004). Recent studies have described two different types of radial migration: cellular locomotion, in which the cells use the radial glial fibers as substrate to migrate (Hatten 1999; Noctor et al. 2001) and somatic translocation, where the cells migrate independently of the radial glia and extending a long process to attach to the pial surface and retract afterward during the migration pushing the cell upward (Nadarajah et al. 2001; Nadarajah & Parnavelas 2002).

2.3.2. Tangential migration

Tangential migration is mainly used for interneurons to reach the cortex from the basal ganglia where they are born. This type of migration is perpendicular to the radial glial fibers and thus uses distinct kind of substrate

to migrate (Rakic 1972; Rakic 1974; Marín & Rubenstein 2001). These neurons can migrate as a chain, giving support to each other, as in the rostral migratory stream (Lois & Alvarez-Buylla 1994), following axons as a guidance to reach their final destination (Wray et al. 1994; Yoshida et al. 1996) or guided by chemoattractant molecules in their individual trip over the extracellular matrix to their final destination (Flames et al. 2004).
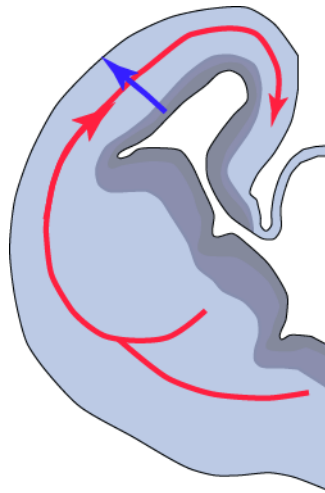
Figure 7: Main types of neuronal migration in the cerebral cortex. Schematic diagram showing the radial migration (arrow in blue), which is mainly followed by cells originated in the ventricular zone of the pallium and the tangential migration (arrow in red) followed by cells outside of the pallium as interneurons.

2.4. Neuronal migration in the Hippocampus

2.4.1. Cajal-Retzius cells

One of the first populations of neurons that migrate along the telencephalon during development are the Cajal-Retzius cells (CR cells) (Figure 9). They represent a transient class of neurons found at the surface of the developing cortex and the hippocampus. They are the earliest neurons to be born and invade the preplate as early as E10 (König et al. 1977; König & Schachner 1981) (Figure 8). Also, they have an important role in the layer organization of the cortex and hippocampus (del Río et al. 1995). It has been described that they originated from three different sites in the telencephalon: the pallial–subpallial boundary (PSB) laterally, the septum rostro-medially,

and the cortical hem caudo-medially (Bielle et al. 2005). Around 85-95% of the hippocampal CR cells originate in the hem (Takiguchi-Hayashi et al. 2004; Yoshida et al. 2006).
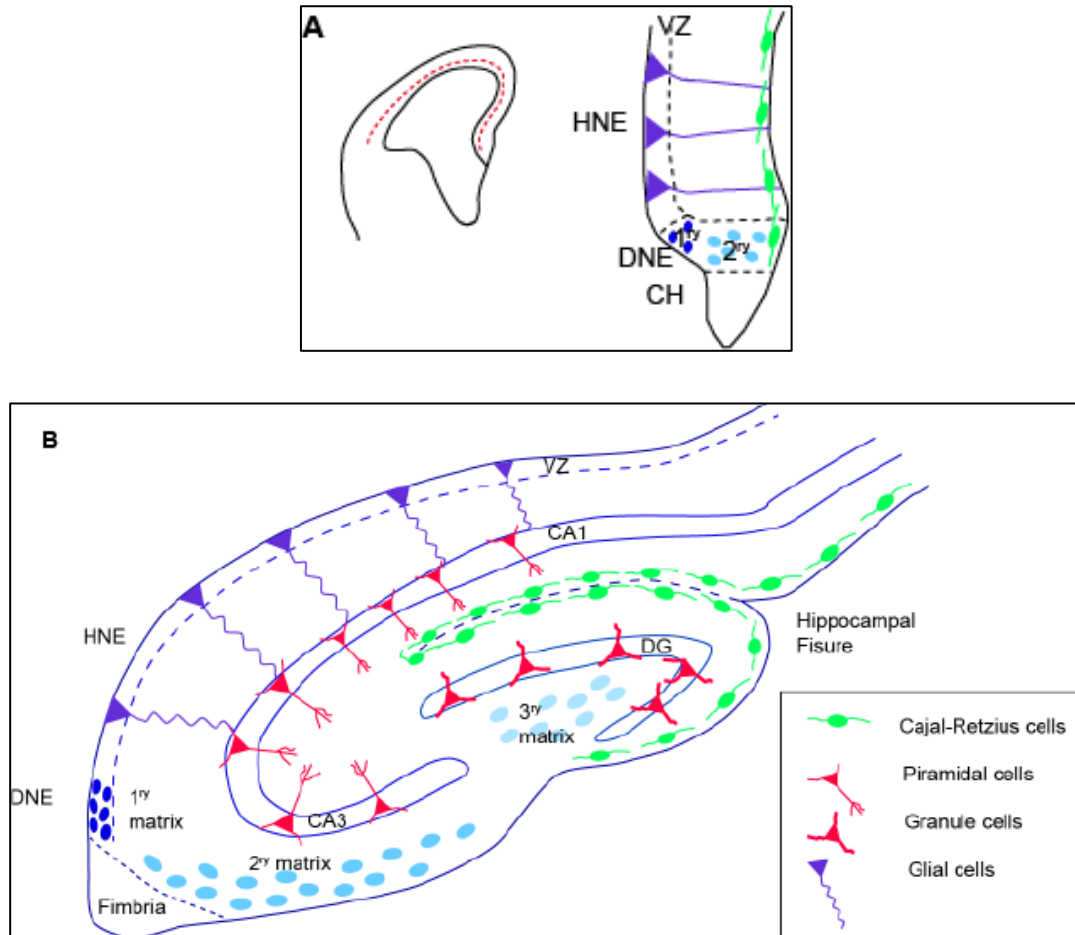
Figure 8: Cell migration and development of the hippocampus: Schematic representation of the hippocampus and its different type of cell migrations at E14.5 (A) and at birth (B). Cajal-Retzius cells (green), born around E12.5 in the cortical hem, just under the presumptive dentate neuroepithelium (DNE), lined the pial surface. At E14.5, the dentate precursors of the primary matrix (dark blue circles) are located in the VZ and start to migrate towards the pial side of the cortex forming the secondary matrix (blue circles). In the VZ of the hippocampal neuroepithelium (HNE), radial glial precursors (purple cells) give rise to hippocampal neurons. At E17.5 the hippocampal fissure is formed and DG precursor cells migrate to and accumulate there, forming the tertiary matrix (light blue). Cajal-Retzius cells are also present and follow the hippocampal fissure. At this stage the glial scaffold extends from the CH to the hippocampal fissure and pial surface, directing the migration of dentate precursor cells. From the HNE, hippocampal neurons (red triangles) are born and migrate along radial glial cells towards their location in the hippocampal fields, CA1 and CA3 and after that, the blades of the DG start to form. Granule

neurons in the DG (red triangles) appear first in the upper blade, below the hippocampal fissure. The continuous migration of CR cells reaches the pial side and promotes the formation of the lower blade of the DG. Precursor cells in the primary and secondary matrix will soon disappear, but cells in the tertiary matrix continue actively dividing and producing granule neurons through postnatal DG development; cortical hem (CH); ventricular zone (VZ); primary matrix (1ry); secondary matrix (2ry); tertiary matrix (3ry); dentate gyrus (DG). (Adapted from Urbán & Guillemot 2014).

CR cells main function is related to radial migration of neurons and the formation of cortical layers controlling, among other things, the radial glia morphology, which is the substrate for migrating neurons. CR cells express the protein Reelin in the marginal zone (MZ) of the developing hippocampus framing the area for the attachment of radial glia cells to lead neurons to their final position in CA or DG fields. CR cells also have a role in the development of hippocampal connections (Del Río et al. 1997).

2.4.2. Hippocampal projection neurons

Neurogenesis in the mice hippocampus starts at E10-E11 and lasts well beyond birth (Angevine 1965). Pyramidal neurons in the Ammon's horn are mainly generated from the neuroepithelium adjacent to the *hippocampal primordium* and undergo radial migration to reach their final destination (Figure 8) (Altman & S. A. Bayer 1990a; Nakahira & Yuasa 2005; Kitazawa et al. 2014). Also, the hippocampal laminar formation occurs in a birthdate dependent inside-out pattern where earlier born neurons occupy the deepest region meanwhile later born neurons occupy the superficial region (Bayer 1980; Rakic & Nowakowski 1981; Altman & S. A. Bayer 1990b). The generation of pyramidal neurons between the hippocampal regions (CA1 and the CA3) is different probably because of the different U-shape of CA3 and the proximity to the DG and hilus.

CA1 cells are mostly generated in the VZ between E12-E18 with a peak around E14-E16. After they left the VZ, multipolar-shaped some cells may undergo another round of division and move slowly into the intermediate

zone (IZ) (Nakahira & Yuasa 2005; Kitazawa et al. 2014) where they remain for several days (Altman & S. A. Bayer 1990b). The generation of CA3 cells starts also around E12-E18, having a birth peak one day before than CA1 cells (Angevine 1965) and remaining longer in the IZ (Altman & Bayer 1990b). Thereafter, CA1 and CA3 cells continue their migration to the preplate splitting it in the hippocampal plate, which will become the pyramidal layer and the subplate that will be the prospective *SO*. The marginal zone above the hippocampal plate will become the prospective *SR* and *SLM*.

2.4.3. Hippocampal interneurons

GABAergic interneurons in the hippocampus are local circuit neurons responsible for inhibitory activity, thereby controlling the activity of principal excitatory cells, such as pyramidal cells in the hippocampus and GC in the DG. In mice, the majority of interneurons are generated at E12–13, and DG interneurons at E13–14 (Soriano et al.,1986; Soriano et al., 1989a; Soriano et al., 1989b).
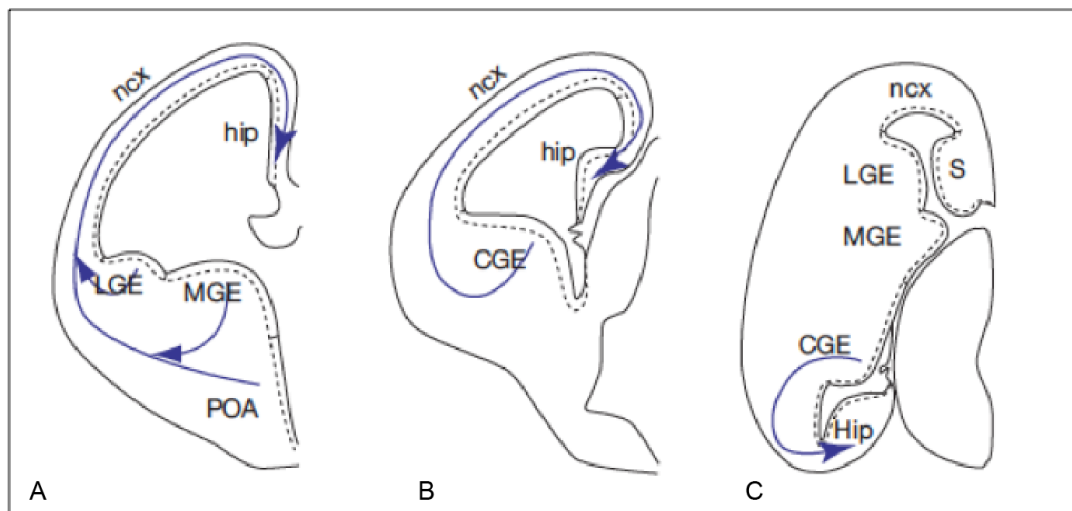
Figure 9: Tangential migration of the interneurons. Schematic representation of coronal sections through the rostral (A) and caudal (B) cortex at E13.5 showing the tangential migration of the interneurons that will populate the hippocampus originated in subpallial regions (C) Schematic representation of a horizontal section through the brain at E13.5 showing the route that follow

the interneurons from Caudal Eminence to the hippocampus. (ncx, neocortex; hip, hippocampus; LGE, lateral ganglionic eminence; MGE, medial ganglionic eminence; POA, pre-optic area; CGE, caudal ganglionic eminence; S, septum). Adapted from (Li & Pleasure 2014).

Interneurons residing in the hippocampus are derived from the ventral telencephalon, the *subpallium*, and need longer tangential migration times to reach the hippocampus (Marín et al. 2010). It has been shown that hippocampal interneurons originate in the ganglionic eminences of the subpallium, mainly from the medial and the caudal ganglionic eminences (MGE and CGE, respectively, Pleasure et al. 2000; Wichterle et al. 2001; Nery et al. 2002; Tricoire et al. 2011). The preoptic area has been shown also to contribute with interneurons to the hippocampus (Gelman et al. 2009) (Figure 9).

Previous studies with the *Dlx1* and *Dlx2* transcriptions factors expressed in the ganglionic eminences (GEs) showed that mutant mice with mutations in these genes lead to the loss of most of the interneurons, not only in the neocortex but also in the hippocampus (Pleasure et al. 2000; Cobos et al. 2005). They originate in the GEs and migrate towards the hippocampus following similar routes as neocortical interneurons, through the MZ (marginal zone) and IZ/SVZ (Intermediate zone/Subventricular zone) streams. While MGE (medial ganglionic eminence) cells migrate laterally and spread widely throughout the cortex, the CGE (caudal ganglionic eminence) derived cells (E12.5–E13.5) migrate caudally to the most-caudal end of the telencephalon and move toward the MZ before entering the hippocampus (Yozu et al. 2005). Also, it is known that the first interneurons enter the hippocampus on, or slightly after, E14 with peak invasion occurring between E15 and E18. The MZ path contributes the most hippocampal interneurons (Manent et al. 2006). They first reach the subiculum and the CA1 field, and then the CA3 field at E16, and the DG primordium 1day later, at E17 (Manent et al. 2006). CGE-derived interneurons are added slightly later than MGE-derived interneurons (Rubin et al. 2010; Tricoire et al. 2011).

2.4.4.   Dentate gyrus cells

Dentate gyrus originates from the dentate neuroepithelium (DNE) also called the primary matrix, located adjacent to the cortical hem and the dentate notch, in the medial wall of the lateral ventricle. It becomes clearly distinguishable around E14.5 (Figure 10).
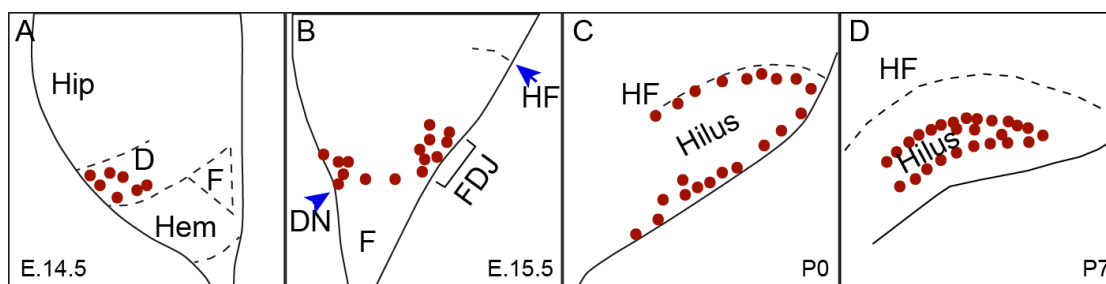
Figure 10: Granule cell migration. Schematic representation of the development of the DG. Granule cells (red dots) start originating from the dentate neuroepithelium at E14.5 (A). After that they will migrate to reach the FDJ (B) where they will keep dividing and will follow to the prospective DG region (C). Finally, they will migrate radially to form the granule cell layer of the DG. (Hip, Hippocampus; D, Dentate; F, fimbria; DN, dentate notch; FDJ, fimbrio-dentate junction; HF, hippocampal fissure) (Adapted from Li et al. 2009).

At the beginning of the last week of rodent embryonic development, progenitor cells migrate out of the DNE and towards the subpial surface in a process that depends on hem-derived Cajal-Retzius cells (Rickmann et al. 1987; Del Río et al. 1997). This new migratory progenitor population will constitute the secondary matrix. Meanwhile, the primary radial glia develops and is the lead for dentate precursors and granule neurons to migrate and organize. Once the progenitors reach the hippocampal fissure, they accumulate into the *hilus* and form another proliferating niche, the tertiary matrix. GCs are generated during DG development from precursors of all three matrices and form the GCL (Figure 8 and 10). By early postnatal stages, the tertiary matrix becomes the only source of dentate progenitors and GCs.

31

Later, proliferation in the DG becomes more restricted and it will be confined to the subgranular zone (SGZ) where will remain throughout live.

3. Adult Neurogenesis

The transition of proliferative and multipotent Neural Stem Cells (NSCs) to differentiated neurons is called neurogenesis. Neurogenesis occurs from early embryonic to early postnatal stages, however in recent years it has been discovered that neurogenesis remains active at adult stages in a few neurogenic zones (Götz & Huttner 2005; Ming & Song 2011a; Paridaen & Huttner 2014).

There are mainly two places in the murine central nervous system where adult neurogenesis has been well characterized (Figure 11). The SGZ in the DG of the hippocampus will produce GCs to contribute to the dentate itself (Altman & Das 1965; Gould & Cameron 1996; Kempermann et al. 1997; Gage 2002), and the subependymal zone of the lateral ventricles, also called Ventricular-Subventricular Zone (V-SVZ) will contribute with neurons that will migrate to reach the olfactory bulb (Lois & Alvarez-Buylla 1994; Merkle et al. 2007; Ventura & Goldman 2007; Young et al. 2007; Brill et al. 2009). Both regions have been shown to be active in adult human brains too with the V-SVZ producing new neurons that will incorporate to the striatum and SGZ to the DG (Eriksson et al. 1998; Spalding et al. 2013; Ernst et al. 2014).
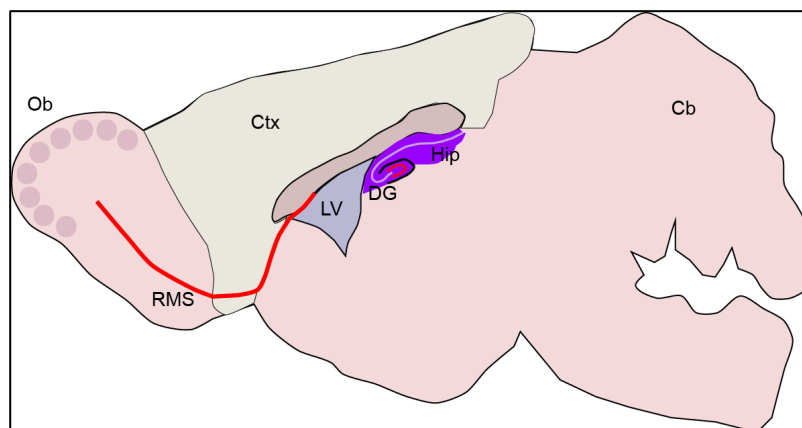
Figure 11: Stem Cell in the Adult Brain. Representation of the two main niches of stem cell in the adult brain, the SGZ in the hippocampus and the SVZ in the lateral ventricles (red lines) (Ob, olfactory bulb; Ctx, cortex; Cb, cerebellum; RMS, rostral migratory stream; LV, lateral ventricle; DG, dentate gyrus; Hip, hippocampus.

One of the main difference between the SGZ and SVZ is that in SGZ the cells that will contribute to the population of adult NSC are completely dissociated from the embryonic germinative zone where they are born (Altman & S. a Bayer 1990; Li et al. 2009). As mention before, during the development of the DG, the cells originated in the neuroepithelium adjacent to the cortical hem migrate and incorporate to the GCL of the DG. Later in adulthood, NSCs from the SGZ produce GCs that will be integrated in the GCL of the DG. On the contrary, the NSCs from the SVZ differentiate into neuroblast before they incorporate to the Rostral Migratory Stream (RMS) in their way to the olfactory bulb. In this context, the regulation of the signals that maintain both NSC niches in adult will be slightly different.

3.1. The Subventricular Zone (SVZ)

The germinal region of the olfactory bulb in adults is located in the wall of the lateral ventricle and has similar characteristics as the embryonic VZ or SVZ. The V-SVZ (Lim & Alvarez-Buylla 2016) as it was mentioned before is one of the two canonical places where neurogenesis occurs in the adult brain (Lois & Alvarez-Buylla 1994). NSCs from this region generate neuroblasts (type A cells) that migrate through the RMS to reach the olfactory bulb. Once they arrive there, they differentiate and integrate mainly as interneurons. NSCs, also called type B1 cells express a number of glial markers such as GFAP (glial fibrillary acidic protein), GLAST (Glutamate aspartate transporter) and BLBP (Brain lipid binding protein). Type B1 cells can be in a quiescent or an activated state (Codega et al. 2014; Mich et al. 2014). When they are in an activated state, they will express Nestin, an intermediate filament generally considered as a marker of NSCs. These Nestin positive cells give rise to

transient amplifying precursors (type C cells), which generate neuroblasts (type A cells) that move through the RMS (Doetsch & Alvarez-Buylla 1996) into the olfactory bulb where they migrate radially to become interneurons.

3.2. The Subgranular Zone

The SGZ is the niche of the adult stem cells that will generate the GCs. Thus, defects in the generation and integration of GCs play an important role in different neurological disorders such as depression (Dranovsky & Hen 2006) and epilepsy (Parent et al. 2006). In fact, it is already known that newly generate neurons confer an extra degree of plasticity and have effects in learning and certain types of contextual memory (Jessberger et al. 2009; Sahay et al. 2011). Hence, in the last years, many studies have been trying to unveil the integration process of these new neurons into the adult hippocampal circuits.

It is well known that adult stem cells are tightly restricted to the generation of one (GCs of the DG) or a few types of neurons (granule neurons and periglomerular neurons in the V-SVZ) (Zhao et al. 2008; Ming & Song 2011b) whereas embryonic neurogenesis is, thus, tightly linked to cell fate specification. These processes are dependent on specific signals and factors that specify subtype identities during development and they can also control some aspects of the behavior of adult stem cells.

3.2.1. Cellular types in the SGZ

In the hippocampus, adult NSCs, also called type-I cells or radial glial-like cells, generate exclusively granule neurons in the DG (Figure 12). Those cells, NSCs, express the same markers as embryonic stem cells (*Nestin*, *Sox2* and GFAP). Type-I cells follow a well characterized cell lineage that include intermediate cell progenitors (IPCs) as type IIa (non-radial intermediate or transient amplifying progenitors cells that express *Nestin*, *Sox2* and *Tbr2*), type IIb (neuronally determined intermediate or transient

amplifying progenitor cells, that also express *Nestin*, *Prox1*, *NeuroD1* and DCX (doublecourtin)) and type III (migratory neuroblast-like that stop expressing Nestin but maintain neural markers as Prox1, NeuroD or DCX) (Nicola et al. 2015).

Type I	Type IIa	Type IIb	Type III	
		Nestin		
GFAP	Tbr2	DCX	DCX	
Nestin	Nestin	NeuroD1	NeuroD1	NeuN
Sox2	Sox2	Prox1	Prox1	Prox1

| Radial glia-like cell | Neuronal progenitor | Neuroblast | Immature neuron | Mature neuron |

ML

GCL

SGZ
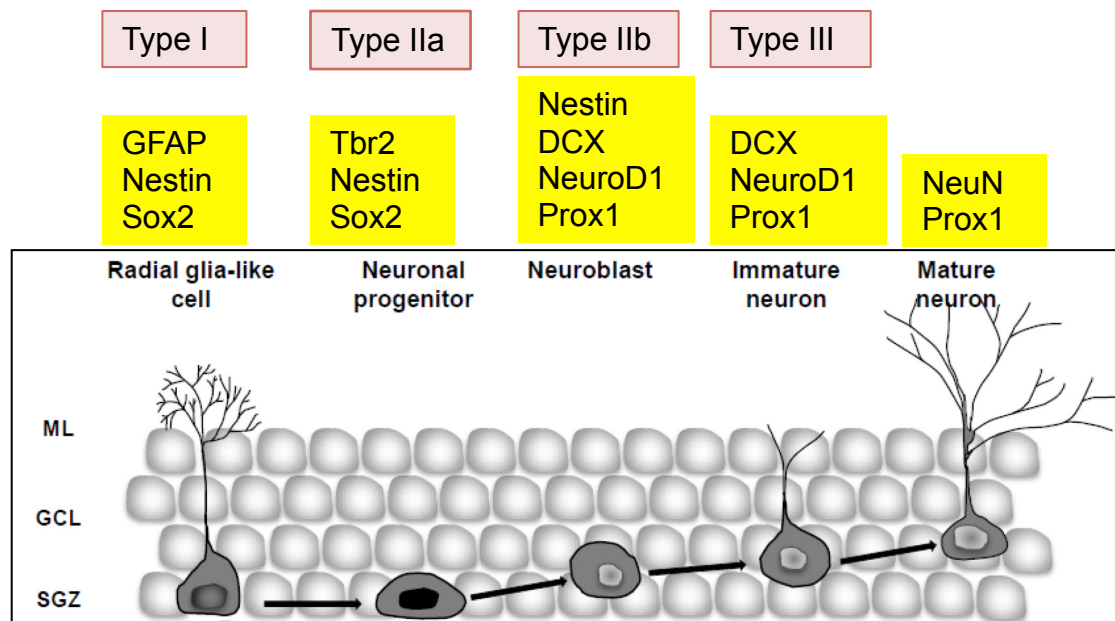
Figure 12: Markers and cell types in the Subgranular Zone of the DG. Schematic diagram illustrating the sequential types of cells in the process of neurogenesis in the adult hippocampus showing the transition from radial-like glia cell to neural progenitor cell in the adult SGZ. Adapted from Faigle and Song, (Faigle & Song 2013).

3.2.2. Molecules that regulate the neurogenesis

As mention before, neurogenesis in mammalian brain involves multiple and complex processes that include proliferation, fate specification, differentiation, maturation, migration, and functional integration of newborn cells into the existing neuronal circuitry. Thus, adult NSCs are quiescent and settle in a very complex environment containing signals that modulate its behavior (Fuchs et al. 2004; Blank et al. 2008; Faigle & Song 2013).

3.2.2.1. BMPs and Wnts

Molecules such as BMPs and Wnts, involved in the development of the

hippocampus are also present in the adult neurogenic niche with a different role. BMPs are necessary to maintain the quiescence of NSCs and also the differentiation and maturation of GC (Bond et al. 2014). Wnts, on the other hand, which act as organizer of hippocampal development at earlier stages, have also a role in postnatal and adult neurogenesis (Zhang et al. 2011; Ortiz-Matamoros et al. 2013; Varela-Nallar & Inestrosa 2013). They are secreted by astrocytes and stem cells in the adult hippocampus and can directly induce neurogenic genes such as *Neurog2*, *NeuroD1* or *Prox1* in intermediate progenitors (IP) to differentiate in GC that will be integrated in the GCL and play a role in synapse formation and maturation of postmitotic neurons (Kuwabara et al. 2009).

3.2.2.2.   Notch

Notch receptors and their ligands are broadly expressed during all stages of hippocampal development (Pleasure et al. 2000). Loss of essential component of *Notch* signaling as RBPJk or Jagged1 leads to defects in stem cell proliferation and maintenance but not in DG formation (Breunig et al. 2007; Lavado & Oliver 2014). During brain development, the activation of the Notch pathway is essential to expand the NSC population size by dividing symmetrically and later, in adult life, maintaining the size of the NSC pool by balancing quiescence versus activated NSC (Hitoshi et al. 2002; Ables et al. 2010). Indeed, loss of *Notch* caused a significant increase in new neurons at the expense mainly of progenitors cell types and activation of *Notch* pathway instead produce an increment of the glial progenitors cells in SGZ (Breunig et al. 2007).

3.2.2.3.   Other signals that regulate the NSC niche

Other molecules involved in the maintenance of the adult stem cells are growth factors such as neurotrophins, neurotransmitters, and neurogenic transcription factors. Most of them have a different role during development and in adult neurogenesis. Thus, for example, an increment of growth factors and neurotrophins, such as FGF2 (Fibroblast Growth Factor-2) and BDNF (Brain Derived Neurotrophic Factor) result in an increase in the production of

newly born neurons in the DG (Rai et al. 2007; Zhao et al. 2007; Li et al. 2008), while lack of neurotrophins as NT-3 (neurotrophin 3) results in an impairment of differentiation (Shimazu et al. 2006). Neurotransmitters, such as glutamate and its receptors, or GABA, produce diverse effects that help to keep the equilibrium of the niche regulating proliferation (Glutamate through NMDA receptors) (Deisseroth et al. 2004; Nacher & McEwen 2006) or maintaining the quiescence of radial glia-like NSC by GABA produced from local parvalbumin expressing interneurons (Song et al 2012). In addition, a pool of transcription factors with diverse known effects in brain development also play a role in the establishment of the SGZ environment. For example, *Tbr2* is involved in the proliferation and differentiation of NSC into intermediate progenitors (IPs) or *Prox1* in the acquisition of GC identity.

3.2.3. Shh in the development of the Dentate Gyrus

Sonic Hedgehog (SHH) is a protein with diverse and important roles during CNS development. Among the three known ligands of the Hedgehog family (SHH, IHH and DHH), only *Shh* is expressed in the CNS (Echelard et al. 1993). Acting as a morphogen, SHH is involved in the patterning of the brain and other regions (Charytoniuk et al. 2002). During the development of the neural tube, SHH morphogen gradient establish the differential expression of homeodomain transcription factors along the dorso-ventral axis to specify neuronal identity. In the ventral forebrain, SHH is necessary for the generation of cells in the medial and lateral ganglionic eminences (Kohtz et al. 1998). In addition to controlling cell fates, SHH promotes proliferation and inhibits differentiation of neuronal and non-neuronal cell types, as in GC in the cerebellum (Dahmane and Ruiz i Altaba 1999), or oligodendrocyte precursors (Davies and Miller 2001). Lack of SHH during development produce severe defects in the CNS, such as a fused telencephalic vesicle, single fused optic vesicle and externally, an apparent proboscis (Chiang et al. 1996; Roessler et al. 1996). Lately, its function has been extensively studied in neural stem cell and progenitors (Machold et al. 2003; Ahn & Joyner 2005).

3.2.3.1.   SHH signaling in the SGZ

Secreted SHH protein acts in a concentration- and time- dependent manner to initiate diverse cellular responses. SHH is released from the cell and initiate signaling through binding to its canonical receptor Ptc (*Patched*, *Ptc1* and *Ptc2* in mammals). This results in the derepression of Smo (Smoothened), and the internalization of the Smo complex into the cell to activate GLI family proteins. The GLI family of proteins is composed of three multifunctional transcription factors (GLI1, GLI2 and GLI3) that can either act as an activator or repressor. When SHH signal is activated, GLI3 and GLI2 act as activators. Cells that respond to Shh upregulate the expression of Gli1 and play a role as a secondary enhancer of the Shh signaling. In the absence of SHH, GLI proteins are largely inactive through the activity of SUFU, suppressor of fuse protein that is an inhibitor of SHH, leading to its degradation or the formation of its repressor form.

Recent studies have identified the important role of *Shh* signaling in the establishment and maintenance of stem cell niches in the adult brain (Machold et al. 2003; Ahn & Joyner 2005; Han et al. 2008; Breunig et al. 2008). Mice with conditional null alleles of either *Shh* or *Smo*, show in a dramatic loss of neural progenitors in the postnatal SVZ and hippocampus. Also, loss of *Shh* signaling results in defects in the DG and the olfactory bulb (Machold et al. 2003). Moreover, the impairment of the cilia, where *Shh* signaling is typically transduced, produce morphological abnormalities in the glial-like neural precursors resulting in an hypoplasic hippocampus (Breunig et al. 2008; Han et al. 2008). These data suggest that precursors in the hippocampus are SHH responsive. Indeed, experiments of fate mapping with transgenic mice reveals that embryonic dentate NSCs are responsive to SHH during late gestation before they settle in their permanent niche in the SGZ. Even more, they will keep this responsiveness while they remain as quiescent all along adulthood (Ahn & Joyner 2005; Encinas et al. 2011).

3.2.4. The transcription factor *Emx2* during brain development

The transcription factor *Empty Spiracles Homeobox 2 (Emx2)* is a vertebrate homeobox gene related to the Drosophila *empty spiracles (ems)* gene (Dalton et al. 1989). *Emx2* starts its expression in the initial development and affecting the early dorsal telencephalic regionalization (Fukuchi-Shimogori & Grove 2003; Shimogori et al. 2004). In coordination with other transcription factors such as *Pax6*, *Sp8* and *Coup-Tf1*, *Emx2* is involved in the specification of the cortical area map which give rise to the primary areas of the cortex (Bishop et al. 2000; Armentano et al. 2007; Sahara et al. 2007). In addition, studies of *Emx2$^{-/-}$;Pax6$^{-/-}$* and *Emx2$^{-/-}$;Otx2$^{-/-}$* double mutants mice shows a role for *Emx2* in the development of the diencephalon (Suda, Y., et al. 2001; Kimura et al. 2005). Also, *Emx1$^{-/-}$;Emx2$^{-/-}$* mutant mouse data suggest that *Emx2* participates in the developing of the medial pallium (Yoshida et al. 1997; Shinozaki et al. 2004).

3.2.4.1. Expression pattern of *Emx2* during mouse development

Expression of *Emx2* starts in the early development (E8.5) where it is initially restricted to the anterior dorsal neuroectoderm and having stronger expression at E9.5 with a posterior boundary within the roof of the presumptive diencephalon. At this stage there is also expression in the floor of the diencephalon and will continue later in specific regions of the presumptive diencephalon. Around E12.5 and posterior stages, *Emx2* appears in the presumptive cortex but is not uniformly distributed, being restricted to the progenitor cells. Along the anterior-posterior axis the signal is much stronger in the posterior dorsal telencephalon with a sharp posterior boundary and a decreasing intensity in progressively in the more anterior regions (Simeone et al. 1992).

At the hippocampus anlage, *Emx2* is visible at E12.5, mainly and abundantly in the ventricular neuroepithelium, the source of all pyramidal neurons of the hippocampus and most of the GC of the DG (Angevine 1965b;

Stanfield & Cowan 1979). Also, *Emx2* is detected underneath the *pia*, in the secondary matrix, where GC of the DG are forming (Schlessinger et al. 1975). Around E15.5 *Emx2* is specifically expressed in the developing nuclear complex of the amygdala and the hippocampus particularly in the forming blades of the DG. The protein was also detected in the SGZ during the second postnatal week, suggesting that *Emx2* expression persists postnatally (Mallamaci et al. 1998). Indeed, EMX2 protein was recently found in adult NSCs present in the subependymal layer of the lateral ventricles and in the DG of the hippocampus, probably participating in the control of transition from symmetrically to asymmetrically dividing neural precursors (Gangemi et al. 2001).

3.2.4.2.   Phenotype of *Emx2^{-/-}* mutant mouse

Major abnormalities have been observed in the brain of the *Emx2^{-/-}* mutant mouse (Pellegrini et al. 1996b; Mallamaci et al. 2000; Savaskan et al. 2002; Shinozaki et al. 2004; Oldekamp et al. 2004; Zhao et al. 2006;). Not only is the DG missing but also the hippocampal proper and the medial limbic cortex are reduced and the development of neocortical plate and olfactory bulb is impaired and disorganized. Histologically, the hippocampus shows major alterations, with a severe reduction in the fimbria and fornix and an abnormally large communication between the two lateral ventricles and the third (Pellegrini et al. 1996; Yoshida et al. 1997). These defects are reminiscent of those found in patients affected by schizencephaly, which is caused by mutations in the *Emx2* gene. This very rare congenital disease is characterized by full-thickness clefts within the cerebral hemispheres (Brunelli et al. 1996).

The *Emx2^{-/-}* mutant mouse cortex shows alterations in the cortical area map, In particular, the caudo-medial cortex, which includes the visual and auditory cortices, is shrunken. This occurs at the expense of the rostro-lateral areas, motor and somatosensory cortex which are augmented and its identity altered (Bishop et al. 2000; Mallamaci et al. 2000). The laminar organization of the cortex is also impaired, due to a reduction in the number of CR cells (Mallamaci et al. 2000).

As mentioned earlier, *Emx2* is widely expressed in the hippocampus at almost all ages. At E18.5 shows that this gene is present in every subdivision of the DG, with strong expression in radially and tangentially migrating neurons and the tertiary matrix, and weaker expression in the granule layer (Oldekamp et al. 2004). Lack of *Emx2*, therefore, produce alterations in the hippocampus and the DG, probably not only because of the changes of patterning produced in the medial cortex but also, for the loss of *Emx2* in the hippocampus and DG itself. There is reduced expression of marker of genes that function in cell division such as *Ki67*, or specification such as *Mash1* (Pleasure et al. 2000), showing that these two mechanisms, cell division (Muzio et al. 2005) and migration (Oldekamp et al. 2004) are affected.

OBJECTIVES

The origin and development of the cells that populate the GCL of the DG embryonically has been extensively studied. Previous works from Altman and Das (1967) described also the DG as one of the place in the brain where adult neurogenesis is happening. The interface of the GCL and the hilus, known as Subgranular Zone is the adult neurogenic niche where NSC are generated to give rise GCs not only embryonically but in adult life.

Our main objective in this work is to better understand the mechanisms that control the formation of the SGZ as a neurogenic niche. For that, we marked the following objectives:

Chapter 1

A) To define the embryological origin of the cells that will populate the SGZ as NSC in the adult.
B) To determine how Shh controls the formation of the DG SGZ, identifying the source of Shh that is acting as a ligand of the NSC, and when and where these cells are distribute.

Chapter 2

C) To understand the mechanisms that are involved in the Shh signaling and the interactions with others proteins in the origin and development of the NSC.
D) To determine the role of *Emx2* gene thought Shh signaling in the origin, maintenance and migration of the embryonic neural stem cells originated in the ventricular zone of the ventral hippocampus.

MATERIAL AND METHODS

4. Animals and Genotyping

Experiments were performed in different strains of mice. All of them were maintained in the C57BL6/J background, and according to the protocols approved by the Institutional Care and Use Committee at UCSF. Timed pregnant dams were generated and we considered the plug date as E0.5. For tamoxifen Induction Tamoxifen (T5648, Sigma) was dissolved in corn oil (C8267, Sigma) at 20 mg/ml. Pregnant females were injected intraperitoneally (i.p.) with 3 mg of tamoxifen per 40 g animal. Neonates were injected subcutaneously with 50 ml of tamoxifen stock solution.

The following mouse lines were obtained from Jackson laboratories:

$Gli1^{nLacZ}$ (stock 008211)

$Gli1^{CreERT2}$ (stock 007913)

$Rosa^{Yfp}$ (stock 006148),

$Emx1^{Cre}$ (stock 05628),

Nes^{Cre} (stock 003771)

Shh^{GfpCre} (stock 005622)

$Shh^{CreERT2}$ (stock 005623)

$Shh^{Flox/Flox}$ (stock 004293)

$Smo^{Flox/Flox}$ (stock 004526)

$Ai14^{Flox/Flox}$ (stock 007914)

$Olig2^{Cre}$ (kindly provided by Dr. D. Rowitch (UCSF))

$Neurod6^{Cre}$ (Dr. S. Goebbels and Dr. K.A. Nave (Max Planck))

$Emx2^{-/-}$ (Dr. J. L. Rubenstein (UCSF)).

To identify all the genotypes, PCRs with appropriate primers were performed.

For *Emx2*:

*Emx2*R_WT: ACCTGAGTTTCCGTAAGACTGAGACTGTGAGC

*Emx2*F: CACAAGTCCCGAGAGTTTCCTTTTGCACAACG

*Emx2*R_MT: ACTTCCTGACTAGGGGAGGAGTAGAAGGTGG

For *Gli1^{LacZ}*

LacZ200F: TTATGGCAGGGTGAAACGCAGGTC

LacZ200R: AAACCGACATCGCAGGCTTCTG

Or

oIMR7888: GGG ATC TGT GCC TGA AAC

oIMR8770: TCT GCC AGT TTG AGG GGA CGA C

oIMR9034: AGG TGA GAC GAC TGC CAA GT

For *Shh^{CreGFP}* ; *Gli1^{CreERT2}*; *Emx1^{Cre}*; *Nes^{Cre} Shh^{CreERT2}*; *Olig2^{Cre}* and *Neurod6^{Cre}*;

Cre400F: GCATTACCGGTCGATGCAACGAGTGATGAG

Cre400R: GAGTGAACGAACCTGGTCGAAATCAGTGCG

For *Ai14$^{F/F}$*

Ai14-wt9020: AAG GGA GCT GCA GTG GAG TA

Ai14-wt9021: CCG AAA ATC TGT GGG AAG TC

Ai14-mut9103: GGC ATT AAA GCA GCG TAT CC

Ai14-mut9105: CTG TTC CTG TAC GGC ATG G

For *Rosa^{Yfp}*

Rosa-21306: CTG GCT TCT GAG GAC CG

Rosa-24500: CAG GAC AAC GCC CAC ACA

Rosa-24951: AGG GCG AGG AGC TGT TCA

Rosa-24952: TGA AGT CGA TGC CCT TCA G

For $Smo^{Flox/Flox}$

oIMR1834: CCA CTG CGA GCC TTT GCG CTA C

oIMR1835: CCC ATC ACC TCC GCG TCG CA

oIMR6916: CTT GGG TGG AGA GGC TAT TC

oIMR6917: AGG TGA GAT GAC AGG AGA TC

For $Shh^{Flox/Flox}$

25035: CAG AGA GCA TTG TGG AAT GG

25036: CAG ACC CTT CTG CTC ATG G

PCR protocol:

94ºC for 3 min (1 cycle)

94ºC for 45 sec

60ºC for 45 sec

72ºC for 45 sec (35 cycles)

Finally, an extension for 7 min at 72ºC (1 cycle) and 4ºC (hold). Agarose electrophoresis was used to visualize PCR products.

To collect embryos at E15.5 and E18.5 we sacrificed timed pregnant females with CO_2. Fetuses were extracted by cesarean section. E15.5 embryos were placed into cold 1x PBS to dissect the brain, then, the brains were transferred to PFA 4% for 4hr at 4ºC. For E18.5 the pups were perfused

with a syringe, using first 1ml of cold PBS and after that, 3 ml of PFA 4%. Dissected brains were transferred into PFA 4% for 1hr at 4ºC.

All brains were section by cryostat in 5 sets of 16 μm, so were cryoprotected in 30% sucrose in PBS until they sink and then embedded in OCT compound and stored at -80ºC.

For postnatal and posterior stages, animals were perfused with paraformaldehyde (PFA) 4% and the dissected brains were postfixed with PFA 4% for 2 hr at 4ºC. Tissues were cryoprotected in 30% sucrose, embedded in OCT, and then kept at -80ºC for long-term storage. Perinatal tissues were sectioned at 20 μm and P7 tissues at 16 μm for X-gal staining. For immunohistochemistry, brain sections made on a cryostat at 12 μm were directly collected on slides for perinatal tissues or cut at 30 μm for P15 or older tissues as floating sections in 1x PBS and mounted onto slides after staining.

5. X-gal staining

X-gal staining was developed at 37ºC overnight in the staining solution (5 mM $K_3Fe(CN)_6$, 5 mM $K_4Fe(CN)_6$, 5 mM EGTA, 0.01% deoxycholate, 0.02% NP40, 2 mM $MgCl_2$, and 1 mg/ml X-gal). Sections were postfixed with 10% formalin at room temperature overnight. Slides were then counterstained with nuclear-fast red (H-3403, Vector Laboratories) at room temperature for 10 min before proceeding for dehydration (70%, 95%, 100% ethanol, xylene twice) and cover-slipped with Mount-Quick (Ted Pella).

6. Immunohistochemistry

Cryostat sections were air-dried and rinsed 3 times in 0.1M PBS plus 0.3% Triton before blocking for 1 hour in 10% normal lamb serum diluted in 0.1M PBS with 0.3% Triton to prevent non-specific binding. When DAB staining is needed, sections were incubated in a solution of 3% hydrogen peroxide in PBS for 30 m before blocking. Primary antibodies were diluted in

the same blocking solution and sections were incubated in primary antibody overnight at 4°C. The primary antibodies were as follows: rabbit anti-Prox1 (1:1000); rat anti-Ctip2 (1:1000; Abcam); rabbit anti-Ki67 (1:250; Neomarker); chicken anti GFP (1:500; Aves Lab); rat anti-GFP (1:1000; Nacalai Tesque), rabbit anti-GFAP (1:500; Dako); rat anti-GFAP (1:200; Termofisher) rabbit anti-Phospho-Histone 3 (1:500; Upstate); rabbit anti-Blbp (1:1000; Chemicon); rabbit anti-Tbr2 (1:1000; gift from Dr. R. Hevner, University of Washington); Rabbit anti-Laminin (1:500; Sigma-Aldrich); rabbit anti-Calretinin (1:1000; Chemicon); rabbit anti-Otp (1:1000; gift from Dr. F. Vaccarino, Yale University); guinea pig anti-Sox10 (1:1000; gift from Dr. M. Wegner, Institut für Biochemie); rabbit anti-Olig2 (1:1000; gift from Dr. D. Rowitch, UCSF), rabbit anti-Dcx (1:500; Abcam); rabbit anti-Sox2 (1:1000; Epitomics); and rabbit anti-DsRed (1:500; Clontech).

Primary antibodies were detected using Alexa Fluor-conjugated secondary antibodies (1:500, Invitrogen) in the same blocking buffer for 2h at room temperature and counter stained with DAPI for 0.5h and then washed with PBS and cover slipped with gel mount (Sigma). For DAB biotinylated secondary antibody were used, then rinsed with 0.1M PBS for 3 times and incubated for 1hr in ABC complex (Avidin-Biontin-Peroxidase, Vector Labs) that were prepared in advance. To develop brown color, 0.05 % 3,3'-diaminobezidine (DAB) with 0.01 % hydrogen peroxide in PBS were used. Finally, the tissue was dehydrated as in X-gal staining.

7. Environment Enrichment

For environment enrichment, six to ten mice were housed in the One Cage 2100 system, which is almost triple the size of the regular cage. The cages were also equipped with igloos, tunnels, running wheels, and various toys.

8. Microscope

Images were acquired using a Nikon E600 microscope equipped with a cooled charge-coupled device camera (QCapture Pro; QImaging). Fluorescent photographs were taken using a Zeiss LSM 510 and 710 confocal microscopes. For confocal image analysis, each fluorophore were scanned sequentially and Z-stacks of the images obtain were collapsed into a single projection image or presented as individual optical sections.

9. Statistical analysis

All statistical analyses were done with SPSS15 software. The statistical significance of single comparison on discrete data was performed using the nonparametric Chi-square's test. For continuous data the statistical significance of single comparisons was performed using two-tailed t-test with Welch's correction when required (non-equal variances) or Mann-Whitney nonparametric test when data did not fit to a normal distribution (assessed by Shapiro-Wilk normality test). For multiple comparisons we used ANOVA with a Tukey HSD posthoc to determine the significance between groups after checking our data fitted to a normal distribution (assessed by Shapiro-Wilk normality test) and the variance was equal (determined by Levene's test).

RESULTS

CHAPTER 1

10. The Ventral Hippocampus Is the Embryonic Origin for Adult Neural Stem Cells in the Dentate Gyrus

Guangnan Li, Li Fang, Gloria Fernández, and Samuel J. Pleasure

10.1. Hh-responsive cells are concentrated in the ventral hippocampal neuroepithelium during late gestation

Previous studies reported that during the last week of gestation in rodents, a migratory stream from the dentate neuroepithelium adjacent to the cortical hem courses through the fimbrio-dentate junction (FDJ) and either assumes a subpial route or fans out into the hilus (Altman and Bayer, 1990a; Li et al., 2009). Prospective NSCs destined for the SGZ are believed to derive from this migratory stream (Altman and Bayer, 1990a) or directly translocate from the dentate primordium (Eckenhoff and Rakic, 1984). Taking into consideration the findings that NSCs responding to Hh can be labeled during late gestation (Ahn and Joyner, 2005; Li et al., 2009) and that Hh-signaling is required to establish SGZ progenitors (Han et al., 2008; Machold et al., 2003), we reasoned that upon perceiving Hh in the dentate VZ or along the migratory stream, precursors are induced or specified to become dentate NSCs. To test this hypothesis, we decided to begin with the Hh-responding line Gli1^{nLacZ} (Bai et al., 2002) to study the static distribution of Hh-responding cells at the perinatal ages when the prospective SGZ NSCs can be traced by the tamoxifen inducible line Gli1^{CreERT2} (Ahn and Joyner, 2005; Li et al., 2009).

The rodent hippocampus is situated at the medio-temporal edge of the neocortex and straddles the thalamus along its septo-temporal axis. Dorsal to the thalamus is the dorsal hippocampus whereas ventral to the thalamus is the ventral hippocampus. Sagittal sections at different medio-lateral levels (shown as schemas in Figure 1A and 1E) allow us to comprehensively examine the distribution of Gli1^{nLacZ+} cells throughout the developing hippocampus including both the dorsal and ventral arms.

To our surprise, at E17.5 Gli1^{nLacZ+} cells were basically absent from the dorsal dentate primordium (arrowheads in Figure 1B', C'). By contrast, *Gli1nLacZ* expression occupied the whole VZ of the ventral hippocampus at the far end of the temporal pole (arrowhead in Figure 1B"), about half at the mid-level (arrowhead in Figure 1C"), but only about one-third at the transitional level (arrowhead in Figure 1D'). At the most temporal level,

Gli1nLacZ+ cells were noticeably distributed from VZ to the forming DG (arrow in Figure 1B").

Figure 1: Perinatal distribution of *Gli1nLacZ* Hh-responding cells in the hippocampus (**A**) Schemas of *Gli1nLacZ* distribution at E17.5 were shown at the three levels of the sagittal sections. (**B-D**) From medial to lateral, three levels of sagittal sections for *Gli1nLacZ* staining at E17.5 were shown. At E17.5, *Gli1nLacZ* expression occupied the whole ventricular zone (VZ) of the ventral hippocampus at the far end of the temporal pole (**B"** arrowhead), half at the mid-level (**C"** arrowhead), but only one-third at the transitional level (**D'** arrowhead). A stream of Gli1-nLacZ+ cells from VZ to the dentate pole were noticeable at the end of the temporal pole (**B"** arrow). *Gli1nLacZ+* cells were clearly absent in the dorsal dentate primordium (**B', C'** arrowheads). (**E**) Schemas of *Gli1nLacZ* distribution at P0 were shown at the three levels of the sagittal sections. (**F-H**) From medial to lateral, three levels of sagittal sections for *Gli1nLacZ* staining at P0 were shown. At P0, *Gli1nLacZ* expression covered the whole VZ of the ventral hippocampus at all levels (**F"**, **G"** and **H'** arrowheads). By contrast, *Gli1nLacZ* remained absent from the

dentate primordium in the dorsal hippocampus (**F'** and **G**' arrowheads). At the transitional level, *Gli1nLacZ+* cells spread from ventral to dorsal (**H'** arrows). Sparse *Gli1nLacZ+* cells were also detected in the dorsal DG displaying a gradient with the lowest in the septal pole (**F', G'** and **H'** arrows).

By P0, *Gli1nLacZ* remained absent from the dorsal dentate primordium (arrowheads in Figure 1F', G'), and only sparse *Gli1nLacZ* + cells were detectable in the dorsal DG (arrows in Figure 1F' and G'). However, *Gli1nLacZ* expression now covered the whole VZ of the ventral hippocampus at all levels (arrowheads in Figure 1F", G" and H'). *Gli1nLacZ+* cells were observed in the ventral forming DG at the more lateral/septal level (arrows in Figure 1G"). At the transitional level, *Gli1nLacZ+* cells were distributed from the ventral to the dorsal arm around the fimbria (arrows in Figure 1H'). The perinatal distribution of Hh-responding cells in the hippocampus prompted us to investigate whether the descendants of these perinatal Hh-responding cells, when most of them are still restricted in the ventral hippocampus by birth, give rise to the NSCs that settle in the SGZ at all septo-temporal levels.

10.2. Postnatal fate-mapping analysis of cells responding to Hh at prenatal and perinatal ages

In our previous study, we showed that some derivatives of the Hh-responding cells labeled at E17.5 constituted the postnatal radial glia in the SGZ of the DG (Li et al., 2009). In light of our new finding that *Gli1nLacZ+* cells mostly populated the VZ of the ventral hippocampus at this age, we wished to know how these cells contribute to the dentate gyrus at all septo-temporal levels. To address these questions, we turned to fate mapping analysis using the *Gli1^{CreERT2}* line (Ahn and Joyner, 2004) crossed to the *Cre* reporter line Ai14 (Rosa-CAG-LSL-tdTomato-WPRE) (Madisen et al., 2010). After independent tamoxifen injections at E15.5, E17.5 or P0, the distribution of recombined cells was examined at P15 (Figure 2A-I). If the recombined cells generate the NSCs eventually located in the SGZ, we expected that

radial NSCs and clusters of granule cells (the progeny of the NSCs) would be labeled by tdTomato (tdT) expression by this age.
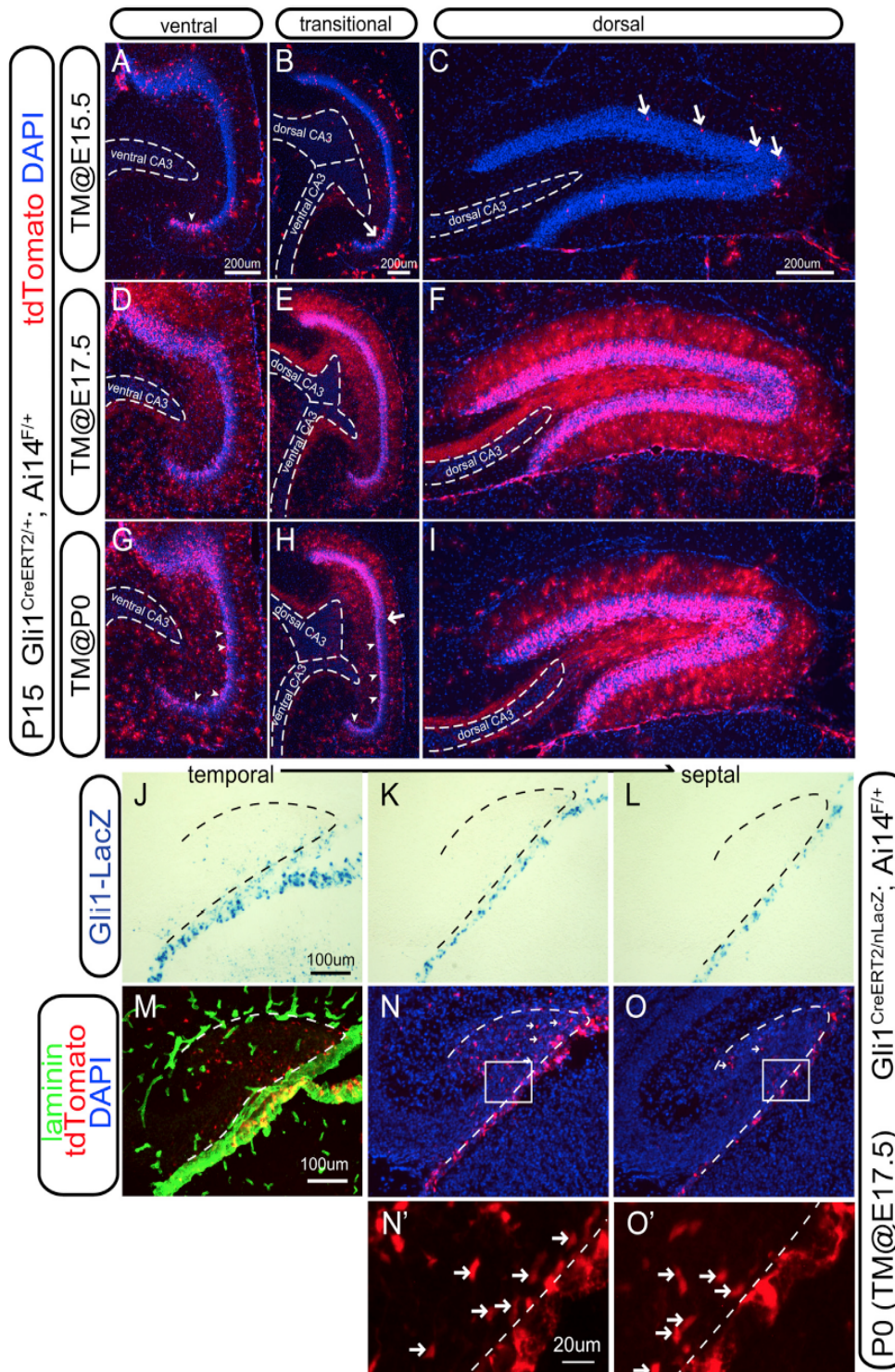
**Figure 2: Fate-mapping analysis of Hh-responding cells by *Gli1^{CreERT2}*
with prenatal or perinatal tamoxifen injections:** (**A**-**I**) The distribution of tdT+
cells in the dentate gyrus was examined at P15 in mice carrying both *Gli1^{CreERT2}*
and *Cre* reporter Ai14 after tamoxifen (TM) injection at E15.5 (**A-C**), E17.5 (**D-F**)
and P0 (**G-I**), of which the ventral (**A, D, G**), transitional (**B, E, H**) and dorsal (**C, F,
I**) aspects were shown respectively. (**J-O**) Mice carrying *Gli1^{CreERT2}*, *Gli1nLacZ* and
Ai14 were analyzed at P0 after tamoxifen injection at E17.5. At P0, the
representative sagittal sections of the dorsal DG from temporal (**J**) to septal (**I**)
levels were shown for *Gli1nLacZ* distribution. In the meantime, the distributions of
tdT+ cells representing the progeny of the recombined cells were shown with the
next sections corresponding to (**J-K**). The complete set of the alternative sections
for the *Gli1nLacZ* and tdT+ cells were shown in the **Figure S1**. Basement
membrane of the meninges and blood vessels were labeled by Laminin expression
(**M**). Of note, tdT+ cells were detectable at the septal level (arrows in **n** and **o**)
where *Gli1nLacZ* expression was absent in the dentate field (**K** and **L**). Boxed
areas in **Figure 2N** and **Figure 2O** were shown at the higher magnification in
Figure 2N' and **Figure 2O'**, the arrows in which highlighted the presence of tdT+
cells at the entrance of the hilus.

When tamoxifen was injected at E15.5, a small number of tdT+ clusters
were found in the suprapyramidal blade of the ventral DG (arrowhead in
Figure 2A), whereas very few isolated tdT+ cells were seen in the transitional
ventral DG (arrow in Figure 2B) and in the dorsal DG (arrows in Figure 2C).
When tamoxifen was injected at E17.5, tdT+ clusters were found in the DG at
all the septo-temporal levels (Figure 2D-F). At the current dosage of tamoxifen
(3mg/40g animal), 69±4% of the Blbp+ cells displaying radial orientation in the
SGZ were also tdT+ at P15 (Figure S1B, B' and c), whereas 61±6% of the
Sox2+ cells were also tdT+ (Figure S1A, A' and c). The pattern of tdT+
clusters labeled at E15.5 showed minimal overlap with those labeled at E17.5,
indicating that the effect of tamoxifen was transient and diminished by 48hrs.
When tamoxifen was injected at P0, tdT+ clusters were found in the inner
aspect of the GCL in the ventral DG (arrowheads in Figure 2G-H, the arrow in
Figure 2H indicated the boundary between ventral and dorsal DG).
Meanwhile, tdT+ clusters continued to heavily make up the dorsal DG at all
levels (Figure 2I). Therefore, the Hh-responding cells in the ventral
hippocampus start to make a large contribution to the ventral DG around
E15.5 and to the dorsal DG around E17.5.

10.3. Progeny of Hh-responding cells from the temporal pole arrive in the dentate septal pole ahead of the appearance of local Hh-responding cells

Static analysis showed that *Gli1nLacZ*+ cells were initially concentrated in the ventral hippocampus and then later appeared in the developing DG in a temporal (high)-to-septal (low) gradient. We define these two populations as early Hh-responding cells in the VZ of ventral hippocampus, and late Hh-responding cells in the local DG, respectively. The expression of *Gli1nLacZ* in the late Hh-responding cells might be due either to the retention of the LacZ protein after they leave their origin or to actively responding to local Shh after they reach the forming DG. We wished to determine the spatial relationship of the progeny of early Hh-responding cells relative to the late Hh-responding cells in the developing DG at birth. To address this, we examined the progeny of the Hh-responding cells marked by tamoxifen injection at E17.5 after crossing the *Gli1^{CreERT2}* line with Ai14 in the mice also carrying *Gli1nLacZ* to identify late Hh-responding cells at the same time points and anatomic levels. At P0, we examined the expression of both tdT and LacZ using alternate sagittal sections covering all septo-temporal dentate levels (the complete data set is in Figure S1D). X-gal staining rather than antibody staining was used to maximize the detection sensitivity for LacZ. Interestingly, at more temporal levels, tdT+ cells (Figure 2M) had a wider distribution than *Gli1nLacZ*+ cells (Figure 2J). At more septal levels, tdT+ cells were still present (arrows in Figure 2N, 2N', 2O, 2O'), whereas nLacZ+ cells were scarce (Figure 2K) or completely absent (Figure 2L) from the dentate plate, despite the presence of nLacZ+ cells in the meninges labeled by Laminin (presumed to be meningeal fibroblasts) (Figure 2M). These results demonstrated that progeny marked at E17.5 with the Gli1-CreERT2 line can reach more septal levels before late Hh-responding cells are established locally at the same septo-temporal levels in the developing DG.

10.4. The descendants of the Hh-responding cells from the ventral hippocampal VZ display a continuous stream into the dorsal DG.
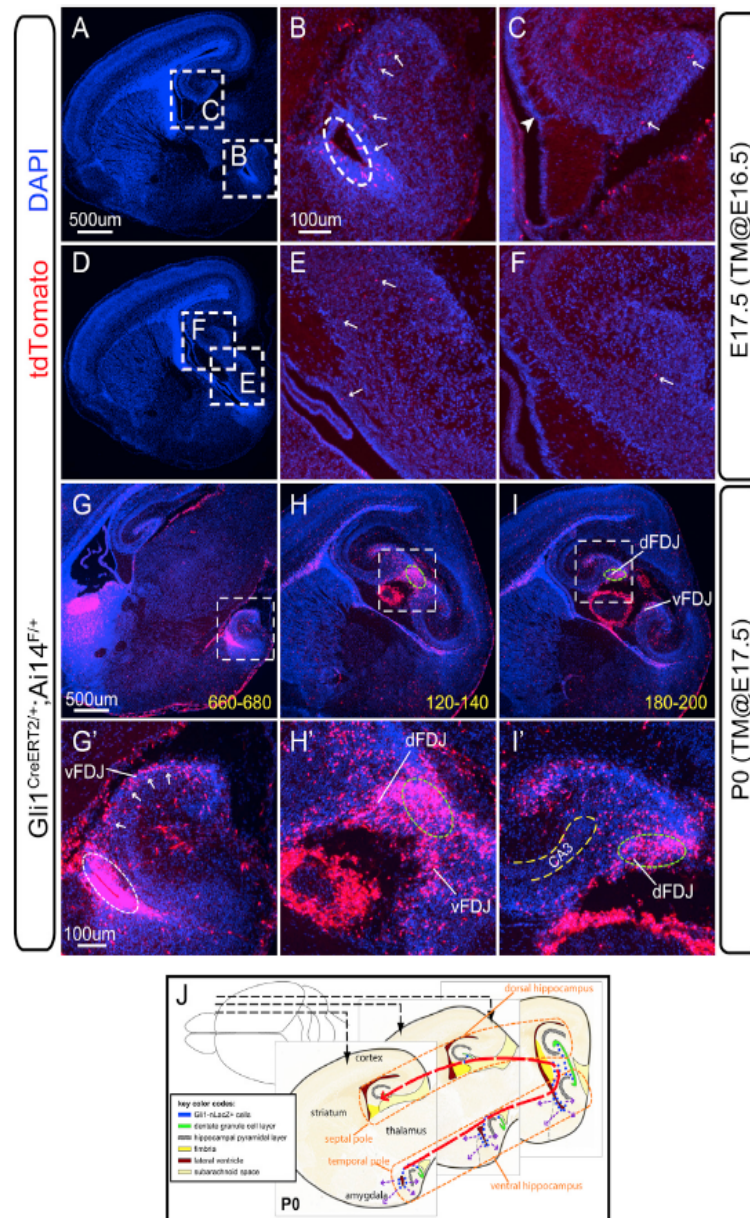
Figure 3: The short-term distribution for the progeny of Hh-responding cells derived from the ventral hippocampus (**A-F**) The distribution of tdT+ cells in the Gli1$^{CreERT2/+}$;Ai14$^{F/+}$ animals were shown one day after tamoxifen (TM) induction at E16.5. The two representative sagittal levels (**A and D**) were used for analysis. Boxed areas were shown at the higher magnification in **B, C, E and F**. From the temporal pole to the septal pole, the tdT+ cells (arrows in **B, E, F and C**) displayed a gradient distribution. **(G-I)** The distribution of tdT+ cells in the Gli1$^{CreERT2/+}$;Ai14$^{F/+}$

animals were shown two day after tamoxifen (TM) induction at E17.5. The three representative sagittal sections were chosen to highlight the main features of the tdT+ cells from the newborns (P0), whereas a series of sections from every 60μm were shown in the **Figure S2**. The progeny of Hh-responding cells were identified by tdT expression. Throughout the whole hippocampus, the VZ of the temporal hippocampus was the most heavily labeled by tdT (white oval in **G'**). There was a remarkable cell stream in the vFDJ regions (arrows in **G'**). The tdT+ cells were continuous from the vFDJ into the dFDJ at the transitional level (green oval in **H** and **H'**) and tapered off in the dorsal hippocampus toward the septal pole (green oval in **I** and **I'**). The thickness distance as micron from the first section (in the **Figure S2**.) was shown at the bottom-right corners in **G, H and I**. dFDJ, dorsal fimbrio-dentate junction; vFDJ, ventral fimbrio-dentate junction. **(J)** The schema shows the temporal-to-septal distribution (red arrow) of the progeny of the Hh-responding cells originated from the VZ of the ventral hippocampus at the perinatal age. In addition, the VZ of the amygdalo-hippocampal region also gives rise to other cells in different directions (purple arrows).

The above data inspired us to determine the spatial connection between the progeny of the Hh-responding cells and the ventral hippocampal VZ. To do this, we initially analyzed the distribution of tdT+ cells one day after tamoxifen induction at E16.5 (Figure 3A-F). We confirmed that heavy recombination indeed occurred in the VZ of temporal hippocampus (oval in Figure 3B) but was completely absent from the VZ of the dorsal dentate (arrowhead in Figure 3C). From temporal to septal hippocampus (arrows in Figure 3B-E-F-C), the gradient distribution of tdT+ closely mimicked the pattern of *Gli1nLacZ*+ cells at the similar age (Figure 1B-C).

Then we analyzed the representative sagittal levels (Figure 3G-I) and the serial sagittal sections (Figure S2) for the distribution of tdT+ cells at P0 with tamoxifen induction at E17.5. The tdT+ cells formed a continuous stream (arrows in Figure 3G') from the VZ at the temporal pole of the ventral hippocampus (white oval in Figure 3G') to the forming ventral dentate GCL, which showed close apposition to the meninges at the ventral fimbrio-dentate junction (vFDJ) (Figure 3G, G'). Of note, the tdT+ cells seen in the mantle of the amygdalo-hippocampal region could have arisen from the amygdalo-hippocampal VZ (oval in Figure 3G'). At the medio-lateral level where the dorsal and ventral dentate gyri joined each other (green oval in Figure 3H, H'), a large number of tdT+ cells were apparent. The higher cell density in this

region probably indicated ongoing local proliferation. In the dorsal hippocampus, most tdT+ cells localized in the dorsal fimbrio-dentate junction (dFDJ) (green oval in Figure 3I, I'), and some of them were distributed further into the hilus at the same longitudinal levels (Figure 3I'). The presence of the tdT+ cells near the upper blade indicated there might be *de novo* induction of Hh-responding cells (Figure 3I'). Quite strikingly, the tdT+ cells at the dFDJ had little connection to the dorsal dentate neuroepithelium at any levels and this cell population likely represented the "intrinsic component" first described by Altman et al. (Altman and Bayer, 1990a). All these data taken together reinforce our new model (Figure 3J) that the progeny of the Hh-responding cells from the ventral hippocampus VZ feed into the dentate gyrus during late gestation in the temporo-septal direction (red arrow in Figure 3J), initially staying in the vFDJ/dFDJ close to the meninges and then radiating into the hilus before the SGZ forms.

10.5. Hh-responding cells in the hippocampus of Hh signaling mutants

What is the anatomic Shh source for the Hh-responding cells in the VZ of the ventral hippocampus? Previous studies suggested that Shh from the subpallial septum might regulate NSCs in the adult DG through the long-range axonal targeting via the septo-hippocampal pathway (Lai et al., 2003). However, it is not clear whether Shh from the septum would regulate the developing DG, particularly at these ages when the septo-hippocampal projection is not yet fully developed (Super and Soriano, 1994). In order to pinpoint the Hh-producing cells that interact with the dentate precursors, we compared the distribution of the Hh-responding cells around birth between $Emx1^{Cre}Shh^{F/F}$ and $Emx1^{Cre}Smo^{F/F}$ conditional mutants. If other Hh members (Dhh or Ihh) within the *Emx1* domain or Hh sources (Shh or other members) outside the *Emx1* domain (essentially the dorsal forebrain) were required for the development of the DG, Hh-responding cells would be expected to be unaffected in the $Emx1^{Cre}Shh$ cKO.

67
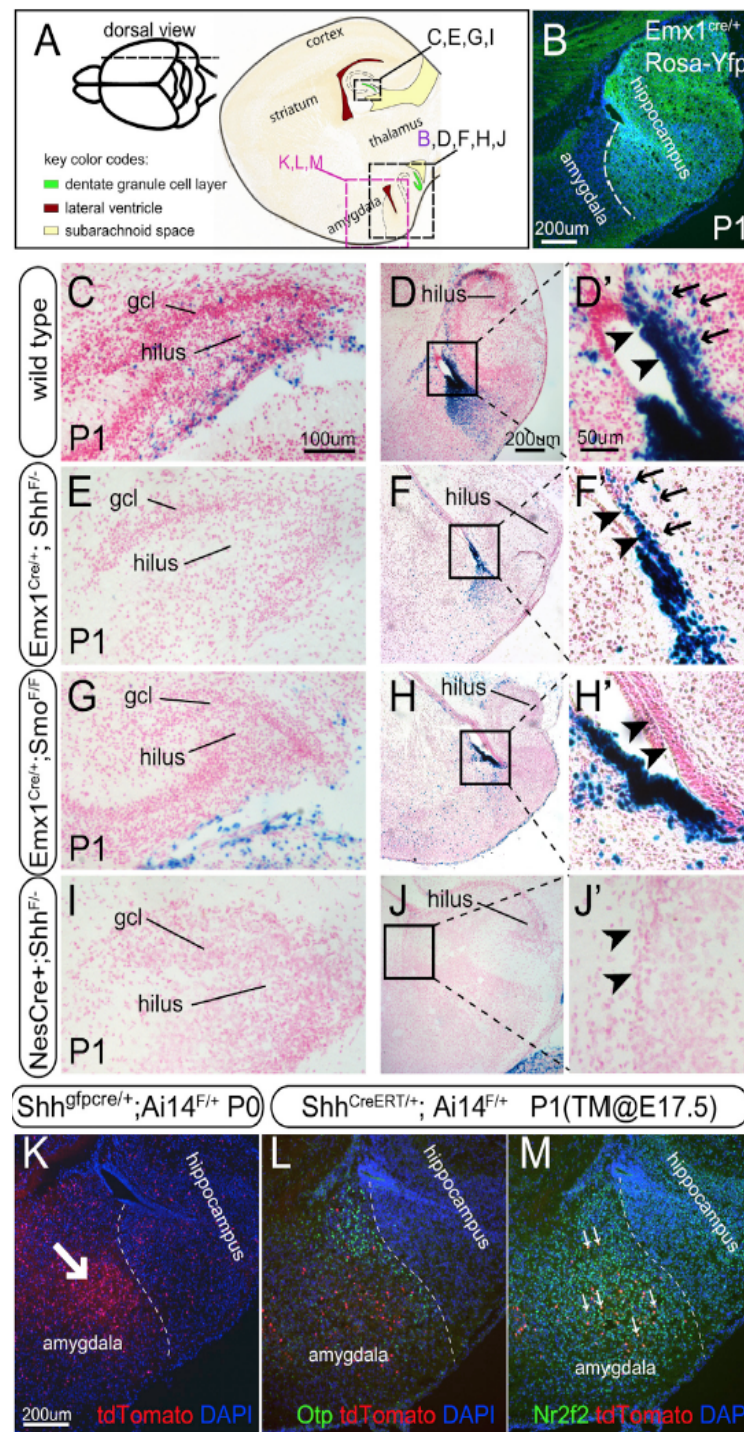
Figure 4: Perinatal distribution of *Gli1nLacZ* in various *Shh* signaling conditional mutants. (**A**) The schemas are illustrated for the sagittal sections from the P1 animals shown in **B**-**M**. (**B**) With the cre reporter *RosaYfp*, *Emx1Cre* showed recombination in the ventral hippocampus. (**C**, **D** and **D'**) In the control, *Gli1*nLacZ+ cells were detected in the hilus of both dorsal (**C**) and ventral (**D**) DG, and particularly in the VZ of the ventral hippocampus (arrowheads in **D'**). *Gli1nLacZ+* cells were obvious in the region away from the VZ (arrows in **D'**). (**E**, **F** and **F'**) In the *Emx1-Shh* conditional knockout, *Gli1nLacZ+* cells were absent from the hilus of both dorsal and ventral DG (**E**, **F**) but still present in the

VZ of the ventral hippocampus (**F'**). *Gli1nLacZ+* cells were still evident in the region away from the VZ (arrows in **F'**). (**G**, **H** and **H'**) In the *Emx1-Smo* conditional knockout, *Gli1nLacZ+* cells were absent in the dorsal (**G**) and ventral hippocampus (**H** and arrowheads in **H'**) without affecting their distribution in the VZ of the amygdala (**H**, **H'**). (**I**, **J** and **J'**) In the *Nes^{Cre}-Shh* conditional knockout, *Gli1nLacZ* activity was completely abolished in the hippocampus and the VZ of the amygdalo-hippocampal region. (**K**-**M**) A domain of *Shh*-producing cells was located in the amygdala. At P0, cumulative fate-mapping with the *Shh^{GfpCre}* and *Ai14* lines showed a tdT+ domain in the amygdala (arrow in **K**). The fate-mapping analysis with *Shh^{CreERT2}* and *Ai14* upon tamoxifen injection at E17.5, showed a subset of tdT+ cells at P1 in the amygdala as in (**K**). They were co-labeled with Nr2f2 (arrows in **M**) but not overlapped with the Otp+ cells (**L**).

By crossing *Emx1^{Cre}* to the cre reporter *Rosa^{Yfp}*, we confirmed that at P1 Emx1^{Cre} showed recombination in the ventral hippocampus (Figure 4B), including its VZ (Figure S3B and B'). By P1, *Gli1nLacZ+* cells were found in the dorsal DG of the wild type control (Figure 4C) but mostly absent from the *Emx1;Shh* cKO at the same anatomical level (Figure 4E). When one copy of the *Gli1nLacZ* was present, *Gli1nLacZ+* cells were completely abolished throughout the DG along the whole longitudinal axis in both Emx1-Shh and *Emx1;Smo* cKOs (Figure 4E, F, G and H). However, the *Gli1nLacZ+* cells in the VZ of the ventral hippocampus were entirely missing only in *Emx1-Smo* mutants (arrowheads in Figure 4H') not *Emx1-Shh* mutants (arrowheads in Figure 4F'), even though they were not as abundant as in the control (arrowheads in Figure 4D'). In the Emx1-Shh cKO, *Gli1nLacZ+* cells (likely due to the slow turnover of nLacZ) were also detected in a region slightly away from the VZ of the ventral hippocampus (arrows in Figure 4F'), as in the control (arrows in Figure 4D').

It has been reported that *Gli1nLacZ* expression is affected by the functional copy number of Shh (Garcia et al., 2010). We reasoned that different copy numbers of Shh and *Gli1nLacZ* would give us further insights into the formation of *Gli1nLacZ+* cell stream from the VZ of the ventral hippocampus and the *de novo* induction of Hh-responding cells in the forming DG. To facilitate the analysis, the developing dorsal dentate can be divided into upper and lower portions by a line connecting the tip of the CA3 field and the apex of the dentate pole. In relation to the Gli1$^{Z/+}$;Shh$^{F/F}$ animals (Figure

S3D, D', E, E'), when one copy of the Shh flox allele was replaced with a Shh null allele in the Gli1$^{Z/+}$;Shh$^{F/-}$ animals, the number of *Gli1nLacZ+* cells in the dorsal dentate was dramatically reduced in both portions (Figure S3F, F'), the *Gli1nLacZ* expression showed a decreased level in the VZ of the ventral hippocampus and the stream of the *Gli1nLacZ+* cells emanating from the VZ was also reduced (Figure S3G, G'). Interestingly, all of these phenotypes could be restored in the Gli1$^{Z/Z}$;Shh$^{F/-}$ animals when an extra copy of *Gli1nLacZ* was present (Figure S3H, H', I and I'). However, when the remaining Shh flox allele was floxed out in the *Emx1* domain in the *Emx1$^{cre/+}$;Gli1$^{Z/Z}$;Shh$^{F/-}$* animals, most of the *Gli1nLacZ+* cells were abolished in the upper portion of the dorsal dentate whereas residual *Gli1nLacZ+* cells were still present at the entrance of the hilus in the lower portion (Figure S3J, j'), which appeared to be continuous with the *Gli1nLacZ+* cell stream from the VZ of the ventral hippocampus (Figure S3K, K'). The *Gli1nLacZ* distribution pattern in the *Emx1$^{cre/+}$;Gli1$^{Z/Z}$;Shh$^{F/-}$* animals was phenocopied in the *Neurod6$^{cre/+}$;Gli1$^{Z/+}$;Shh$^{F/F}$* animals when two copies of the Shh floxed allele were removed from the pallial neuronal lineage (Goebbels et al., 2006) (Figure S3L, L', M and M') but not the ventral hippocampal VZ (Figure S3C, C'). Therefore, Shh from the neuronal cells within the *Emx1* domain contributes to the *de novo* Hh-responding activity seen locally in the DG, whereas *Hh* from outside the *Emx1* domain is responsible for the Hh-responding activity in the VZ of the ventral hippocampus in the *Emx1$^{cre/+}$;Gli1$^{Z/Z}$;Shh$^{F/-}$* animals.

This somewhat unexpected finding led us to ask whether Shh was the only Hh family member responsible for the Hh-responding activity in the amygdalo-hippocampal region. We used the CNS-specific cre (*Nes^{Cre}*) to conditionally remove *Shh*. The *Nes^{Cre};Shh* conditional mutants showed complete absence of Hh-responding cells in both DG (Figure 4I) and the VZ of the ventral hippocampus (Figure 4J, J'). The CA fields in the ventral hippocampus also showed a distorted appearance due to the development of hydrocephalus and/or patterning defects in the *Nes^{Cre};Shh* conditional mutant (Figure 4J and data not shown). Therefore, we conclude that Shh is the sole

ligand required for Hh-responding cells in the ventral hippocampus but that Shh is produced by both a local source for the forming DG and an extracortical source for the VZ of the ventral hippocampus.

Crossing Shh^{GfpCre} mice with Ai14 allowed cumulative fate mapping for Shh expressing cells revealing that a domain of tdT+ cells was localized within the amygdala, close to the ventral hippocampus (arrow in Figure 4K). By crossing the tamoxifen inducible $Shh^{CreERT2}$ line with Ai14, a subset of tdT+ were found in the same amygdalar domain when the expression was examined at P1 after tamoxifen injection at E17.5 (Figure 4L), suggesting that amygdalar *Shh* was actively expressed at E17.5. This is in line with the Shh mRNA expression pattern in the Allen Brain Atlas Database (http://developingmouse.brain-map.org/data/search/gene/index.html?term=shh). These tdT+ cells coexpressed the transcription factor Nr2f2 (displaying high level of expression in the amygdala) (arrows in Figure 4M), but were excluded from the Otp domain (Figure 4L). The timing and location of the *Shh* expression in the amygdala suggested that it is a likely *Shh* source regulating the Hh-responding cells in the ventral hippocampus.

10.6. Shh signaling conditional mutants support a complex anatomical origin for dentate stem cells

The analysis above showed that all the Hh-responding activity was abolished in both the hilar region and the VZ of the ventral hippocampus in the *Emx1;Smo* cKOs, whereas in the *Emx1;Shh* cKOs Hh-responding activity was eliminated only in the hilar region but was still present in the VZ of the ventral hippocampus. We wished to further examine the migratory streams of the developing DG in the *Emx1;Shh* cKOs and *Emx1;Smo* cKOs with the generic proliferation marker Ki67 (Figure 5A-G) and neurogenic precursor marker Tbr2 (Figure 5H-N).
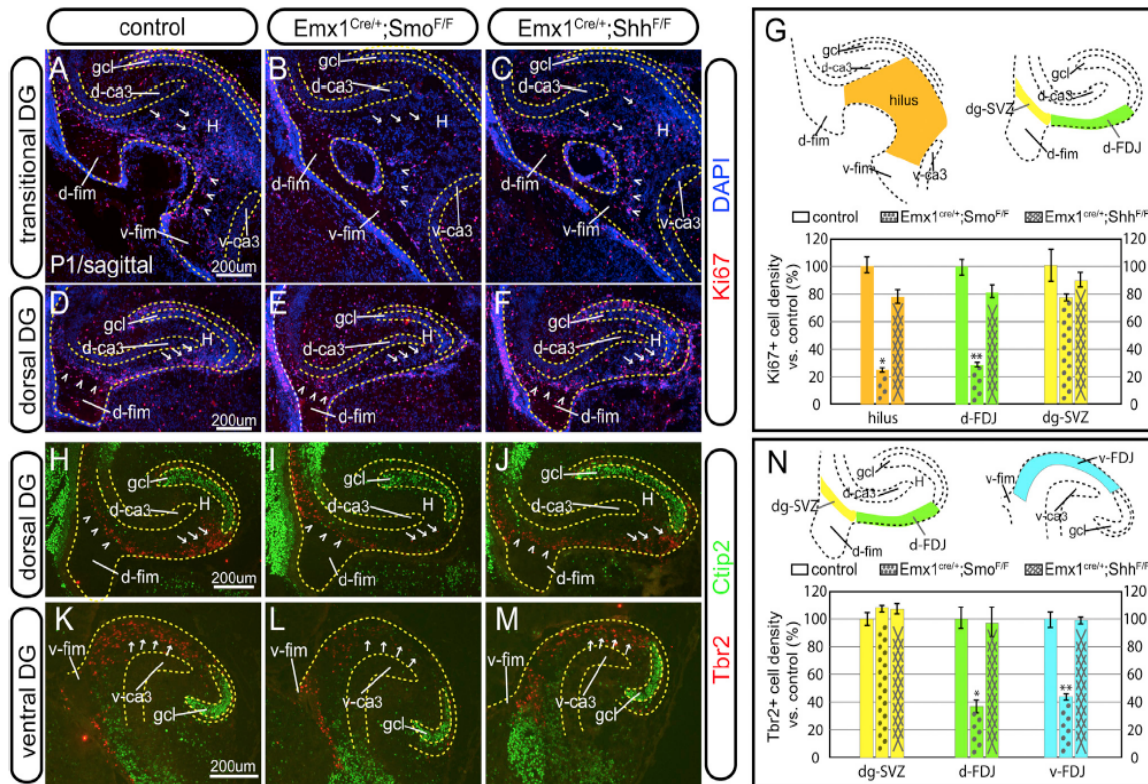
Figure 5: The dentate migratory streams in the Shh signaling conditional mutants. (**A-F**) Ki67+ proliferative cells at P1 were shown at the transitional level (**A**-**C**) and in the dorsal DG (**D**-**F**) for the control (**A**, **D**), *Emx1;Smo* cKO (**B**, **E**) and *Emx1;Shh* cKO (**C**, **F**), respectively. Compared to the control, Ki67+ proliferating cells in both the hilar region (arrows in **A**-**C**) and the hilar entrance from the ventral hippocampus (arrowheads in **A**-**C**) were severely compromised in the *Emx1;Smo* cKO but only mildly affected in the *Emx1;Shh* cKO. In the dorsal hippocampus, they showed comparative number of Ki67+ cells at the SVZ of the dentate primordium (arrowheads in **D**-**F**). However, compared to the control (arrows in **D**), Ki67+ cells in the dFDJ were greatly diminished in the *Emx1;Smo* cKO (arrows in **E**) but only slightly reduced in the *Emx1;Shh* cKO (arrows in **F**). (**G**) Quantification is shown for the density of Ki67+ cells in various regions from the control, *Emx1;Smo* cKO and *Emx1;Shh* cKO. Compared to the control ($100\pm6\%$ and $100\pm6\%$), the Ki67+ cell densities found in the hilus (orange) and d-FDJ (green) were only $25\pm2\%$ (n=5, $p<0.001$) and $29\pm2\%$ (n=5, $p<0.001$) for the *Emx1;Smo* cKO, whereas they were $78\pm5\%$ (n=5, $p<0.05$) and $81\pm5\%$ (n=5, $p<0.05$) for the *Emx1;Shh* cKO. In the dg-SVZ (yellow), the Ki67+ cell densities in the *Emx1;Smo* cKOs and *Emx1;Shh* cKOs were $77\pm3\%$ (n=5, p= 0.13) and $89\pm6\%$ (n=5, p=0.42) as much as the controls ($100\pm12\%$). **H-M**) Tbr2+ neurogenic cells at P1 were shown in the dorsal DG (**H-J**) and the ventral DG (**K-M**) for the control (**H**, **K**), *Emx1;Smo* cKO (**I**, **L**) and *Emx1;Shh* cKO (**J**, **M**), respectively. Similar to the Ki67 pattern, they showed comparative number of Tbr2+ cells at the SVZ of the dentate primordium (arrowheads in **H**-**J**). However, compared to the control (arrows in **H**), Tbr2+ cells in the dFDJ were greatly diminished in the *Emx1;Smo* cKO (arrows in **I**) but only slightly reduced in the *Emx1;Shh* cKO (arrows in **J**). In relation to the control (arrows in **K**), Tbr2+ cells in the vFDJ were greatly diminished in the *Emx1;Smo* cKO (arrows in **L**) but only slightly reduced in the *Emx1;Shh* cKO (arrows in **M**). (**N**) Quantification is shown

for the density of Tbr2+ cells in various regions from the control, *Emx1;Smo* cKO and *Emx1;Shh* cKO. In the dg-SVZ (yellow), Tbr2+ cell densities were comparable among the three genotypes: 100±5% for the control, 108±3% for the *Emx1;Smo* cKO (n=5, p= 0.39) and 107±4% for *Emx1;Shh* cKO (n=5, p=0.58). However, compared to the control (100±8% and 100±6%), the Tbr2+ cell densities found in the d-FDJ (green) and v-FDJ (cyan) were 37±3% (n=5, p<0.001) and 45±3% (n=5, p<0.001) for the *Emx1;Smo* cKO, whereas they were 97±5% (n=5, p=0.6) and 104±3% (n=5, p=0.14) for the *Emx1;Shh* cKO. Data are shown as mean±SEM and p values for the indicated sample sizes were returned by Student's *t*-test for two-tailed distribution with unequal variance. dg-SVZ, subventricular zone of dentate gyrus; gcl, granule cell layer; d-ca3, dorsal CA3; v-ca3, ventral CA3; H, hilus; d-FDJ, dorsal fimbrio-dentate junction; v-FDJ, ventral fimbrio-dentate junction; d-fim, dorsal fimbria; v-fim, ventral fimbria

The removal of the obligatory Hh co-receptor Smo from the pallial region by *Emx1^{Cre}* resulted in a severe reduction of Ki67+ cell density by 75±2% in the hilar region at the transitional level of the DG (arrows in Figure 5B) in relation to the control (arrows in Figure 5A). However, the removal of Shh by the same cre driver only led to a moderate proliferation decrease by 22±5% (arrows in Figure 5C). Noticeably, compared to the control (arrowheads in Figure 5A), Ki67+ cells at the entrance of hilus from the ventral hippocampus were more affected in the *Emx1;Smo* cKO (arrowheads in Figure 5B) than the *Emx1;Shh* cKO (arrowheads in Figure 5C). Similarly, Ki67+ and Tbr2+ cells in the dorsal FDJ were significantly diminished by 71±2% and 63±3%, respectively, in the *Emx1;Smo* cKO (arrows in Figure 5E, **i**) but only slightly decreased by 19±5% and 3±5%, respectively, in the *Emx1;Shh* cKO (arrows in Figure 5F, J), as compared to the control (arrows in Figure 5D, H). In contrast, the dorsal SVZ of the dentate was minimally affected in both *Emx1;Smo* and *Emx1;Shh* cKOs, as judged by Ki67 and Tbr2 (arrowheads in Figure 5D-F and H-J, respectively). Tbr2+ cells in the migratory stream of the ventral hippocampus were also reduced by 55±3% in the *Emx1;Smo* cKO but had little change (104±3% over the control) in the *Emx1;Shh* cKO (arrows in Figure 5K-M). All these data strengthen the model that progeny of the Hh-responding cells from the VZ of the ventral hippocampus serve as the critical source for the cells migrating into the dorsal DG, and a *Shh* source outside the *Emx1* domain essentially controls the size of this stream whereas the role of local *Shh* source in the DG is dispensable for this process.

10.7. Shh sources for the postnatal dentate gyrus
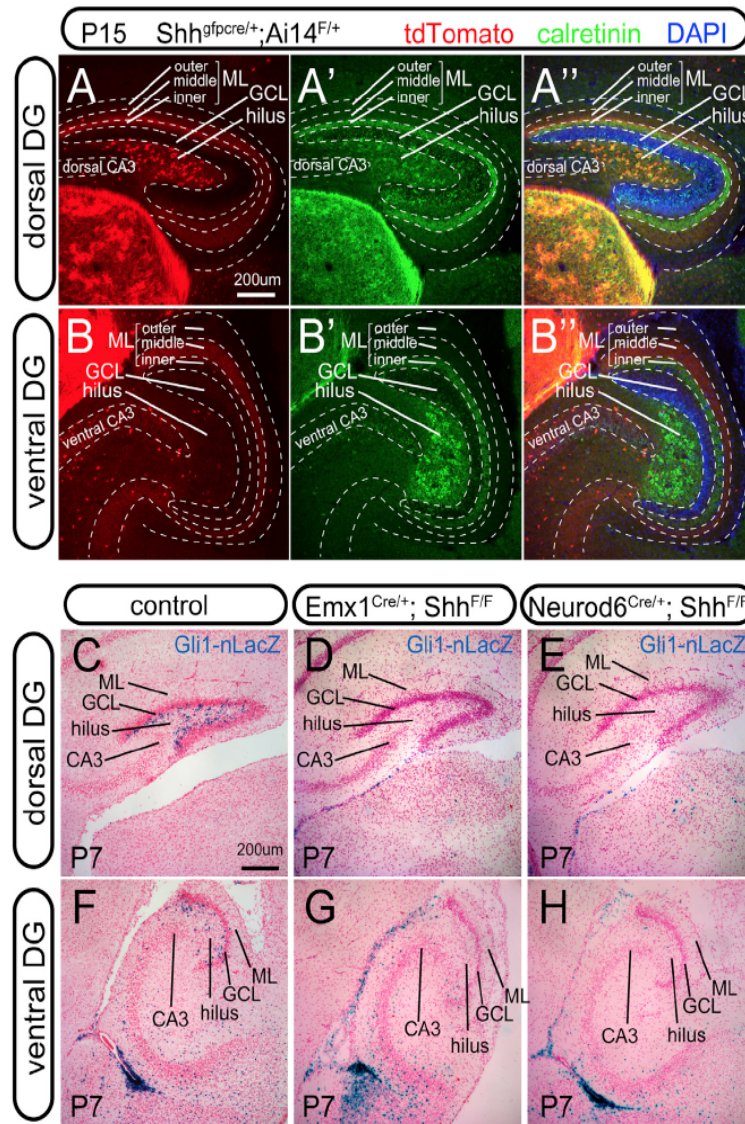
Figure 6: The Shh sources for the postnatal DG. (**A-B**) At P15, cumulative fate-mapping of the Shh producing cells with the Shh^{GfpCre} and Ai14 lines was shown in the dorsal and ventral DG (**a** and **b**, respectively). In the dorsal dentate gyrus, tdT expression was colocalized with hilar mossy cell marker Calretinin (**A'**, **A''**). In the dorsal and ventral dentate gyrus, tdT expression was also detected in the mid-molecular layer (**A''**, **B'**, **B''**) where the neurons of the medial entorhinal cortex project their fibers. (**C-H**) At P7, *Gli1nLacZ+* cells were present in the hilus of both dorsal and ventral DG in the control (**c** and **f**), but completely abolished in the *Emx1;Shh* cKO (**D** and **G**) and *Neurod6;Shh* cKO (**E** and **H**). GCL, granule cell layer; ML, molecular layer; SGZ, subgranular zone.

The cumulative fate mapping analysis with the *Shh^GfpCre* line (Harfe et al., 2004) showed complex dynamics of distribution for the Shh-lineage in the developing DG. Some of the cells derived from the *Shh* lineage were oligodendrocyte progenitors in the prenatal and perinatal DG (Figure S4A-C). However, conditional mutant mice deleting *Shh* from the oligodendrocyte lineage with *Olig2^Cre* (Schuller et al., 2008) had very little alteration to the Hh-responding cells in the DG as examined at P7 (Figure S4D). The Shh-lineage was fate-mapped postnatally to the hilar mossy cells, as defined by Calretinin+ staining in the dorsal DG (Figure 6A, A', A") but not the ventral DG (Figure 6B, B', B"). Mossy cells derived from the Shh lineage projected to the inner molecular layer of the DG (Figure 6A, A"). In addition, neurons in the medial entorhinal cortex (MEC) (Figure S4E-G), which project to the middle molecular layer of the DG (Figure 6A", B"), were also part of the *Shh* lineage.

In order to evaluate the contribution of neuronal (mossy cells and/or MEC) Shh to the Hh-responding activity in the postnatal DG, the distribution of *Gli1nLacZ*+ cells was examined at P7 in the mutant mice in which *Shh* was conditionally removed from the neocortical and hippocampal neurons by Neurod6-cre (Goebbels et al., 2006). Compared to the control (Figure 6C, F), the loss of Hh-responding activity in the hilus of *Neurod6-Shh* cKO (Figure 6E, H) was almost as effective as *Emx1;Shh* cKO (Figure 6D, G). Therefore, the neuronal *Shh* is the key source responsible for the Hh-responding activity locally in the DG.

10.8. The role of the local Shh in SGZ formation and maintenance

Our data favors the new model that ventral hippocampus-derived NSCs contribute to the NSCs in the SGZ. However, if the local Shh plays a critical role in the formation of the SGZ, its absence would result in severe SGZ deficiency. To test this, we looked into SGZ formation at P15 by removing either *Smo* or *Shh* from the hippocampus with *Emx1^Cre* and compared their phenotypes for SGZ formation. In relation to the control

(Figure 7A), there was a complete lack of the radial glia marker Blbp in the SGZ of *Emx1;Smo* cKO (Figure 7A) but only a mild decrease of the Blbp cell density by 28±4% in the SGZ of *Emx1;Shh* cKO (Figure 7C, I) and 18±3% in *Neurod6;Shh* cKO (Figure 7D, I). Consistently, the radial glial scaffolding in the DG, visualized by GFAP staining, was severely affected in the *Emx1;Smo* cKO but relatively intact in the *Emx1;Shh* cKO and *Neurod6;Shh* cKO (Figure S5A-D, A'-D'). In addition, we examined the length of the two blades of the dentate gyrus among these mutants. In comparison with the control, the length of the upper and lower blades were 61±1% and 24±1% in the *Emx1;Smo* cKO, whereas they were 81±5% and 76±3% in the Emx1-Shh cKO, and 102±4% and 98±3% in the *Neurod6;Shh* cKO (Figure S5E). Compared to the complete absence of proliferation in the SGZ of *Emx1;Smo* cKO (Figure 7F, Figure S5G, G'), there was a relatively milder proliferation defect in the *Emx1;Shh* cKOs and *Neurod6;Shh* cKOs as judged by Ki67 (a decease by 35±3% and 27±2%, respectively, (Figure 7G, H, J, in relation to the control) and Tbr2 (a decrease by 60±7% and 38±4%, respectively, (Figure S5F-I, J, in relation to the control). Consequently, the thickness of the GCL was affected among the different genotypes: about 8 cells in the control, 4 cells in *Emx1;Smo* cKO and 6 cells in *Emx1;Shh* cKO or *Neurod6;Shh* cKO (Figure S5F'-I'). The divergent phenotypes in SGZ formation between *Emx1;Smo* and *Emx1;Shh* (or *Neurod6;Shh*) cKOs further validate the model that the Hh-responding cells retained in the ventral hippocampus of the *Emx1;Shh* cKO or *Neurod6;Shh* cKO (but completely absent from the *Emx1;Smo* cKO) are responsible for the initial formation of the SGZ, whereas Shh from the *Emx1* domain is relatively dispensable for this in light of the only slightly compromised SGZ in its absence.

As we showed previously that *de novo* local Hh-responding activity was mostly abolished in the *Neurod6;Shh* cKO (Figure 6E, H, and Figure S3L, L'), we asked in the same genetic background whether Hh-responding cells from the ventral hippocampus can contribute to dorsal dentate development, in particular, SGZ formation, by genetic fate-mapping analysis with the $Gli1^{CreERT2}$ line. For that purpose, we examined animals by P15 with tamoxifen

injection at birth using Ai14 as the cre reporter. We confirmed that *Neurod6^{Cre}* showed recombination activity mostly in the outer GCL with little in the inner GCL (Figure 7K, K') but not in the SGZ at all (Figure 7K") (Goebbels et al., 2006). In *Gli1$^{creERT2/+}$;Ai14$^{F/+}$;Shh$^{F/F}$* animals, tdT+ cells occupied both the inner GCL and SGZ, as indicated by colabeling with the stem cell marker Sox2 (Figure 7L, L' and L"). Strikingly, in *Gli1$^{creERT2/+}$;Neurod6$^{cre/+}$;Ai14$^{F/+}$;Shh$^{F/F}$* animals, tdT+ cells not only populated the outer GCL but also in the inner GCL (Figure 7M, M') with a few co-expressing Sox2 in the SGZ (arrows in the Figure 7M"). These data taken together indicate that even in the absence of local Shh in the forming DG, descendants of Hh-responding cells in the ventral hippocampus still contribute to the GCL and a few of them also take up residence in the SGZ, whereas in the presence of local Shh, more descendants can be retained in the SGZ, supporting the idea that the local Shh serves to maintain NSCs in the SGZ.

Figure 7: The formation of the SGZ in the *Emx1;Smo*, *Emx1;Shh* and *Neurod6;Shh* cKOs. (**A**-**D**) SGZ formation was assessed with the radial glial marker Blbp in the control (**A**), *Emx1;Smo* cKO (**B**), *Emx1;Shh* cKO (**C**) and *Neurod6;Shh* (**D**). There was a complete lack of Blbp+ cells in the SGZ of *Emx1;Smo* cKO (**B**) but only a moderate decrease in the *Emx1;Shh* cKO (**C**) and *Neurod6;Shh* cKO (**D**). The arrangement of Blbp+ cells in the SGZ was shown at the higher magnification in the insets. (**E**-**H**) Proliferative Ki67+ cells in the SGZ were shown for the control (**E**), *Emx1;Smo* cKO (**F**), *Emx1;Shh* cKO (**G**) and *Neurod6;Shh* (**H**). Ki67+ cells were completely abolished in the *Emx1;Smo* cKO (**F**) but only mildly affected in the *Emx1;Shh* cKO (**K**) and *Neurod6;Shh* cKO (**D**). (**I**) Quantification of Blbp+ cell densities in the SGZ was made for the control, *Emx1;Shh* cKO and *Neurod6;Shh* cKO. It was 72±4% (n=5, p<0.01) in the Emx1-Shh cKOs and 82±3% (n=5, p<0.01) in the *Neurod6;Shh* cKOs, as compared to the controls (100±6%). (J) Quantification of Ki67+ cell densities in the SGZ was made for the control, *Emx1;Shh* cKO and *Neurod6;Shh* cKO. It was only 65±3% (n=5, p<0.01) in the *Emx1;Shh* cKOs and 73±2% (n=5, p<0.01) in the *Neurod6;Shh* cKOs, as compared to the controls (100±7%). (k-m). Fate-mapping analysis in the absence of local *Shh* in the DG. Animals were examined by P15 with tamoxifen injection at birth using Ai14 as the cre reporter. In *Neurod6$^{cre/+}$;Ai14$^{F/+}$;Shh$^{F/F}$* animals (**K**) , tdT+ cells were mostly restricted in the outer GCL (**K'**) but absent from the SGZ as indicated by the lack of colabeling with Sox2, the marker for NSCs (**K"**). In *Gli1$^{creERT2/+}$;Ai14$^{F/+}$;Shh$^{F/F}$* animals (**L**), tdT+ cells were present mostly in the inner GCL (**L'**) and SGZ (**L"**). By contrast, in *Gli1$^{CreERT2/+}$;Neurod6$^{Cre/+}$;Ai14$^{F/+}$;Shh$^{F/F}$* animals (**M**), despite the lack of local *Shh* in the dentate, tdT+ cells were present in both inner GCL (**M'**) and SGZ (arrows in **M"**), in addition to the outer GCL. Data are shown as mean±SEM and p values for the indicated sample sizes are calculated by Student's *t*-test for two-tailed distribution with unequal variance. CL, granule cell layer; SGZ, subgranular zone.
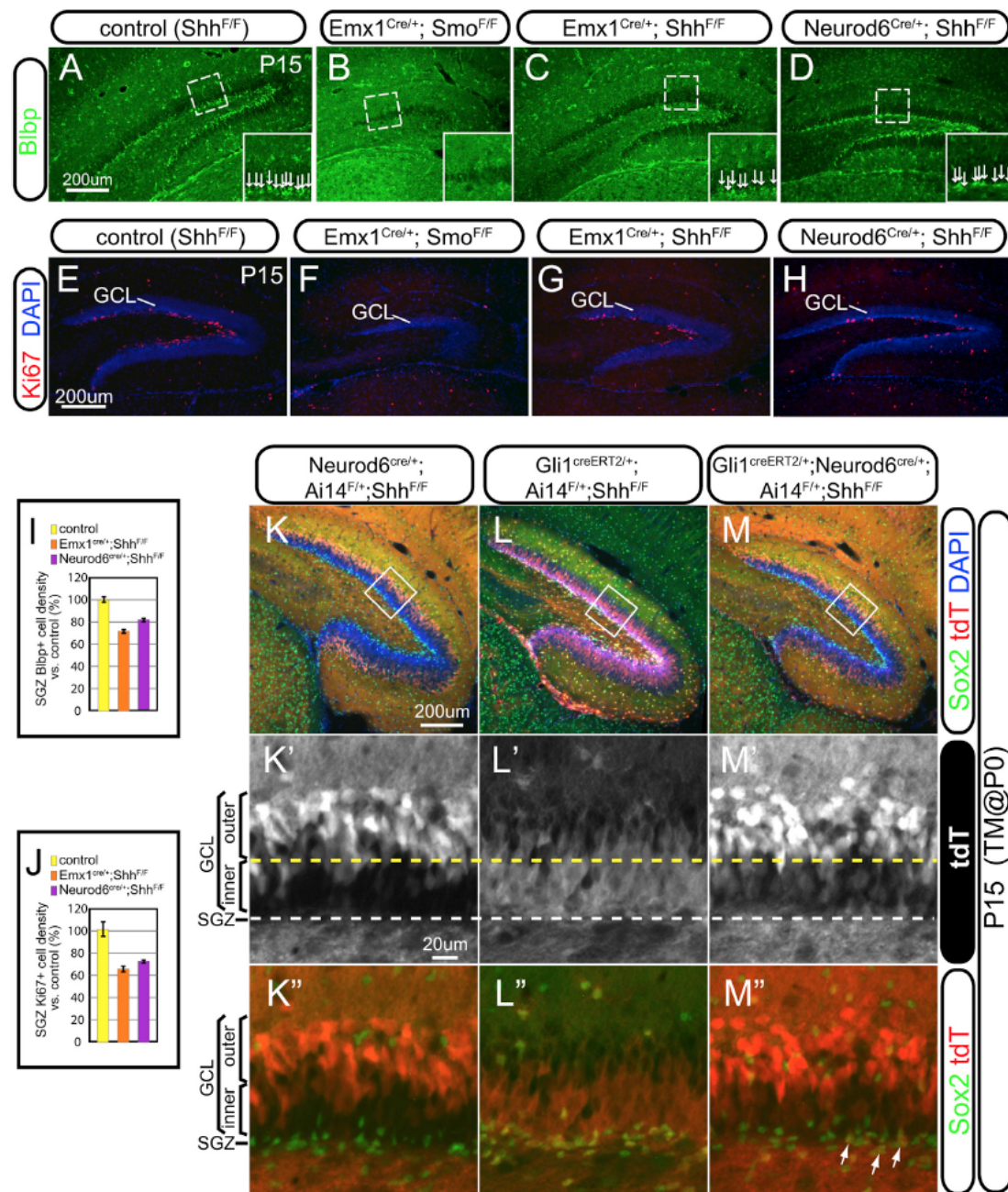
10.9. The descendants of the prenatal Hh-responding cells contribute to the LL-NSCs in the SGZ

The long-term fate of the descendants derived from the prenatal Hh-responding cells hasn't been determined yet. By crossing the *Gli1^CreERT2* line with the *Cre* reporter *Ai14*, we could evaluate the tdT expressing cells over a long time after tamoxifen injection at E17.5. In order to increase neurogenesis in aging animals (van Praag et al., 2000), we also subjected them to environment enrichment (EE) for two months and then examined the SGZ

when they reached one-year of age (Figure 8A). A number of radially oriented tdT+ cells still retained the expression of the radial glia marker Blbp (arrows in Figure 8B, C). More importantly, some of the tdT+ cells also expressed the immature neuronal marker Dcx (arrows in Figure 8D, E). Therefore, some of the descendents derived from the prenatal Hh-responding cells maintain the characteristics of NSCs and they are still neurogenic even in aged animals.
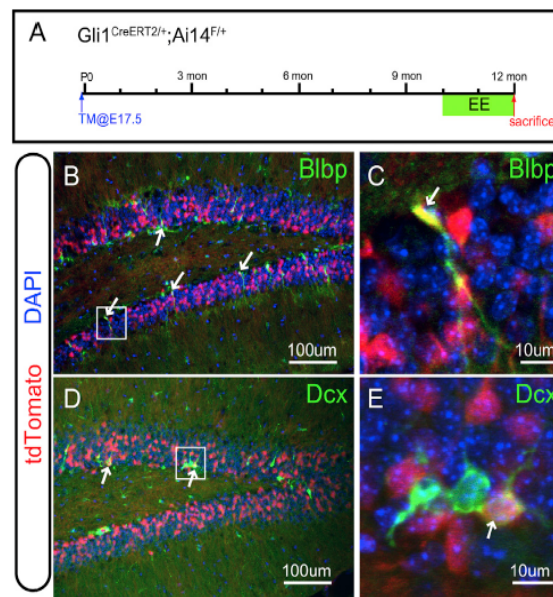
Figure 8: The long-term fate mapping of the prenatal Hh-responding cells in the dentate gyrus. (**A**) The schema shows the strategy for the long-term fate mapping of the prenatal Hh-responding cells in the dentate gyrus. By crossing the *Gli1^CreERT2* line with the *Ai14* line, the cell fate of the Hh-responding cells labeled by tamoxifen injection at E17.5 was examined in the one-year-old animals after environment enrichment (EE) for two months (green box). (**B-C**) Some tdT+ cells were marked by the neural stem cell marker Blbp in the SGZ (arrows in **B**) in the one-year-old animals. The boxed area in (**B**) is shown at the higher magnification in (**C**). (**D-E**) Some tdT+ cells were also labeled by the immature neuronal marker Dcx (arrows in **D**) in the one-year-old animals. The boxed area in (**D**) is also shown at the higher magnification in (**E**).

10.1. Suplementary Figures
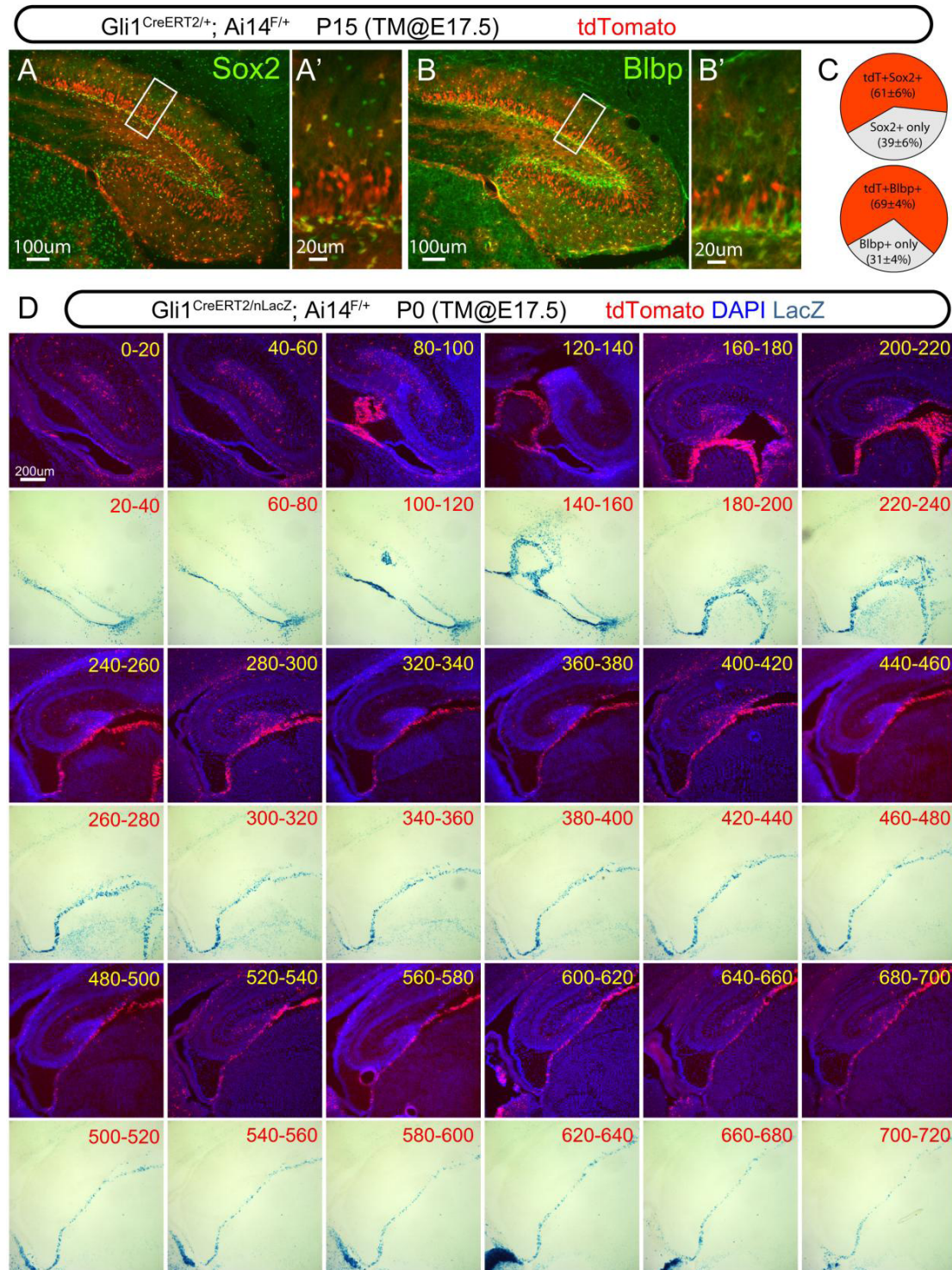
Figure S1 (related to Figure 2): (**A**-**C**) The labeling efficiency of *Gli1*^*CreERT2*
in the SGZ was assessed by P15 with tamoxifen injection (3mg/40g animal) at
E17.5 after crossing to the *Cre* reporter *Ai14*. tdT+ cells in the SGZ were shown
to express the radial glia markers Sox2 (**A**) and Blbp (**B**). Boxed areas in (**A**)
and (**B**) were shown at the higher magnification in (**A'**) and (**B'**), respectively.
About 61±6% of the total Sox2+ cells in the SGZ along the septo-temporal axis

were tdT+ (upper panel in **c**), and about 69±4% of the Blbp+ cells with radial processes in the SGZ were also tdT+ (lower panel in **C**). (**D**) Alternate sections were used for analyzing the spatial distribution of *Gli1*[nLacZ+] and tdT+ cells respectively for the *Gli1*[CreERT2/nLacZ]*;Ai14*[F/+] mice. The tdT+ cells at P0 represented the descendants of Hh-responding cells labeled by tamoxifen induction at E17.5. The number in each panel represents the thickness distance from the first panel. tdT+ cells clearly occupied the septal levels (about 480mm away from the first panel) where the *Gli1nLacZ* expression was no longer detectable.
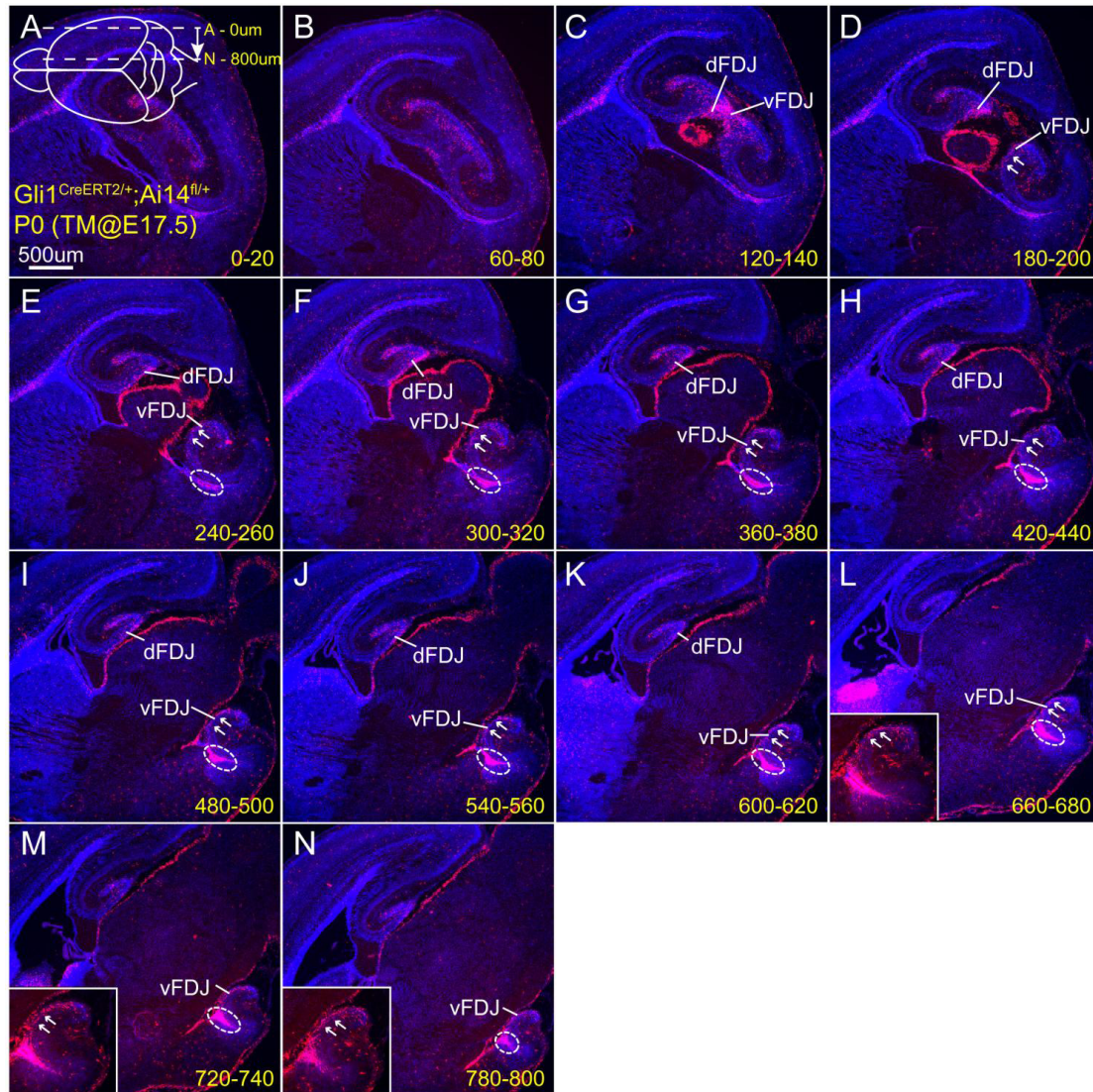
Figure S2 (related to Figure 3): (**A**-**N**). The distribution of tdT+ cells in the *Gli1*[CreERT2/+]*;Ai14*[F/+] animals were shown every 60μm by birth after tamoxifen (TM) induction at E17.5. The thickness distance as micron from the first section was shown at the bottom-right corner. Throughout the whole hippocampus, the VZ of the temporal hippocampus was the most heavily labeled by tdT (white ovals in **E-N**). The tdT+ cell stream was noticeable in the vFDJ region (arrows in **D-N**). The tdT+ cells were continuous from the vFDJ into the dFDJ at the transitional level (**C**) and tapered off in the dorsal

hippocampus toward the septal pole. dFDJ, dorsal fimbrio-dentate junction; vFDJ, ventral fimbrio-dentate junction.
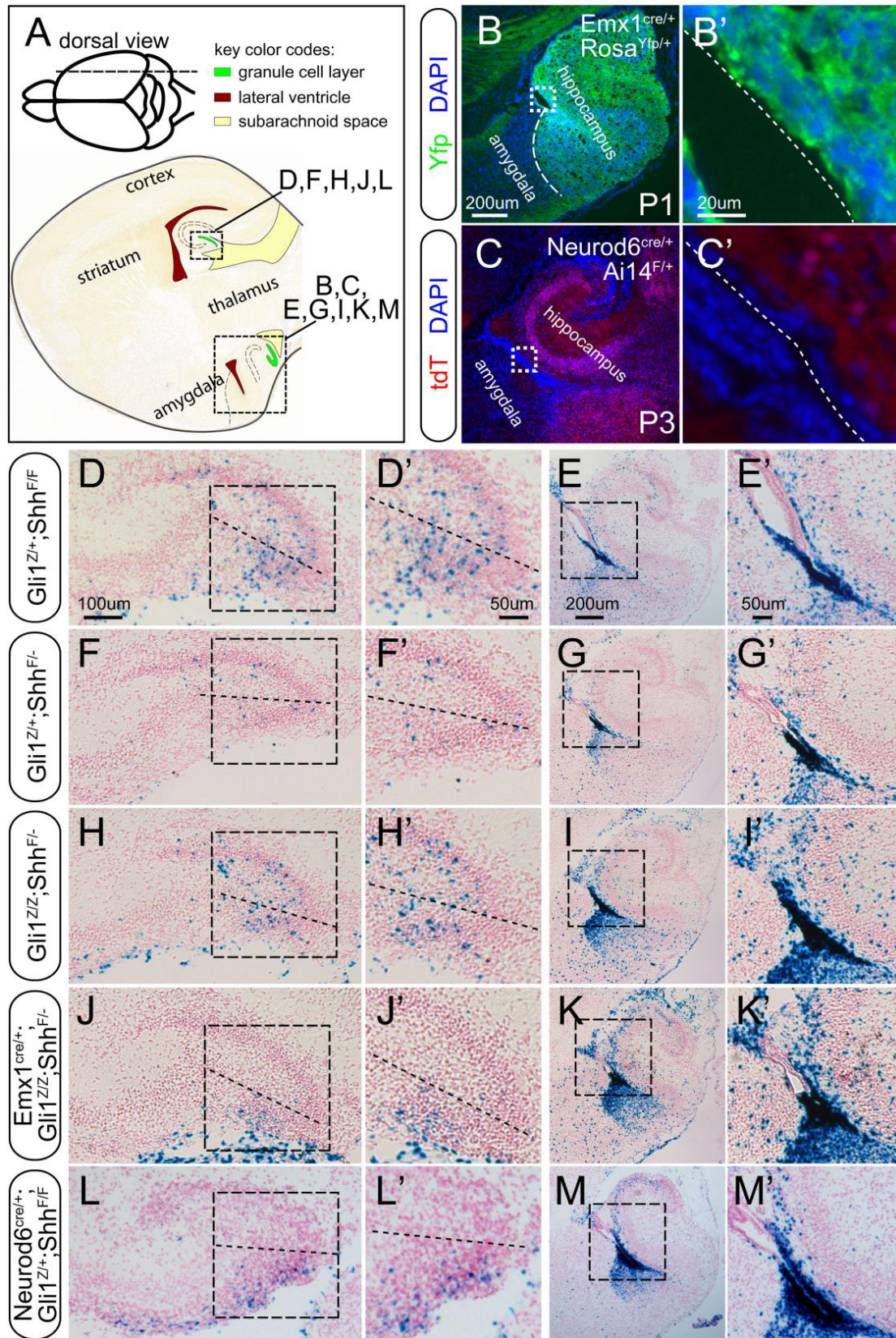
Figure S3 (related to Figure 4): (A) the schemas are illustrated for the sagittal sections from the P1 animals shown in **B**-**M**. (**B**) In the *Emx1^{Cre/+};Rosa^{Yfp/+}* animal at P1, *Emx1^{Cre}* showed the recombination activity in the ventral hippocampus as the expression of Yfp (**B**), which also covered its VZ (along the dotted line in **B'**). Boxed area in **b** was shown at the higher magnification in **B'**. (**C**) In the *Neurod6^{Cre/+};Ai14^{F/+}* animal at P3, *Neurod6^{Cre}* showed the recombination activity in the ventral hippocampus as the expression of tdTomato (**C**), which didn't cover its VZ (along the dotted line in **C'**). Boxed area in **C** was shown at the higher magnification in **C'**. (**D-E**) In the *Gli1^{Z/+};Shh^{F/F}* animals, *Gli1nLacZ+* cells were localized at the entrance of the hilus in the dorsal DG (**D** and **D'**). The dorsal dentate can be divided into upper and lower portions by a line connecting the tip of the CA3 field and the apex of the dentate pole. Some of *Gli1nLacZ+* cells could be detectable in the upper portion (**D'**). *Gli1nLacZ+* cells were clearly identifiable to form a stream out of the VZ of ventral hippocampus into the forming DG (**E** and **E'**). Boxed areas in **D** and **E** were shown at the higher magnification in **D'** and **E'**. (**F**-**G**) In the *Gli1^{Z/+};Shh^{F/-}* animals, one copy of the *Shh* flox allele was replaced with a *Shh* null allele. The number of *Gli1nLacZ+* cells in the dorsal dentate was dramatically reduced in both portions (**F** and **F'**). The stream of *Gli1nLacZ+* cells leaving the VZ of ventral hippocampus was slightly diminished and there was a decrease in the expression of *nLacZ* in the VZ (**G** and **G'**). Boxed areas in **F** and **G** were shown at the higher magnification in **F'** and **G'**. (**H-I**) In the *Gli1^{Z/Z};Shh^{F/-}* animals, an extra copy of *Gli1nLacZ* was present in relation to the animals in **F**-**G.** The distribution of *Gli1nLacZ+* cells was restored in both dorsal DG (**H** and **H'**) and ventral hippocampus (**I and I'**) close to the level seen in the *Gli1^{Z/+};Shh^{F/F}* animals. Boxed areas in **H** and **I** were shown at the higher magnification in **H'** and **I'**. (**J**-**K**) In the *Emx1^{cre/+};Gli1^{Z/Z};Shh^{F/-}* animals, the remaining Shh flox allele was floxed out in the Emx1 domain. Most of the *Gli1nLacZ+* cells were abolished in the upper portion of the dorsal dentate whereas residual *Gli1nLacZ+* cells were still present at the entrance of the hilus in the lower portion (**J** and **J'**), which appeared to be continuous with the *Gli1nLacZ+* cell stream from the VZ of the ventral hippocampus (**K** and **K'**). Boxed areas in **J** and **K** were shown at the higher magnification in **J'** and **K'**. (**L-M**) In the *Neurod6^{cre/+};Gli1^{Z/+};Shh^{F/F}* animals, two copies of the *Shh* flox alleles were removed from the pallial neuronal lineage. The distribution of *Gli1nLacZ+* cells (**L**, **L'**, **M** and **M'**) was quite similar to the *Emx1^{cre/+};Gli1^{Z/Z};Shh^{F/-}* animals. Boxed areas in **l** and **m** were shown at the higher magnification in **L'** and **M'**.
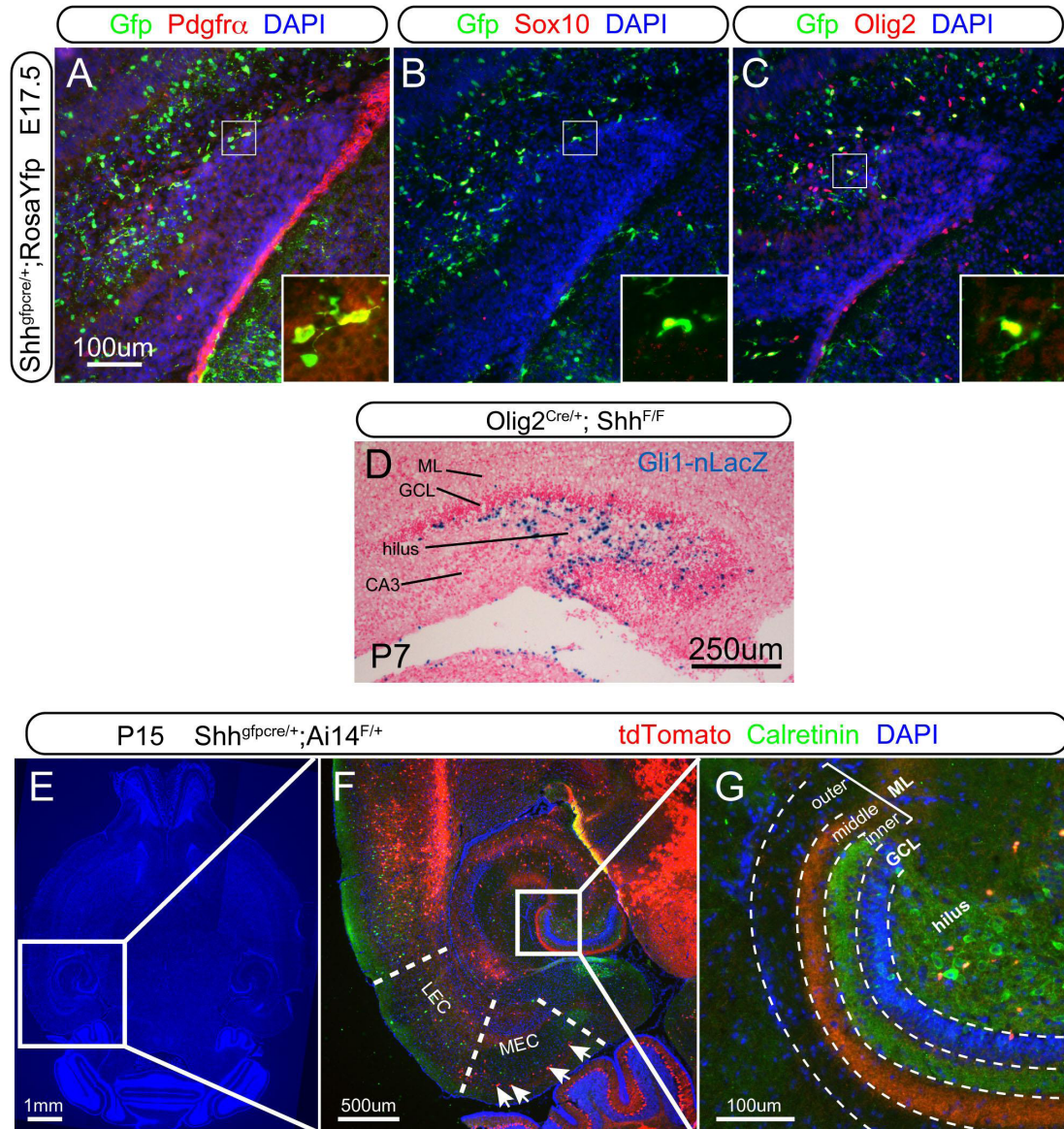
Figure S4 (related to Figure 6): (**A**-**C**) The *Shh* lineage expressed markers for oligodendrocyte progenitor cells (OPCs) in the dentate gyrus at E17.5. By crossing *Shh^{GfpCre}* with *Rosa^{Yfp}*, the *Shh* lineage marked as *Yfp*+ cells (enhanced with Gfp antibody staining) in the dentate gyrus at E17.5 was colabeled with oligodendrocyte progenitor cell (OPC) markers -- Pdgfrα (**A**), Sox10 (**B**) and Olig2 (**C**). (**D**) In the *Olig2$^{cre/+}$;Shh$^{F/F}$* animals, Shh was removed from the oligodendrocyte lineage. However, the distribution of the *Gli1nLacZ*+ cells in the dorsal DG was unaffected by P7. (**E**-**G**) By crossing *Shh^{GfpCre}* with the cre reporter *Ai14*, a horizontal section at P15 (**E**) showed the *Shh* lineage also marked the cells in the MEC (arrows in **f**), which made projection to the middle molecular layer in the DG (**G**). LEC, lateral entorhinal cortex; MEC, medial entorhinal cortex.
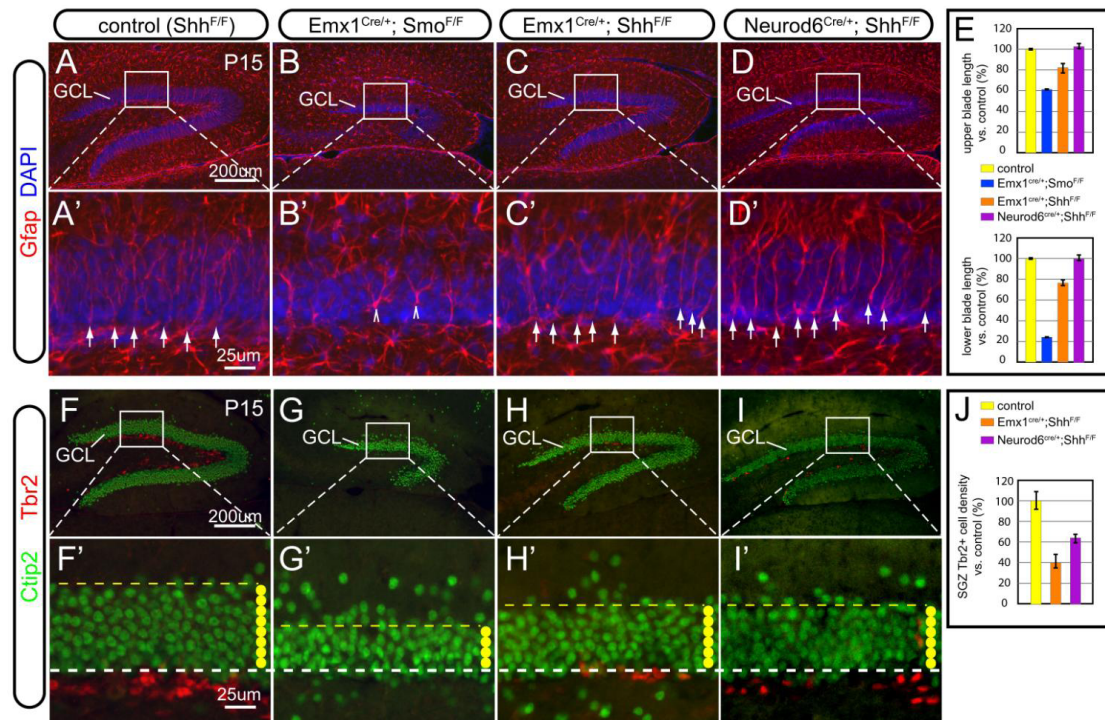
Figure S5 (related to Figure 7): (**A**-**D**) and (**A**'-**D**') GFAP staining at P15 showed the radial glial scaffolding in the control (**A**, **A'**), *Emx1;Smo* cKO (**B**, **B'**), *Emx1;Shh* cKO (**C**, **C'**), *Neurod6;Shh* cKO (**D**, **D'**). Compared to the control (arrows in **A'**), the radial glia spanning the GCL poorly developed in the *Emx1;Smo* cKO (arrowheads in **B'**), whereas the radial glial fibers were rather intact in the *Emx1;Shh* cKO (arrows in **C'**) and *Neurod6;Shh* cKO (arrows in **D'**). (**E**) Quantification was made for the length of the upper and lower blades in the control, *Emx1;Smo*, Emx1-Shh and *Neurod6;Shh* cKOs. In relation to the control, the length of the upper and lower blades were 61±1% (n=5, p<0.001) and 24±1% (n=5, p<0.001) in the *Emx1;Smo* cKO, whereas they were 81±5% (n=5, p<0.01) and 76±3% (n=5, p<0.01) in the *Emx1;Shh* cKO, and 102±4% (n=5, p<0.01) and 98±3% (n=5, p<0.01) in the *Neurod6;Shh* cKO. (**F**-**I**) and (**F'**-**I'**) Ctip2+ cells in the GCL and Tbr2+ neurogenic precursors in the SGZ were shown for the control (**F, F'**), *Emx1;Smo* cKO (**G, G'**), *Emx1;Shh* cKO (**H, H'**) and *Neurod6;Shh* cKO (**i, i'**). *Emx1;Smo* cKO displayed complete deficiency for the Tbr2+ cells in the SGZ and the thinnest GCL (~4 cells thick, yellow dots in **G'**). *Emx1;Shh* cKO also had diminished number of Tbr2+ cells in the SGZ and thinner GCL (~6 cells thick, yellow dots in **H'** and **I'**), compared to the control (~8 cells thick, yellow dots in **F'**). (**J**) Quantification of Tbr2+ cell densities in the SGZ was made for the control, *Emx1;Shh* cKO and *Neurod6;Shh* cKO. As compared to the control (100±9%), it was 40±7% (n=5, p<0.001) in the *Emx1;Shh* cKO and 62±4% (n=5, p<0.001) in the *Neurod6;Shh* cKO.
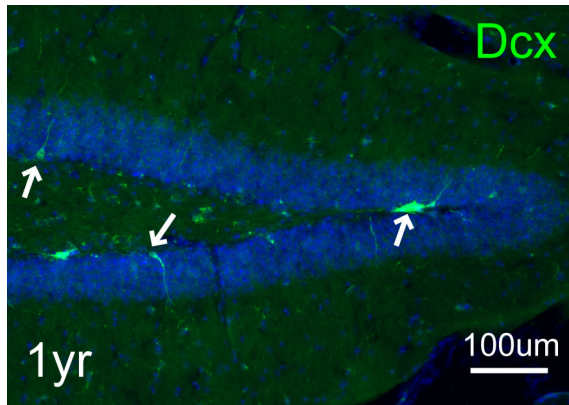
Figure S6 (related to Figure 8): Only very few Dcx+ immature neurons (arrows) were detectable in the DG in one year old animals.

CHAPTER 2

11. Interaction of *Emx2* and *Shh* to modulate the embryonic neural stem cells of the ventral hippocampus

11.1. Ectopic distribution of Hh responsive cells in the hippocampus of the *Emx2$^{-/-}$* mutant mice

In Chapter 1 we show that the ventral hippocampus is the origin for a subset of adult NSC settling in the DG. We also showed that Shh is critical for the origin and maintenance of these cells. Although we already know several important features of these stem cells, there are multiple questions that still remain unclear. In this chapter we will try to identify the genes involved in the generation and migration of NSC on their route to the DG from their origin in the ventricular zone of the ventral hippocampus.
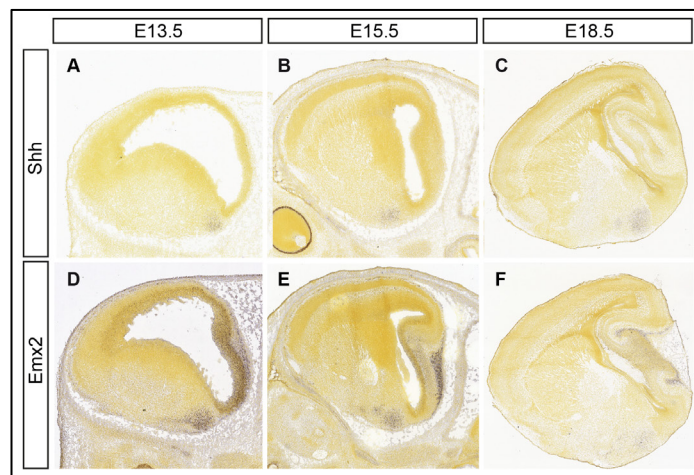
Figure 1: Expression pattern of Shh and *Emx2* genes (Brain Allen Atlas): Sagittal sections of E13.5 (A, D), E15.5 (B, E) and E18.5 (C, F) showing the mRNA expression pattern of *Shh* (A-C) and *Emx2* (D-F) in the amygdalo-hippocampal region.

The transcription factor *Emx2* is expressed specifically in the hippocampus, starting early during development. This expression is maintained in cell progenitors and specifically in the SGZ during the second postnatal week (Mallamaci et al. 1998). Prominent defects in the hippocampus and dentate gyrus of the *Emx2$^{-/-}$* mutant mice have been well described in previous studies (Pellegrini et al. 1996b; Oldekamp et al. 2004; Zhao et al. 2006). For instance it is

known that the shape and size of the hippocampus is modified and reduced and the DG is almost missing in these mutants (Oldekamp et al. 2004; Pellegrini et al. 1996a; Tole et al. 2000; Simeone et al. 1992). Closer analyses of the DG showed a lost of GC and disorganization of the radial glial fibers used as scaffold by the putative granular cells to reach their final destination (Rickmann et al. 1987; Oldekamp et al. 2004).
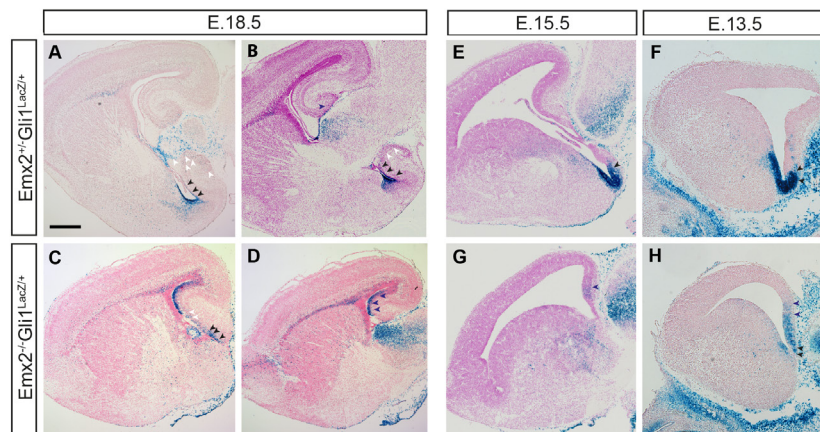
Figure 2: Static distribution of Shh responsive cells in mice lacking *Emx2* gene show an ectopic distribution in dorsal ventricular zone (dVZ) of most lateral sections of hippocampus. Sagittal sections of *Emx2$^{+/-}$Gli1$^{LacZ/+}$* at E18.5 (A and B), E15.5 (E) and E13.5 (F) and *Emx2$^{-/-}$Gli1$^{LacZ/+}$* mutant mice at E18.5, (C and D); E15.5, (G) and E13.5, (H) showing the expression pattern of LacZ protein under the *Gli1* promoter in lateral levels of the hippocampus (dorsal and ventral regions).). Scale bar (in A) A-H, 500µm.

Previous work from our laboratory showed that the Sonic Hedgehog protein produced in the amygdalo-hippocampal region adjacent to the ventricular zone of the ventral hippocampus, is the source of Shh to which the embryonic granular cells are responding and consequently expressing Gli1, (Shh responsive cells) (Li et al. 2013). The similar expression pattern of *Shh* and *Emx2* in this region (Figure 1), along with the *Emx2* mutant phenotype, suggested to us that *Emx2* might modulate the expression of Shh, affecting the origin and migration of these cells to reach their final destination in the Subgranular Zone of the dorsal DG (Li et al. 2013).

To test this hypothesis, we first studied the localization of Gli1 positive cells at different ages in the hippocampus of the *Emx2^{-/-}* mutant mice by crossing the mutants with *Gli1^{nLacZ}* transgenic reporter mice line (which express LacZ under the Gli1 promoter) (Figure 2, A-H). The expression pattern analysis at E18.5 revealed that Gli1 positive cells are restricted in the wild type animals to the DG of the dorsal hippocampus, where we already have described that these cells are arriving by migrating along the transitional hippocampus (Figure 2 A, B). At similar levels in the *Emx2^{-/-}* mutant mice, we found Gli1+ cells neither in the presumptive DG nor in the transitional hippocampus. We also found high expression of LacZ corresponding to Gli1+ cells in the VZ/SVZ in the ventral hippocampus of control mice, where these cells are born and start their migration to the dorsal and ventral DG. In mutants in the same area, this expression is reduced suggesting a defect in the origin and migration of this population of cells (Figure 2 A-D).

This difference in the expression pattern of Gli1 is also found at younger stages, where we found in control animals the same lacZ expression in the ventral regions of the ventricle while in *Emx2^{-/-}* mutant mice this expression is reduced in the same area. The study of the *Emx2^{-/-}* mutant mice also revealed an ectopic population of cells expressing Gli1 in the VZ of the dorsal hippocampus (Figure 2, C-D) at E18.5 compared with the controls. We wondered where this ectopic population came from by analyzing the Gli1 expression pattern at early stages. We found an enlargement of the Gli1 expression in dorsal regions of the hippocampus at E15.5 (Figure 2, E and G) and E13.5 (Figure 2, F and H) in the *Emx2* KO mice that correspond with the VZ of the dorsal hippocampus at later stages (Figure 2, C-D). Since previous studies have shown that Shh has an important role in the origin and maintenance of the LL-NSC of the SGZ in the DG and that Gli1+ cells are responding to Shh, and are NSC (Ahn & Joyner 2005), we wished to further study and characterize the misexpression of Gli1+ cells along the dorsal prospective hippocampus and the reduction observed in the ventral ventricular zone of the hippocampus. To do this we used the *Gli1^{CreERT2}* conditional transgenic mice crossed with *Ai14^{F/F}* reporter line as a tool to follow and characterize the Gli1 positive cells and to determine how the lack of *Emx2*

91

affects the population of NSC originated embryonically in the ventral region of the hippocampus.

11.2. Fate mapping of Shh responsive cells in the *Emx2*$^{-/-}$ mutant mice
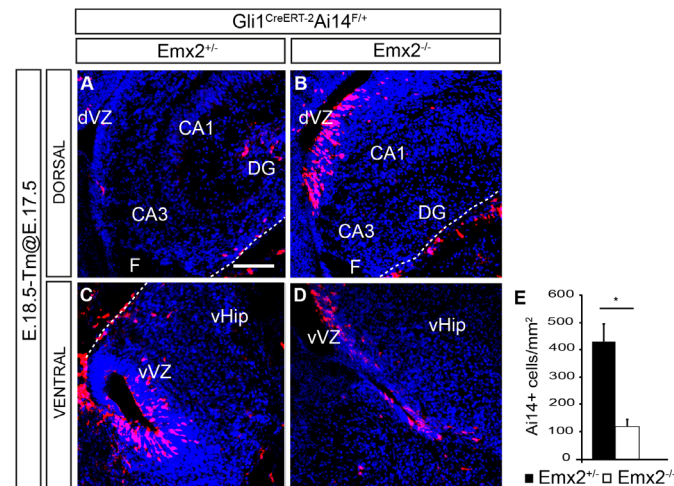
Figure 3: Loss of *Emx2* leads to an accumulation and reduction of Gli1+ cells in the ventricular zone of dorsal and ventral hippocampus respectively. Sagittal sections through the hippocampal region of *Emx2*$^{+/-}$*Gli1*$^{CreERT2+/-}$*Ai14*$^{F/+}$ (control) (A,C) and *Emx2*$^{-/-}$*Gli1*$^{CreERT2+/-}$*Ai14*$^{F/+}$ (mutant) (B,D) E18 mice after E17.5 tamoxifen injection showing the distribution of AI14^{+} (red) cells after the immunohistochemistry and co-stained with DAPI in dorsal (A-B) and ventral (C-D) hippocampus. (CA1, cornus ammonis 1; CA3 cornus ammonis 3; DG, dentate gyrus; F, fimbria; VHip, ventral hippocampus; dVZ, dorsal ventricular zone; vVZ, ventral ventricular zone). Scale bar (in A) A-D, 50 µm.

As *Emx2*$^{-/-}$ mutant mice died at birth due to kidney problems (Simeone et al. 1992), our study ends in the latest gestation stages, so we can not follow the whole development of the DG and the SGZ that continues during the first two postnatal weeks. To better understand how Hh responsive cells distribute in the *Emx2*$^{-/-}$ mutant mice, we analyzed the fate map of Gli1+ cells using the *Gli1*^{CreERT2}; *Ai14*$^{F/+}$ into the *Emx2*$^{-/-}$ line. E17.5 embryos were injected with tamoxifen and then analyzed one day later (Figure 3, A-D). In the dorsal hippocampus of control mice we found that a small group of recombinant cells are already settled in the DG at lateral levels (Figure 3, A). Also, some sparse cells were found in the dorsal ventricular zone and in the basal membrane of

the meninges. The analysis of the *Emx2*^{-/-} mutant mice on the other hand shows no cells in the presumptive DG and an accumulation of recombinant cells in the dorsal ventricular zone and in the basal membrane (Figure 3, B).

In the ventral ventricular zone of the hippocampus we found a reduction of AI14+ cells in the *Gli1*^{CreERT2} mutant mice in comparison to the controls (Figure 3, C-D). We also saw that the phenotype found in the *Gli1*^{CreERT2} mice was pretty similar to the one found in the *Gli1*^{nLacZ} mice both in the dorsal and ventral hippocampus.

This similarity in the expression pattern between the static distribution of Gli1+ cells obtained with the *Gli1*^{nLacZ} and the short term fate mapping that we performed with the *Gli1*^{CreERT2} mice allowed us to characterize the phenotype of the Gli1+ ectopic cells found in the dorsal ventricular zone (Figure 4) and the changes found in the ventricular zone (Figure 6) of the ventral hippocampus.

11.3. The ectopic population of Gli1+ cells in dVZ of the hippocampus correspond mainly to progenitors

Previous studies in Emx2^{-/-} mutant mice showed a lack of GC in the DG (Pellegrini et al. 1996b; Yoshida et al. 1997) and although the mutant dentate is genetically well specified, it doesn't grow and develop properly (Tole et al. 2000). We have shown in the *Gli1*^{nLacZ} and the *Gli1*^{CreERT2} mutant mice an expanded expression of Gli1+ cells in the VZ of the dorsal hippocampus at lateral levels (Figure 1, 2). In order to understand what these Gli1+ cells are we first characterized them with multiple markers.

To assess whether some of the Gli1+ cells belong to the glial lineage we study the co-expression of GFAP (Figure 4, A and D), and Blbp (Figure 4, B and E) with Tdtomato by immunohistochemistry in controls and *Gli1*^{CreERT2}; *Ai14F* mutant mice. GFAP and Blbp are also expressed in neural progenitor cells at embryonic stages (Giachino et al. 2014; Seki et al. 2014) and GFAP labels the fibers of the radial glial cells. We found almost no co-expression of GFAP with AI14+ cells in control animals at E18.5. Only a very few GFAP+

cells appeared around the pia and close to the meninges (Figure 4, A, arrow). In *Emx2*^{-/-} mutant mice, on the contrary, we saw that some of the Ai14 recombinant cells colocalized with GFAP at the dorsal border of the fimbria (Figure 4, D, arrow). Then, we analyzed Blbp (Figure 4, B and E) to confirm that whereas in control mice only a few Ai14+ cells colocalized in the Fimbrio-Dentate Junction (FDJ) with Blbp (Figure 4, B, arrow) and none in the dVZ, in *Emx2*^{-/-} mutant mice, several of the ectopic recombinant cells in dVZ expressed Blbp (Figure 4, E, arrow). Taking advantage of GFAP labeling of the radial fibers used as scaffolding for the newly born neurons to reach the DG (Eckenhoff & Rakic 1984; Rickmann et al. 1987), we next checked the shape of them. In control mice, GFAP is strongly expressed at the border of the fimbria and fibers extend to the entrance of the hilus and project to the pia all around the forming dentate (Figure 4, A). In the *Emx2*^{-/-} mutant mice, fibers are also seen at the border of the fimbria but don't follow the pial surface and spread out in a disorganized way trying to reach the presumptive dentate (Figure 4, D), probably affecting the radial migration of the granule cells. We next used Olig2 to stain the oligodendrocyte lineage, but we found no expression in the dVZ of the hippocampus at this age both in control and mutant mice (Figure 5, A, B). To confirm the ectopic expression of Gli1 correspond to progenitor cells, we next studied the colocalization of several markers such as Nestin, Sox2 and Tbr2. As with the GFAP and Blbp we found multiple Nestin+/Ai14+, Sox2+/AI14+ and Tbr2+/AI14+ cells in the dVZ of the hippocampus in *Emx2*^{-/-} mutant mice and none in the controls (Figure 4, C, F, G-L). Therefore we concluded the loss of *Emx2* gene leads to a misexpression of Gli1 in progenitor cells of the dorsal hippocampus. Later we checked with acute BrdU labeling whether these Gli1+ cells were proliferating (Figure 4, G and J). Although the distribution of BrdU in the VZ and SVZ of the dorsal hippocampus seems similar in controls and *Emx2*^{-/-} mutant mice, the Ai14+ ectopic cells localized in the dVZ of the hippocampus were also stained with BrdU (arrows in Figure 4, J, K and L), pointing out that most of the Gli1+ cells in the dVZ are already dividing.
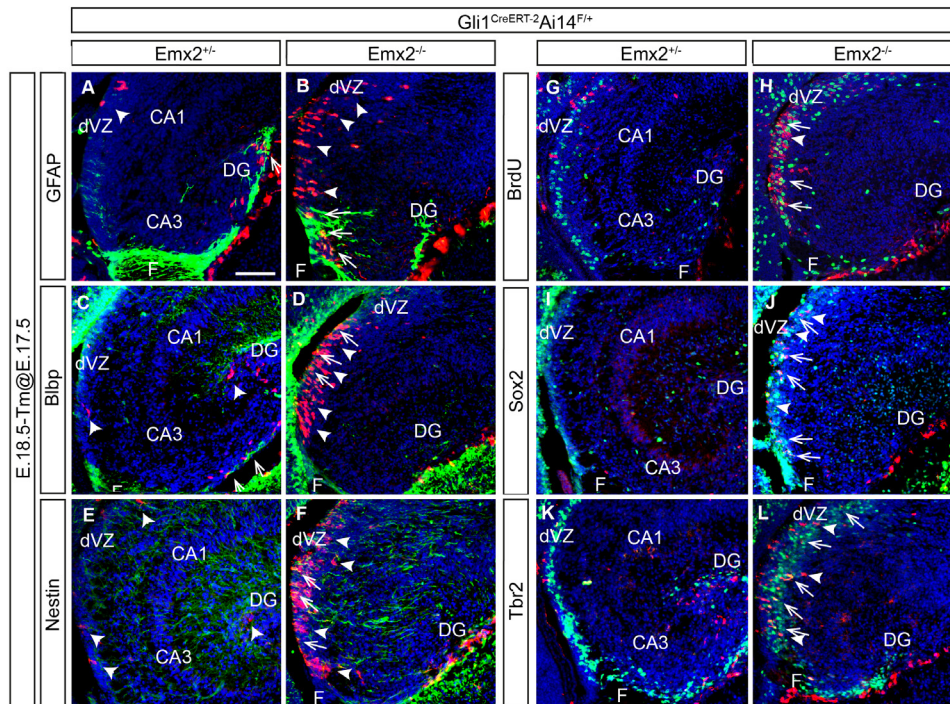
Figure 4: The ectopic population of Shh responsive cells in *Emx2⁻/⁻* mutant mice colocalized with diverse progenitor cell markers. Sagittal sections of dorsal hippocampus of $Emx2^{+/-}Gli1^{CreERT2+/-}Ai14^{F/+}$ control, (A, C, E, G, I and K) and $Emx2^{-/-}Gli1^{CreERT2+/-}Ai14^{F/+}$ mutant E18.5 mice (B, D, F, H, J and L) after received a tamoxifen injection at E17.5 and showing the coexpression of Ai14 with GFAP (A and B), Blbp (C and D), Nestin (E and F), BrdU (G and H), Sox2 (I and J) and Tbr2 (green) (K and L) immunohistochemistry co-stained with DAPI to delimit the areas. (CA1, cornus ammonis 1, CA3 cornus ammonis 3, DG, dentate gyrus, F, fimbria, dVZ, dorsal ventricular zone of the hippocampus; arrowhead, recombinant cells expressing Ai14 (red); arrow, cells colocalizing Ai14 (red) with one of the analyzed maker (green)). Scale bar (in A) A-L, 50 µm.
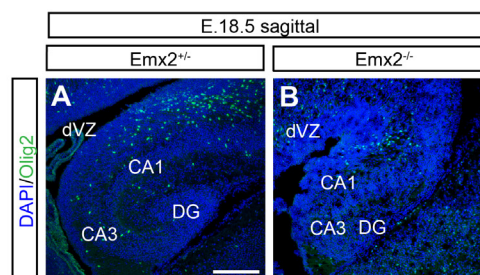
Figure 5: There is no expression of Olig2 markers in the dVZ of controls and *Emx2⁻/⁻* mutant mice. Sagittal sections of the dorsal hippocampus of $Emx2^{-/+}$ controls and $Emx2^{-/-}$ mutant mice (A, B), showing the expression of Olig2 marker and counterstain with DAPI. (CA1, cornus ammonis 1, CA3 cornus ammonis 3, DG, dentate gyrus, dVZ, dorsal ventricular zone of the hippocampus). Scale bar

(in A) A-B, 50 µm.

11.4. Increased number of proliferating and secondary progenitor cells in the dVZ in *Emx2⁻/⁻* mutant mice

Previous studies have shown the loss of *Emx2* affects the proliferation of the progenitor cells in the hippocampus (Muzio et al. 2005). Our experiments show that most of the progenitors that express Gli1 in the *Emx2* mutant mice are in a proliferative state (Figure 4, C, J). To understand better if the loss of *Emx2* gene affects the cell cycle of the progenitor cells of the dVZ, we carried out experiments to quantify the density of those dividing cells in the dVZ of *Emx2* KO and controls at E18.5. The analysis of PH3 in *Emx2⁺/⁺*, *Emx2⁺/⁻* and *Emx2⁻/⁻* mutant mice revealed an approximate doubling of cell density in these proliferative markers in *Emx2⁻/⁻* KO mice compared to controls and heterozygous (Figure 6, A, B, C and D). We found no statistical differences between *Emx2⁺/⁻* and *Emx2⁺/⁺* in PH3 and Ki67. However, BrdU analysis at the same age showed no statistical differences between *Emx2⁺/⁺*, *Emx2⁺/⁻* and *Emx2⁻/⁻* mutant mice (data not shown). We next analyzed the intermediate progenitors using Tbr2 as a marker in the dVZ of the hippocampus. We found an incremental increase of ~30% in the density of Tbr2+ cells in the in *Emx2⁻/⁻* compared with *Emx2⁺/⁻* and *Emx2⁺/⁺* mice (Figure 6, E-H). We found no differences between *Emx2⁺/⁻* and *Emx2⁺/⁺* in Tbr2 cell density. Since ectopic expression of Gli1 at dorsal hippocampus starts at early stages like E13-E15 (Figure 1, E-H) we then analyzed the expression of PH3 and Tbr2 at E15.5 and found an increase of ~60% of PH3+ cells (Figure 7, A-D) in the *Emx2⁻/⁻* compared with *Emx2⁺/⁻* and *Emx2⁺/⁺* mice. On the other hand we didn't find any difference between the three groups of animals in Tbr2+ cells (Figure 7, E-H). These results corroborate our previous data suggesting that the ectopic population of Gli1+ located in the dVZ of the hippocampus correspond to progenitors cells.
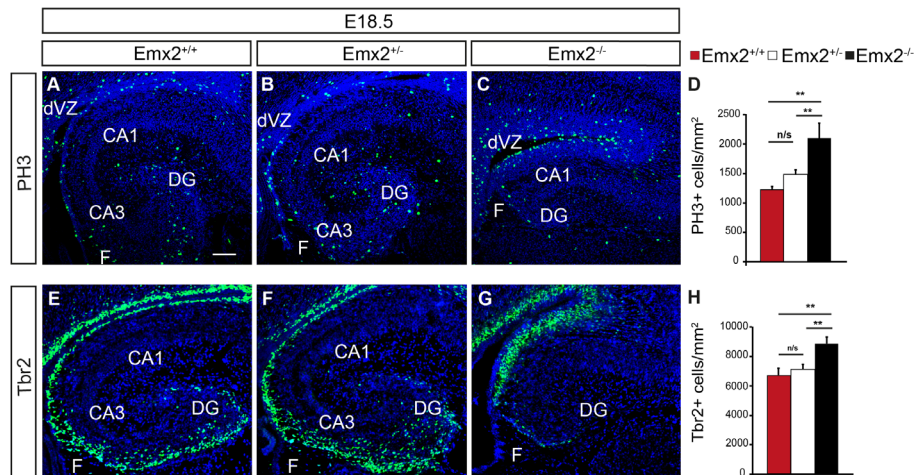
Figure 6: *Emx2 mutant mice show an increase in the density of PH3 and Tbr2 positive cells in the VZ of the dorsal hippocampus.* Sagittal sections of E18.5 (A-C and E-G) wt (A, E), heterocygous (B, F) and *Emx2* mutant mice (C, G), showing immunohistochemistry of PH3 (A-C), or Tbr2 (E-G) marker. Quantification (D, H) of the expression of PH3 (D) or Tbr2 (H) in controls (red bar) het (white bars) and *Emx2*$^{-/-}$ mutant mice (black bars) by cell density in the VZ of dorsal hippocampus. (CA1, *Cornus Ammonis* 1, CA3 *Cornus Ammonis* 3, DG, dentate gyrus, F, fimbria, dVZ, dorsal ventricular zone). Scale bar (in A) A-C, E-C, 50 μm.

Also, at E18.5 we observed differences in the distribution of PH3+ and Tbr2+ cells in the mutants compared with controls. PH3+ cells in *Emx2*$^{-/-}$ mutant mice at E18.5 appeared mainly in the VZ of the dorsal hippocampus, just at the border of the ventricle, while in controls the population of PH3+ cells was homogeneously distributed in the whole hippocampus, including FDJ and DG itself, suggesting that in the mutant, the population that should be dividing in the FDJ and DG in that moment is not there or is not able to proliferate. The intermediate progenitors marker Tbr2 were differentially distributed in *Emx2*$^{-/-}$ and *Emx2*$^{-/+}$ or *Emx2*$^{+/+}$ mice as well, with its distribution in the Emx2$^{-/-}$ mutant mice restricted to the dVZ with a very few cells close to the fimbria, in the FDJ or the DG compared to control mice. Together, the E18.5 and E15.5 PH3, and BrdU data suggest an *Emx2* role through *Gli1* in the control of the cell cycle length, maybe lengthening the cell cycle as other authors have proposed (Muzio et al. 2005). The increase of Tbr2 density number at E18.5 and not earlier at E15.5 in the *Emx2* mutant mice could be at a result of a temporal change in the expression pattern or an accumulation of the cells due to a migration problem,

perhaps because the glial scaffolding is not well formed (Figure 4 A, D). To explore the second possibility we measured the VZ of the dorsal hippocampus. The analysis of the VZ width displayed a ~4-fold increased in the *Emx2* mutant mice compared to controls (Figure 8, A). We next wondered whether the increase in the proliferation rate in the VZ in the *Emx2$^{-/-}$* leads to an increase in the number of immature neurons in that region. So we next performed a X-gal staining in the mice *line Emx2; NeuroD^{LacZ}* in which lacZ is expressed under the promoter *NeuroD*, a postmitotic immature neuronal marker. The analysis of LacZ expression showed an accumulation of immature neurons in the VZ/SV zone of the *Emx2* mutant compared with controls (Figure 8, D, E). The misexpression of Gli1 suggests changes in the expression of Shh in the dorsal hippocampus of the mutant or in adjacent regions. Therefore, we next study the population of recombinant cells in the lines *Emx2$^{+/-}$; Shh^{GFPCre}; Ai14$^{F/+}$* and *Emx2$^{-/-}$; Shh^{GFPCre}; Ai14$^{F/+}$* mice.
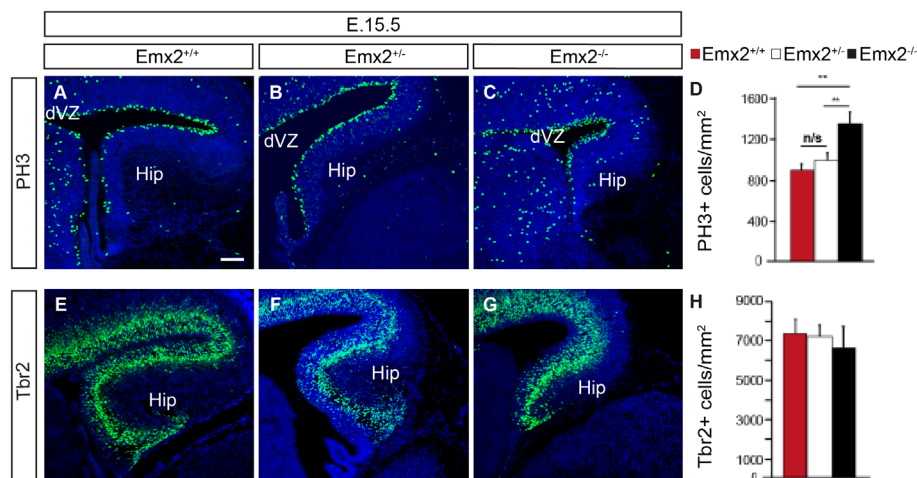
Figure 7: Loss of *Emx2* gene leads to an increase in the dorsal hippocampus proliferation at E15.5. Sagittal sections of E15.5 dorsal hippocampus in *Emx2$^{+/+}$Gli1$^{CreERT2+/-}$Ai14$^{F/+}$* (A and E); *Emx2$^{+/-}$Gli1$^{CreERT2+/-}$Ai14$^{F/+}$*, (B and F) and *Emx2$^{-/-}$Gli1$^{CreERT2+/-}$Ai14$^{F/+}$* mice (C and G), showing distribution of Phospho-Histone 3 (PH3) (A, B and C) and Tbr2 (E, F and G) markers after immunohistochemistry. Quantification (D, H) of the expression of PH3 (D) or Tbr2 (H) in controls (red bar) heterozygous (white bars) and *Emx2$^{-/-}$* mutant mice (black bars) by cell density in the VZ of dorsal hippocampus. (Hip, hippocampus, dVZ, dorsal ventricular zone). Scale bar (in A) A-C, E-C, 50µm.
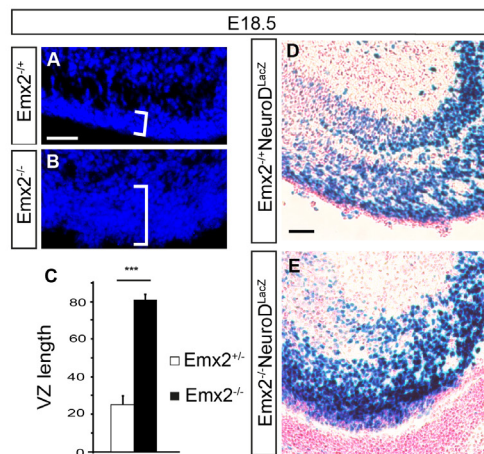
Figure 8: Loss of *Emx2* leads to an increase of the VZ and the immature neuronal marker NeuroD. Sagittal sections of the VZ of the dorsal hippocampal region showing DAPI (A, B) and LacZ (D, E) staining at E18.5 of controls (A, D) and mutant (B, E) mutant mice. D and E sections were counterstain with nuclear fast red to visualized anatomy (C) Quantification of the VZ thickness in controls (white bar) and *Emx2^-/-* mutant mice (black bar). Scale bar (in A) A, B 25 µm; Scale bar (in D) D, E, 50 µm.

11.5. Expression of Shh in the dorsal hippocampus shows few changes in *Emx2^-/-* mutant mice

The misexpression of Gli1 protein in the *Emx2^-/-* mutant mice in progenitors cells pointed us to a possible change in Shh expression. Detection of Shh by immunostaining or in-situ hybridization (ISH) in the brain is very difficult due to low level expression, therefore we chose to use the *Cre* transgenic line under control of the *Shh* promoter, *Shh^GFPCre*, crossed with the *Ai14^Flox* reporter line to follow the *Cre* positive cells which are red because of tdTomato. In this way we could examine the numbers and distribution of cells generated from the Shh expressing lineage. Using this approach we found no clear differences in the distribution and numbers of cells generated from Shh expressing cells at E18.5 (Figure 9, A-D) (Figure 9, arrowheads in B and D). However, as the *Shh^GFPCre* also has GFP expression under the Shh promoter, we can also follow the cells that are actually expressing the protein at that age. We didn't find any expression of GFP in cells close to the dVZ so we are unable to identify the specific source of Shh that might affect the ectopic distribution of Gli1+ cells.
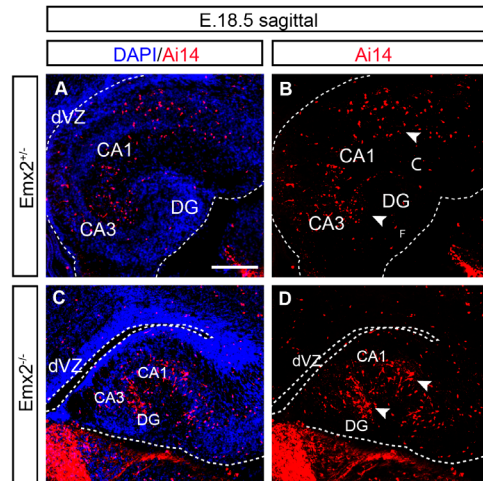
Figure 9: The expression of Shh in the hippocampus. Sagittal sections through the dorsal hippocampus of E18.5 (A-D) $Emx2^{-/+};Shh^{CREGFP};Ai14F^{/+}$ (A, B) and $Emx2^{-/-};Shh^{CREGFP};Ai14F^{/+}$ (C, D) embryos showing the expression of Ai14 under Shh promoter. (CA1, *Cornus Ammonis* 1, CA3 *Cornus Ammonis* 3, DG, dentate gyrus, dVZ, dorsal ventricular zone). Scale bar (in A) A-D, 100 µm.

11.6. The $Emx2^{-/-}$ mutant mice have defects that affect to the source of NSC in the ventral hippocampus

Next we studied the role of Emx2 gene in the VZ of the ventral hippocampus (vVZ). The histological analysis of the vVZ and the expression pattern of *Gli1* revealed a reduction in the number of Gli1+ cells as well as the size of the ventricle at E13.5, E15.5 and E18.5 in the $Emx2^{-/-}$ mutant mice (Figure 2). To pinpoint what kind of cells were affected we performed a broad characterization of the cells in this region. Immunohistochemistry performed at E18.5 of glial markers as GFAP, Blbp, or progenitors as Nestin and Sox2 showed a reduction in their expression in the $Emx2^{-/-}$ mutant mice compared to controls (Figure 10, A-F, I, J). We also observed a reduction in the number of the intermediate progenitors, labeled by Tbr2, and the general mitotic marker BrdU. Hence we concluded the loss of *Emx2* leads to a reduction of the number of progenitor cells and cell division in the vVZ. In chapter 1, we described that Gli1 positive cells originated in the vVZ during the last week of gestation migrate from the caudal (temporal pole) to the dorsal (septal pole) to populate the DG and be part of the SGZ, These cells become the long-lived neural stem cells (LL-NSC). We wished to investigate whether the reduction of progenitor cells and the

divisions in the vVZ in the *Emx2^(-/-)* mutant mice could be also affecting to the population of LL-NSC. As explained before, we cannot follow *Emx2^(-/-)* mutant mice after birth, but we were able to describe defects when they first appear at E17.5, and follow them to E18.5 (Figure 4, A-L). We performed fate-mapping experiments by injecting tamoxifen at E17.5 and analyzing one day later the number and location of the cells originating from Gli1+ cells in the *Emx2* transgenic mice. E18.5 *Emx2^(-/-);Gli1^(CreER-2)* mutant mice showed a reduction of Ai14 recombinant cells in the vVZ compared to controls. We also explored the migratory pathway of the Gli1+ cells (Figure 3, C, D) born in the vVZ and found Ai14+ cells en route to the DG in controls (Figure 3, C), whereas in the *Emx2^(-/-)* mutant mice we found no cells in this migratory route (Figure 3, D). These data provide evidence that *Emx2* is required for the generation and migration of the Gli1+ cells.
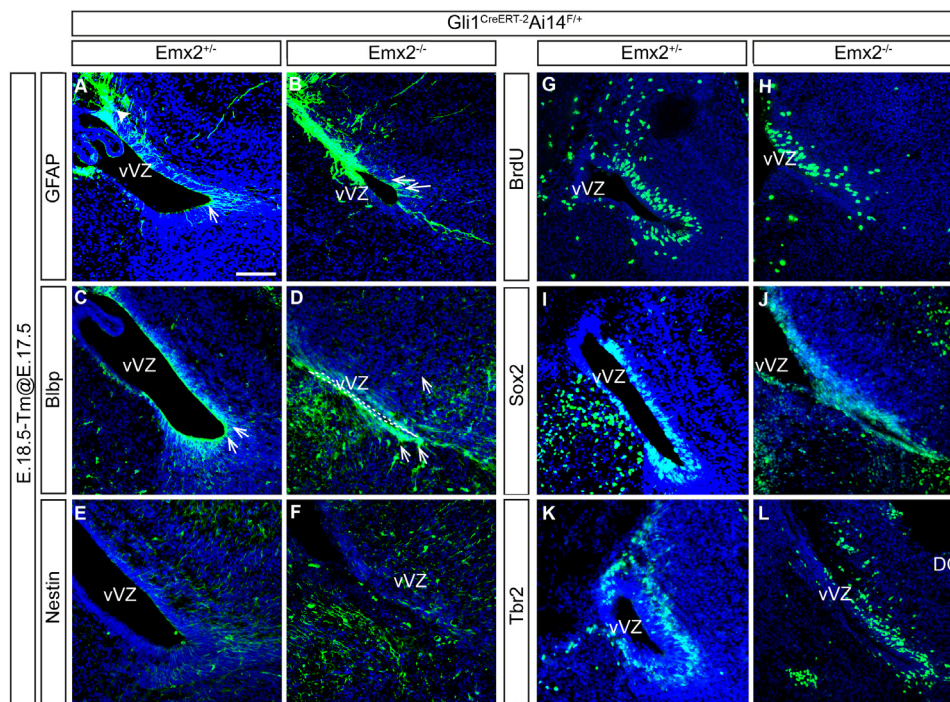
Figure 10: The vVZ of the *Emx2^(-/-)* mutant mice is smaller and the ventricle is thinner than the wt mice. Sagittal sections of ventral hippocampus in *Emx2^(+/-)* control mice, (A, B, C, G, H and I) and *Emx2^(-/-)* mutant mice (D, E, F, J, K and L) at E18.5 showing the expression of diverse markers in vVZ with GFAP (A and D), Blbp (B and E), Nestin (C and F), BrdU (G and J), Sox2 (H and K) and Tbr2 (I and L). (CA1, *Cornus Ammonis* 1, CA3 *Cornus Ammonis* 3, DG, dentate gyrus, F, fimbria, dVZ, dorsal ventricular zone of the hippocampus; arrowhead,

recombinant cells expressing Ai14; arrow, cells colocalizing Ai14 with one of the analyzed maker). Scale bar (in A) A-L, 50µm.

11.7. Loss of *Emx2* leads a reduction of *Shh+* cell density in the amygdalo-hippocampal region

Previous data have suggested that Shh is required for the origin and maintenance of the LL-NSC (Han et al. 2008; Ihrie et al. 2011; Li et al. 2013). In order to understand if the reduction in the number of Gl1+ progenitor cells was regulated directly by the *Emx2* gene or indirectly through Shh we then next analyzed the expression pattern of Shh in the *Emx2* mutant mice. To perform the analysis we used the *Emx2; Shh*^{CreGFP} crossed with the *AI14* reporter line where GFP expression shows the present activity of *Shh* and the Tdtomato the activity at any time (present or past). We found a reduction by half of the density of GFP+ and Tdtomato+ cells in the amydalo-hippocampal region of the *Emx2*$^{-/-}$*; Shh*^{CreGFP} mutant mice at E18.5 compared to controls (Figure 11), this was associated with apoptosis at the same age in the same region (Figure 10). Hence we conclude that *Emx2* is crucial for the survival of the Shh+ cells in the amydalo-hippocampal region and most likely reduction of Shh protein contributes in the origin and maintenance failure of the Gli1+ cells.
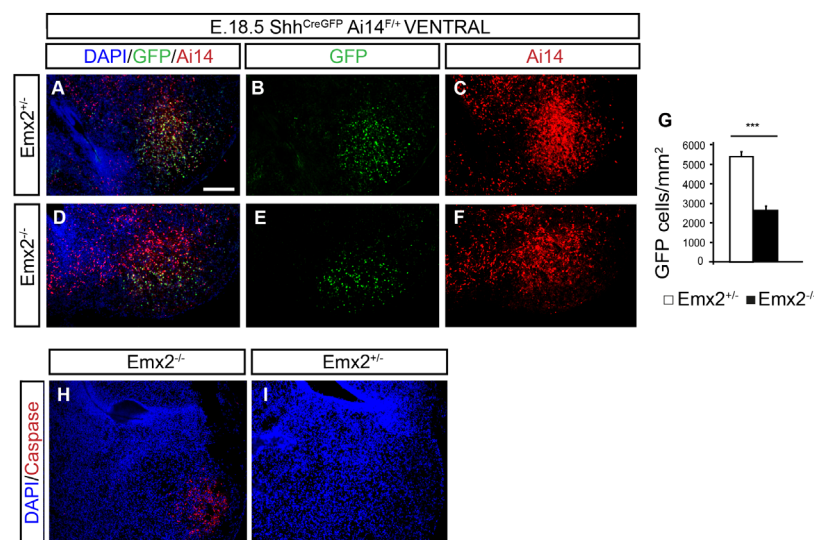
Figure 11: Loss of *Emx2* lead to a reduction of the Shh+ cells in the amygdalo-hippocampal region. Sagittal sections through the amygdalo-hippocampal region showing the expression of Ai14 (A, C, D, F), GFP (A, B, D, E), DAPI (A, D) and caspase in *Emx2*$^{-/+}$*;Shh*^{CREGFP}*;Ai14F*$^{/+}$ (A-C) and *Emx2*$^{-/-}$*;Shh*^{CREGFP}*;Ai14F*$^{/+}$ (C-F) mutant mice at E18.5 (A-F) Scale bar (in A) A-D, H, I

100µm.

DISCUSSION

12. Ventricular zone of the ventral hippocampus a new origin of the LL-NSC

It has been assumed in the literature that the NSCs that will populate the SGZ in the adult come from the dentate neuroepithelium at the equivalent longitudinal level (Altman & S. a Bayer 1990; Eckenhoff & Rakic 1984; Li & Pleasure 2005). Recently it has been shown that Shh plays an important role in the development of the SGZ of the hippocampus (Breunig et al. 2008; Han et al. 2008; Machold et al. 2003) and failures in its signaling pathway lead to a decrease of the SGZ but without showing a complete loss of granule cells. All these data suggested to us that there could be another source of the NSCs. The study of the cells responding to Shh with the transgenic line *Gli1nLacZ* at perinatal stages showed the localization of Gli1+ cells in the ventricular zone of the amygdalo-hippocampal region during late gestation and a gradient of cells in a temporo-septal direction that pointed at the ventricular zone of the ventral hippocampus as a possible origin for the embryonic LL-NSC.

In order to demonstrate the ventral origin of the LL-NSC we perform genetic fate mapping experiments with the Gli1CreERT-2 crossed with the reporter mice Ai14F/F. Thus, under tamoxifen induction we were able to follow the recombinant cells that were positive for Gli1 (i.e. embryonic NSCs) (Ahn & Joyner 2005; Joyner & Zervas 2006) throughout hippocampal development. Our fate mapping results after tamoxifen induction at E17.5 showed that the cells are able to reach all DG levels at postnatal ages. Also, experiments performed with *Gli1nLacZ*; Gli1CreERT-2; AI14F/F transgenic mice allowed us to compare at P0 the population of Tdtomato+ cells induced at E17.5 after a tamoxifen injection with the LacZ+ cells at P0 where we observed that there are two separated populations of cells, the ventral population that reach more septal levels before the local cells in the dorsal dentate start to respond to Shh.

13. Dorsal and Ventral LL-NSC populations respond to Shh from different sources

Ventral and dorsal populations of cells are responding to two different sources of Shh. The experiments with the $Gli1^{LacZ};Emx1^{Cre}; Smo^{F/F}$ KO (the Shh receptor) and $Gli1^{LacZ};Emx1^{Cre}; Shh^{F/F}$ KO confirm those results showing that when we removed the *Smo* receptor from the *Emx1* domain, both population of Shh responding cells are affected whereas in mice Emx1; Shh KO the local population of Gli1+ cells is affected, while the ventral population is almost intact. That was confirmed for the fact that *Gli1LacZ+* cells were completely absent of the $Gli1^{LacZ};Emx1^{Cre}; Shh^{F/F}$ KO transgenic mice.

14. The lack of *Emx2* alters the population of the cells that respond to Shh in the hippocampus

The identification of the origin of the LL-NSC in the ventricular zone of the ventral hippocampus, their posterior migration through the longitudinal axis and the distinct source of *Shh* involved in the formation of the SGZ, are important observations allowing us to better understand hippocampal and the SGZ development. The analysis of the expression pattern of cells that respond to Shh is a powerful tool to elucidate the embryonic origin of the cells that will became the NSCs in the adult SGZ (Ahn & Joyner 2005). These cells, unlike SVZ NSCs, are born embryologically in a different region from where they will settle in the adult (Altman & S. a Bayer 1990). One of the many questions remaining is to identify the molecular mechanisms involved in the origin and migration of the LL-NSC. The analysis of genes expressed in the ventral hippocampus and in the amygdalo-hippocampal region directed us to study the $Emx2^{-/-}$ mutant mice as a tool to understand the development of the

LL-NSC. As we explain in chapter 1, the analysis of *Shh* responding and expressing cells with the transgenic mice *Gli1^{nlacZ}* and *Gli1^{CRE-ERT2}* and *Shh^{CreGFP}* facilitates the identification of the LL-NSCs during their development in the hippocampus..

Loss of *Emx2* produces prominent defects in the hippocampus and DG and consequently in the SGZ where the LL-NSCs will settle. In this context, the analysis of the expression pattern of Shh responding cells appeared altered. Gli1+ cells in the *Emx2^{-/-}; Gli1^{nLacZ}* mice at E18.5 compared to the control revealed differences not only in the dorsal hippocampus, where Gli1+ cells in controls first appear at E17.5 (Li et al. 2013), but also in the ventral hippocampus, where the cells that will originate the LL-NSCs and will later populate the SGZ are drastically decreased in number. These results are corroborated with the short-term fate map of *Emx2^{-/-}; Gli1Cre^{-ERT-2}* crossed with the reporter line *Ai14^{F/F}* upon tamoxifen induction at E17.5 and analyzed 24h later. The defects found in mice without *Emx2* are already well described (Tole et al. 2000; Shinozaki et al. 2004; Gangemi et al. 2006; Zhao, Kraemer, Oldekamp, Cankaya, et al. 2006). The shape and size of the hippocampus is modified and reduced and the DG is almost missing in these mutants (Oldekamp et al. 2004; Pellegrini et al. 1996b; Tole et al. 2000; Simeone et al. 1992). Our analysis of Gli1 expression showed no Gli1+ cells in the hippocampal plate at E18.5, in the DG or in the transitional hippocampus where Gli1+ cells are already present in control mice, in their way to reach the dorsal dentate and the SGZ. Also it is well known that *Emx2^{-/-}* mutant mice showed a loss of GC, described as a diminished in the number or indeed lack of Prox1+ cells (Oldekamp et al. 2004), that is in agreement with the lack of cells Gli1+ in route to reach the dorsal dentate.

A population of Gli1+ cells was found in the VZ/SVZ of the dorsal hippocampus. This ectopic population of cells was already settled in earlier stages during development, suggesting that those cells are starting to respond to *Shh* early than the cells that will populate de dentate in the control mice. One possibility could be that the shift in the patterning that is affecting to the cortex (Zembrzycki et al. 2007; Hamasaki, Leingärtner, Ringstedt &

O'Leary 2004; Cecchi 2002; O'Leary et al. 2007) could also affect the cells originated in the ventral part and now appear in more dorsal region but maintaining ventral properties as the ability to respond to *Shh*.

The analysis of this ectopic population showed a mix of proliferating cells or secondary progenitors that colocalized with the recombinant protein Tdtomato. The lack of Ai14+ in this region in the control mice agrees with our previous studies where we demonstrate that recombinant Ai14+ cells are arriving at E18.5 at the DG and are found also in the transitional hippocampus, but not in other regions of the hippocampus as dVZ (Li et al. 2013). We then found differences in that area between the number of cells that express mitotic markers as PH3, proliferating cells as Ki67 or BrdU. Ki67 as much as BrdU didn't show a statistically significant difference, probably due to a small number of samples but in both cases the tendency was clear for an accumulation of cells dividing in the VZ/SVZ.

Also Tbr2, as a marker of secondary progenitors was augmented in the mutant versus the control mice, causing a SV/SVZ that is thicker in the mutant mouse than the control. Previous studies shown also an accumulation of proliferating cells in that area in *Emx2*$^{-/-}$ mutant mice, suggesting that the progenitors are arrested in that area and that the secondary matrix (or SVZ) is not developed in the mutant (Oldekamp et al. 2004). Nevertheless, the differences are not only in the SVZ adjacent to the dentate neuroepithelium, but also in the hippocampal neuroepithelium pointing at the idea that these cells are not only cells that would populate the DG and the SGZ but progenitors that could belong to different lineage of hippocampal cells that failed to migrate and might switch on their ability to respond to Shh induced by the changes of signals in the mutant hippocampus. Nevertheless, we found no differences between mutant and control mice when we analyzed the expression of *Shh*.

Migrating of cells in the development of the hippocampus is mainly a process depending on radial glia cell. As we have shown and it has been reported before (Oldekamp et al. 2004; Zhao, et al. 2006), the analysis of

GFAP and Blbp populations showed cells with very disorganized fibers. The defect of the fibers that would guide the neural progenitors, not only in the DG but also for the hippocampus, to reach their final destination can also cause the arrest of cells in the VZ/SVZ avoiding the formation of a clear SVZ separated from the VZ in the dorsal hippocampus.

15. The ventricular zone of the ventral hippocampus is reduced in the Emx2-/- mutant mice

As we already have shown, the cells originated in the VZ of the ventral hippocampus are the LL-NSC that will populate the SGZ. This population of cells responds to the source of Shh located in the amygdala and has to migrate to reach the SGZ not only to the ventral DG but also to the dorsal one. The VZ of the ventral hippocampus is smaller in the $Emx2^{-/-}$ mutant than the control mice suggesting that the population of embryonic NSC could be also affected. Our results in the study of the progenitor cell pool by different markers as Nestin, GFAP or Sox2 show a decreased of them confirming our previous hypothesis. We also observed a decrease in mitotic cells in the VZ contributing to the reduction of the progenitor and postmitotic cell pool. Also our results of the fate map of E17.5 upon tamoxifen induction in the $Emx2^{-/-}$ mutant mice showed fewer Tdtomato+ cells in the vVZ corroborating the histological studies.

Since we have proved that *Shh* plays a role in the development of the SGZ (Breunig et al. 2008; Han et al. 2008; Machold et al. 2003) and most likely the source of *Shh* in the amygdala is the one involved in the origin and maintenance of the LL-NSC originated in the VZ of the ventral hippocampus (Li et al. 2013), we checked the status of the *Shh* producing cells in the amygdala. The results showed a reduction in the density of GFP+ cells in the $Shh^{CreGFP};Emx2^{-/-}$ transgenic mice and an increased of Caspase+ cells in the amygdala region. Our results showed *Emx2* gene is necessary for the survival

of the cells in the amygdala, which produce Shh. Although we cannot confirm that the Shh from the amygdala region is the one that controls the proliferation and maintenance of the vVZ NSC, all data point in that direction. Further experiments should be address to confirm this hypothesis.

CONCLUSIONS

Conclusions

1. The ventricular zone of the ventral Hippocampus is the embryonic origin of the neural stem cells which populate the subgranular zone after a long migration to reach the Dentate Gyrus.

2. *Shh* is the only ligand from the Hh family required for the Hh-responding cells originated in the ventral hippocampus.

3. Distinct cortical and extracortical (Amygdala) sources of Shh control the origin and maintenance of both ventral and dorsal NSC of the DG.

4. *Shh* from pallial sources and not from the septum is the only responsible to regulate and maintain the SGZ of the DG at postnatal stages.

5. The loss of *Emx2* causes a decrease in the cells responding to *Shh* in the ventricular zone of the ventral hippocampus and an ectopic expression in the ventricular zone of the dorsal hippocampus.

6. Lack of *Emx2* affect the cell cycle dynamics of progenitors along the ventricular zone of the dorsal hippocampus, where an increase in proliferative cells were observed in the $Emx2^{-/-}$ mutant mice compared to the control.

7. The reduction in the ventricular zone size of the ventral hippocampus in the $Emx2^{-/-}$ mutant mice entails a decrease in the number of progenitor cells.

115

8. *Emx2* is involved in the maintenance and survival of Shh+ cells in the amygdalo-hippocampal region.

Conclusiones

1. La zona ventricular del hipocampo ventral es el origen embrionario de las células madre neurales que poblarán la zona subgranular tras una larga migración, hasta alcanzar el Giro Dentado.

2. *Shh* es el único ligando de la familia Hh requerido por las células que responden a Hh originadas en el hipocampo ventral.

3. Distintas fuentes de *Shh* corticales y extra-corticales (amígdala) controlan el origen y mantenimiento de las células madres neurales del Giro Dentado tanto ventrales como dorsales.

4. *Shh* proveniente de las fuentes paliales y no del septo, es el único responsable de regular y mantener la zona subgranular del Giro Dentado en edades posnatales.

5. La pérdida de *Emx2* produce una disminución de las células que responden a *Shh* en la zona ventricular del hipocampo ventral y una expresión ectópica en la zona ventricular del hipocampo dorsal.

6. La falta de *Emx2* afecta la dinámica del ciclo celular de los progenitores a lo largo de la VZ del hipocampo dorsal, donde se observó un

116

aumento en las células proliferativas en los ratones mutantes *Emx2^{-/-}* en comparación con el control.

7. La reducción en el tamaño de la zona ventricular del hipocampo ventral en el ratón mutante *Emx2^{-/-}* conlleva a su vez una disminución en el número de progenitores.

8. *Emx2* participa en el mantenimiento y supervivencia de las células productoras de Shh en la región amigdalo-hipocámpica.

BIBLIOGRAPHY

Ables, J.L. et al., 2010. Notch1 Is Required for Maintenance of the Reservoir of Adult Hippocampal Stem Cells. *Journal of Neuroscience*, 30(31), pp.10484–10492.

Ahn, S. & Joyner, A.L., 2005. In vivo analysis of quiescent adult neural stem cells responding to Sonic hedgehog. *Nature*, 437(7060), pp.894–7.

Altman, J. & Bayer, S.A., 1990a. Mosaic organization of the hippocampal neuroepithelium and the multiple germinal sources of dentate granule cells. *The Journal of comparative neurology*, 301(3), pp.325–42.

Altman, J. & Bayer, S.A., 1990b. Prolonged sojourn of developing pyramidal cells in the intermediate zone of the hippocampus and their settling in the stratum pyramidale. *Journal of Comparative Neurology*, 301, pp.365–381.

Altman, J. & Bayer, S. a, 1990. Migration and distribution of two populations of hippocampal granule cell precursors during the perinatal and postnatal periods. *The Journal of comparative neurology*, 301(3), pp.365–381.

Altman, J. & Das, G.D., 1965. Autoradiographic and histological evidence of postnatal hippocampal neurogenesis in rats. *The Journal of comparative neurology*, 124(3), pp.319–35.

Amaral, D.G., 1978. A Golgi study of cell types in the hilar region of the hippocampus in the rat. *The Journal of comparative neurology*, 182(4 Pt 2), pp.851–914.

Amaral, D.G., Scharfman, H.E. & Lavenex, P., 2007. The dentate gyrus: fundamental neuroanatomical organization (dentate gyrus for dummies). *Progress in Brain Research*, 163.

Amaral, D.G. & Witter, M.P., 1989. The three-dimensional organization of the hippocampal formation: A review of anatomical data. *Neuroscience*, 31(3), pp.571–591.

Angevine, J.B., 1965a. Time of neuron origin in the hippocampal region. An autoradiographic study in the mouse. *Experimental neurology. Supplement*, p.Suppl 2:1-70.

Angevine, J.B., 1965b. Time of neuron origin in the hippocampal region. An

autoradiographic study in the mouse. *Experimental neurology. Supplement*, p.Suppl 2:1-70.

Armentano, M. et al., 2007. COUP-TFI regulates the balance of cortical patterning between frontal/motor and sensory areas. *Nature neuroscience*, 10(10), pp.1277–1286.

Bayer, S.A., 1980. Development of the hippocampal region in the rat.I. Neurogenesis examined with 3H-thymidine autoradiography. *Journal of Comparative Neurology*, 190, pp.87–114.

Bielle, F. et al., 2005. Multiple origins of Cajal-Retzius cells at the borders of the developing pallium. *Nature neuroscience*, 8(8), pp.1002–12.

Bishop, K.M. et al., 2003. Emx1 and Emx2 cooperate to regulate cortical size, lamination, neuronal differentiation, development of cortical efferents, and thalamocortical pathfinding. *The Journal of comparative neurology*, 457(4), pp.345–60.

Bishop, K.M., Goudreau, G. & O'Leary, D.D., 2000. Regulation of area identity in the mammalian neocortex by Emx2 and Pax6. *Science (New York, N.Y.)*, 288(5464), pp.344–349.

Blank, U. et al., 2008. Signaling pathways governing stem-cell fate. *Blood*, 111(2), pp.492–503.

Bond, A.M. et al., 2014. BMP Signaling Regulates the Tempo of Adult Hippocampal Progenitor Maturation at Multiple Stages of the Lineage. *STEM CELLS*, 32(8), pp.2201–2214.

Breunig, J.J. et al., 2007. Notch regulates cell fate and dendrite morphology of newborn neurons in the postnatal dentate gyrus. *Proceedings of the National Academy of Sciences of the United States of America*, 104(51), pp.20558–63.

Breunig, J.J. et al., 2008. Primary cilia regulate hippocampal neurogenesis by mediating sonic hedgehog signaling. *Proceedings of the National Academy of Sciences of the United States of America*, 105(35), pp.13127–32.

Brill, M.S. et al., 2009. Adult generation of glutamatergic olfactory bulb interneurons. *Nature neuroscience*, 12(12), pp.1524–33.

Broadbent, N.J., Squire, L.R. & Clark, R.E., 2004. Spatial memory, recognition memory, and the hippocampus. *Proc. Natl. Acad. Sci.*, 101, pp.14515–14520.

Brunelli, S. et al., 1996. Germline mutations in the homeobox gene Emx2 in patients with severe schizencephaly. *Nat.Genet.*, 1, pp.94–96.

Burgess, N., Maguire, E.A. & O'Keefe, J., 2002. The human hippocampus and spatial and episodic memory. *Neuron*, 35, pp.625–641.

Caronia-Brown, G. et al., 2014. The cortical hem regulates the size and patterning of neocortex. *Development (Cambridge, England)*, 141(14), pp.2855–65.

Caronia, G. et al., 2010. Bone morphogenetic protein signaling in the developing telencephalon controls formation of the hippocampal dentate gyrus and modifies fear-related behavior. *The Journal of neuroscience : the official journal of the Society for Neuroscience*, 30(18), pp.6291–301.

Charytoniuk, D. et al., 2002. Sonic Hedgehog signalling in the developing and adult brain. *Journal of physiology, Paris*, 96(1–2), pp.9–16.

Chiang, C. et al., 1996. Cyclopia and defective axial patterning in mice lacking Sonic Hedgehog gen function. *Nature*, 383, pp.407–413.

Cobos, I. et al., 2005. Mice lacking Dlx1 show subtype-specific loss of interneurons, reduced inhibition and epilepsy. *Nature Neuroscience*, 8(8), pp.1059–1068.

Codega, P. et al., 2014. Prospective identification and purification of quiescent adult neural stem cells from their in vivo niche. *Neuron*, 82(3), pp.545–59.

Colasante, G. & Sessa, A., 2010. Last but not least: cortical interneurons from caudal ganglionic eminence. *The Journal of neuroscience : the official journal of the Society for Neuroscience*, 30(22), pp.7449–7450.

Dahmane N, R.-A.A., 1999. Sonic hedgehog regulates the growth and patterning of the cerebellum. *Development*, 126, pp.3089–3100.

Dalton, D., Chadwick, R. & McGinnis, W., 1989. Expression and embryonic function of empty spiracles: a Drosophila homeo box gene with two

patterning functions on the anterior-posterior axis of the embryo. *Genes & development*, 3(12A), pp.1940–56.

Davies JE, M.R., 2001. Local Sonic hedgehog signaling regulates oligodendrocyte precursor appearance in multiple ventricular zone domains in the chick metencephalon. *Dev Biol*, 233, pp.513–525.

Deacon, R.R.J. et al., 2002. Effects of cytotoxic hippocampal lesions in mice on a cognitive test battery. *Behav. Brain Res.*, 133, pp.57–68.

Deisseroth, K. et al., 2004. Excitation-neurogenesis coupling in adult neural stem/progenitor cells. *Neuron*, 42(4), pp.535–52.

Doetsch, F. & Alvarez-Buylla, A., 1996. Network of tangential pathways for neuronal migration in adult mammalian brain. *Proceedings of the National Academy of Sciences of the United States of America*, 93(25), pp.14895–900.

Dranovsky, A. & Hen, R., 2006. Hippocampal neurogenesis: regulation by stress and antidepressants. *Biological psychiatry*, 59(12), pp.1136–43.

Echelard, Y. et al., 1993. Sonic hedgehog, a member of a family of putative signaling molecules, is implicated in the regulation of CNS polarity. *Cell*, 15, pp.1417–1430.

Eckenhoff, M.F. & Rakic, P., 1984. Radial organization of the hippocampal dentate gyrus: a Golgi, ultrastructural, and immunocytochemical analysis in the developing rhesus monkey. *The Journal of comparative neurology*, 223(1), pp.1–21.

Encinas, J.M. et al., 2011. Division-coupled astrocytic differentiation and age-related depletion of neural stem cells in the adult hippocampus. *Cell stem cell*, 8(5), pp.566–79.

Eriksson, P.S. et al., 1998. Neurogenesis in the adult human hippocampus. *Nature medicine*, 4(11), pp.1313–7.

Ernst, A. et al., 2014. Neurogenesis in the striatum of the adult human brain. *Cell*, 156(5), pp.1072–83.

Faigle, R. & Song, H., 2013. Signaling mechanisms regulating adult neural

stem cells and neurogenesis. *Biochimica et biophysica acta*, 1830(2), pp.2435–48.

Flames, N. et al., 2004. Short- and long-range attraction of cortical GABAergic interneurons by neuregulin-1. *Neuron*, 44(2), pp.251–61.

Flames, N. & Marín, O., 2005. Developmental mechanisms underlying the generation of cortical interneuron diversity. *Neuron*, 46(3), pp.377–81.

Freund, T.F. Buzsáki, G., 1996. No Title. *Hippocampus*, 6(4), p.345.

Fuchs, E., Tumbar, T. & Guasch, G., 2004. Socializing with the Neighbors: Stem Cells and Their Niche. *Cell*, 116, pp.769–778.

Fukuchi-Shimogori, T. & Grove, E. a, 2003. Emx2 patterns the neocortex by regulating FGF positional signaling. *Nature neuroscience*, 6(8), pp.825–831.

Furuta, Y., Piston, D.W. & Hogan, B.L., 1997. Bone morphogenetic proteins (BMPs) as regulators of dorsal forebrain development. *Development (Cambridge, England)*, 124(11), pp.2203–12.

Gage, F.H., 2002. Neurogenesis in the adult brain. *The Journal of neuroscience : the official journal of the Society for Neuroscience*, 22(3), pp.612–3.

Galceran, J. et al., 2000. Hippocampus development and generation of dentate gyrus granule cells is regulated by LEF1. *Development (Cambridge, England)*, 127(3), pp.469–482.

Gangemi, R.M. et al., 2001. Emx2 in adult neural precursor cells. *Mechanisms of development*, 109(2), pp.323–9.

Gelman, D.M. et al., 2009. The embryonic preoptic area is a novel source of cortical GABAergic interneurons. *The Journal of neuroscience : the official journal of the Society for Neuroscience*, 29(29), pp.9380–9.

Giachino, C. et al., 2014. Molecular diversity subdivides the adult forebrain neural stem cell population. *Stem cells (Dayton, Ohio)*, 32(1), pp.70–84.

Gorski, J.A. et al., 2002. Cortical excitatory neurons and glia, but not GABAergic neurons, are produced in the Emx1-expressing lineage. *The Journal of neuroscience : the official journal of the Society for Neuroscience*, 22(15), pp.6309–14.

Götz, M. & Huttner, W.B., 2005. The cell biology of neurogenesis. *Nature reviews. Molecular cell biology*, 6(10), pp.777–88.

Gould, E. & Cameron, H.A., 1996. Regulation of neuronal birth, migration and death in the rat dentate gyrus. *Developmental neuroscience*, 18(1–2), pp.22–35.

Grove, E. a et al., 1998. The hem of the embryonic cerebral cortex is defined by the expression of multiple Wnt genes and is compromised in Gli3-deficient mice. *Development (Cambridge, England)*, 125(12), pp.2315–2325.

Han, Y.-G. et al., 2008. Hedgehog signaling and primary cilia are required for the formation of adult neural stem cells. *Nature neuroscience*, 11(3), pp.277–84.

Han, Z.-S. et al., 1993. A High Degree of Spatial Selectivity in the Axonal and Dendritic Domains of Physiologically Identified Local-circuit Neurons in the Dentate Gyrus of the Rat Hippocampus. *European Journal of Neuroscience*, 5, pp.395–410.

Hatten, M.E., 1999. Central nervous system neuronal migration. *Annual review of neuroscience*, 22, pp.511–39.

Hébert, J.M. & Fishell, G., 2008. The genetics of early telencephalon patterning: some assembly required. *Nature reviews. Neuroscience*, 9(9), pp.678–685.

Hitoshi, S. et al., 2002. Notch pathway molecules are essential for the maintenance, but not the generation, of mammalian neural stem cells. *Genes and Development*, 16(7), pp.846–858.

Ihrie, R. a. et al., 2011. Persistent Sonic Hedgehog Signaling in Adult Brain Determines Neural Stem Cell Positional Identity. *Neuron*, 71(2), pp.250–262.

Jessberger, S. et al., 2009. Dentate gyrus-specific knockdown of adult

neurogenesis impairs spatial and object recognition memory in adult rats. *Learning & memory (Cold Spring Harbor, N.Y.)*, 16(2), pp.147–54.

Joyner, L. & Zervas, M., 2006. Genetic inducible fate mapping in mouse: establishing genetic lineages and defining genetic neuroanatomy in the ner- vous system. *Developmental Dynamics*, 235, pp.2376–2385.

Kempermann, G., Kuhn, H.G. & Gage, F.H., 1997. More hippocampal neurons in adult mice living in an enriched environment. *Nature*, 386(6624), pp.493–5.

Kessaris, N. et al., 2006. Competing waves of oligodendrocytes in the forebrain and postnatal elimination of an embryonic lineage. *Nature neuroscience*, 9(2), pp.173–9.

Kimura, J. et al., 2005. Emx2 and Pax6 Function in Cooperation with Otx2 and Otx1 to Develop Caudal Forebrain Primordium That Includes Future Archipallium. *Journal of Neuroscience*, 25(21), pp.5097–5108.

Kishi, T. et al., 2006. Topographical projection from the hippocampal formation to the amygdala: A combined anterograde and retrograde tracing study in the rat. *Journal of Comparative Neurology*, 496, pp.349–368.

Kitazawa, A. et al., 2014. Hippocampal pyramidal neurons switch from a multipolar migration mode to a novel "climbing" migration mode during development. *Journal of Neuroscience*, 34, pp.1115–1126.

Kohtz JD, Baker DP, Corte G, F.G., 1998. Regionalization within the mammalian telencephalon is mediated by changes in responsiveness to Sonic hedgehog. *Development*, 125, pp.5079–5089.

König, N. et al., 1977. The time of origin of Cajal-Retzius cells in the rat temporal cortex. An autoradiographic study. *Neuroscience letters*, 4(1), pp.21–6.

König, N. & Schachner, M., 1981. Neuronal and glial cells in the superficial layers of early postnatal mouse neocortex: immunofluorescence observations. *Neuroscience letters*, 26(3), pp.227–31.

Kuwabara, T. et al., 2009. Wnt-mediated activation of NeuroD1 and retro-elements during adult neurogenesis. *Nature neuroscience*, 12(9),

pp.1097–105.

Lavado, A. & Oliver, G., 2014. Jagged1 is necessary for postnatal and adult neurogenesis in the dentate gyrus. *Developmental Biology*, 388(1), pp.11–21.

Lee, S.M. et al., 2000. A local Wnt-3a signal is required for development of the mammalian hippocampus. *Development (Cambridge, England)*, 127(3), pp.457–67.

Li, G. et al., 2009. Identification of a transient subpial neurogenic zone in the developing dentate gyrus and its regulation by Cxcl12 and reelin signaling. *Development (Cambridge, England)*, 136(2), pp.327–335.

Li, G. et al., 2013. The ventral hippocampus is the embryonic origin for adult neural stem cells in the dentate gyrus. *Neuron*, 78(4), pp.658–72.

Li, G. & Pleasure, S.J., 2007. Genetic regulation of dentate gyrus morphogenesis. *Progress in Brain Research*, 163(415).

Li, G. & Pleasure, S.J., 2014. The development of hippocampal cellular assemblies. *Wiley Interdisciplinary Reviews: Developmental Biology*, 3(2), pp.165–177.

Li, Y. et al., 2008. TrkB regulates hippocampal neurogenesis and governs sensitivity to antidepressive treatment. *Neuron*, 59(3), pp.399–412.

Lieberwirth, C. et al., 2016. Hippocampal adult neurogenesis: Its regulation and potential role in spatial learning and memory. *Brain Research*, 1644, pp.127–140.

Lim, D.A. & Alvarez-Buylla, A., 2016. The Adult Ventricular–Subventricular Zone (V-SVZ) and Olfactory Bulb (OB) Neurogenesis. *Cold Spring Harbor Perspectives in Biology*, p.a018820.

Lisman, J.E., 1999. Relating hippocampal circuitry to function: recall of memory sequences by reciprocal dentate-CA3 interactions. *Neuron*, 22(2), pp.233–42.

Lois, C. & Alvarez-Buylla, A., 1994. Long-distance neuronal migration in the adult mammalian brain. *Science (New York, N.Y.)*, 264(5162), pp.1145–

8.

Lorente de Nó, R., 1933. Studies of the structure of the cerebral cortex. I. The area entorhinalis. *J. Psychol. Neurol.*, 45, pp.381–438.

Lorente de Nó, R., 1934. Studies of the structure of the cerebral cortex.II. Continuation of the study of the ammonic system. *J. Psychol. Neurol.*, 46, pp.113–177.

Machold, R. et al., 2003. Sonic hedgehog is required for progenitor cell maintenance in telencephalic stem cell niches. *Neuron*, 39(6), pp.937–950.

Mallamaci, A. et al., 1998. EMX2 protein in the developing mouse brain and olfactory area. *Mechanisms of development*, 77(2), pp.165–72.

Mallamaci, A. et al., 2000. The Lack of Emx2 Causes Impairment of Reelin Signaling and Defects of Neuronal Migration in the Developing Cerebral Cortex. *J. Neurosci.*, 20(3), pp.1109–1118.

Mallamaci, a et al., 2000. Area identity shifts in the early cerebral cortex of Emx2-/- mutant mice. *Nature neuroscience*, 3(7), pp.679–686.

Manent, J.-B. et al., 2006. Glutamate acting on AMPA but not NMDA receptors modulates the migration of hippocampal interneurons. *The Journal of neuroscience : the official journal of the Society for Neuroscience*, 26(22), pp.5901–9.

Mangale, V.S. et al., 2008. Lhx2 selector activity specifies cortical identity and suppresses hippocampal organizer fate. *Science (New York, N.Y.)*, 319(5861), pp.304–309.

Marín, O. & Rubenstein, J.L., 2001. A long, remarkable journey: tangential migration in the telencephalon. *Nature reviews. Neuroscience*, 2(11), pp.780–90.

Merkle, F.T., Mirzadeh, Z. & Alvarez-Buylla, A., 2007. Mosaic organization of neural stem cells in the adult brain. *Science (New York, N.Y.)*, 317(5836), pp.381–4.

Mich, J.K. et al., 2014. Prospective identification of functionally distinct stem

cells and neurosphere-initiating cells in adult mouse forebrain. *eLife*, 3, p.e02669.

Ming, G.-L. & Song, H., 2011a. Adult neurogenesis in the mammalian brain: significant answers and significant questions. *Neuron*, 70(4), pp.687–702.

Ming, G.-L. & Song, H., 2011b. Adult neurogenesis in the mammalian brain: significant answers and significant questions. *Neuron*, 70(4), pp.687–702.

Monuki, E.S. & Walsh, C.A., 2001. Mechanisms of cerebral cortical patterning in mice and humans. *Nature neuroscience*, 4 Suppl, pp.1199–206.

Moreno, N., González, A. & Rétaux, S., 2009. Development and evolution of the subpallium. *Seminars in Cell and Developmental Biology*, 20(6), pp.735–743.

Muzio, L. et al., 2005. A mutually stimulating loop involving Emx2 and canonical Wnt signalling specifically promotes expansion of occipital cortex and hippocampus. *Cerebral Cortex*, 15(12), pp.2021–2028.

Muzio, L. & Mallamaci, A., 2005. Foxg1 confines Cajal-Retzius neuronogenesis and hippocampal morphogenesis to the dorsomedial pallium. *The Journal of neuroscience : the official journal of the Society for Neuroscience*, 25(17), pp.4435–41.

Nacher, J. & McEwen, B.S., 2006. The role of N-methyl-D-asparate receptors in neurogenesis. *Hippocampus*, 16(3), pp.267–70.

Nadarajah, B. et al., 2001. Two modes of radial migration in early development of the cerebral cortex. *Nature neuroscience*, 4(2), pp.143–50.

Nadarajah, B. & Parnavelas, J.G., 2002. Modes of neuronal migration in the developing cerebral cortex. *Nature reviews. Neuroscience*, 3(6), pp.423–32.

Nakahira, E. & Yuasa, S., 2005. Neuronal generation, migration, and differentiation in the mouse hippocampal primordium as revealed by enhanced green fluorescent protein gene transfer by means of in utero electroporation. *Journal of Comparative Neurology*, 483, pp.329–340.

Nery, S., Fishell, G. & Corbin, J.G., 2002. The caudal ganglionic eminence is a source of distinct cortical and subcortical cell populations. *Nature neuroscience*, 5(12), pp.1279–1287.

Neves, G., Cooke, S.F. & Bliss, T.V.P., 2008. Synaptic plasticity, memory and the hippocampus: a neural network approach to causality. *Nature reviews. Neuroscience*, 9, pp.65–75.

Nicola, Z., Fabel, K. & Kempermann, G., 2015. Development of the adult neurogenic niche in the hippocampus of mice. *Frontiers in neuroanatomy*, 9, p.53.

Noctor, S.C. et al., 2004. Cortical neurons arise in symmetric and asymmetric division zones and migrate through specific phases. *Nature neuroscience*, 7(2), pp.136–44.

Noctor, S.C. et al., 2001. Neurons derived from radial glial cells establish radial units in neocortex. *Nature*, 409(6821), pp.714–20.

Oldekamp, J. et al., 2004. bHLH gene expression in the Emx2-deficient dentate cyrus reveals defective granule cells and absence of migrating precursors. *Cerebral Cortex*, 14(9), pp.1045–1058.

Ortiz-Matamoros, A. et al., 2013. Role of wnt signaling in the control of adult hippocampal functioning in health and disease: therapeutic implications. *Current neuropharmacology*, 11(5), pp.465–76.

Oscar Marín et al., 2010. Guiding Neuronal Cell Migrations. *Cold Spring Harbor Perspectives in Biology*, 2(2), pp.1–21.

Parent, J.M. et al., 2006. Aberrant seizure-induced neurogenesis in experimental temporal lobe epilepsy. *Annals of neurology*, 59(1), pp.81–91.

Paridaen, J.T.M.L. & Huttner, W.B., 2014. Neurogenesis during development of the vertebrate central nervous system. *EMBO reports*, 15(4), pp.351–64.

Pellegrini, M. et al., 1996. Dentate gyrus formation requires Emx2. *Development (Cambridge, England)*, 122(12), pp.3893–3898.

Pleasure, S.J. et al., 2000. Cell migration from the ganglionic eminences is required for the development of hippocampal GABAergic interneurons. *Neuron*, 28(3), pp.727–740.

Pleasure, S.J., Collins, A.E. & Lowenstein, D.H., 2000. Unique expression patterns of cell fate molecules delineate sequential stages of dentate gyrus development. *The Journal of neuroscience : the official journal of the Society for Neuroscience*, 20(16), pp.6095–105.

Puelles, L. & Rubenstein, J.L.R., 2015. A new scenario of hypothalamic organization: rationale of new hypotheses introduced in the updated prosomeric model. *Frontiers in neuroanatomy*, 9(March), p.27.

Puelles, L. & Rubenstein, J.L.R., 2003. Forebrain gene expression domains and the evolving prosomeric model. *Trends in neurosciences*, 26(9), pp.469–76.

Rai, K.S., Hattiangady, B. & Shetty, A.K., 2007. Enhanced production and dendritic growth of new dentate granule cells in the middle-aged hippocampus following intracerebroventricular FGF-2 infusions. *The European journal of neuroscience*, 26(7), pp.1765–79.

Rakic, P., 1972. Mode of cell migration to the superficial layers of fetal monkey neocortex. *The Journal of comparative neurology*, 145(1), pp.61–83.

Rakic, P., 1974. Neurons in rhesus monkey visual cortex: systematic relation between time of origin and eventual disposition. *Science (New York, N.Y.)*, 183(4123), pp.425–7.

Rakic, P. & Nowakowski, R.S., 1981. The time of origin of neurons in the hippocampal region of the rhesus monkey. *Journal of Comparative Neurology*, 196, pp.99–128.

Ribak, C.E. & Seress, L., 1983. Five types of basket cell in the hippocampal dentate gyrus: a combined Golgi and electron microscopic study. *Journal of Neurocytology*, 12(4), pp.577–597.

Rickmann, M., Amaral, D.G. & Cowan, W.M., 1987. Organization of radial glial cells during the development of the rat dentate gyrus. *The Journal of comparative neurology*, 264(4), pp.449–79.

del Río, J.A. et al., 1995. Glutamate-like immunoreactivity and fate of Cajal-Retzius cells in the murine cortex as identified with calretinin antibody. *Cerebral cortex*, 5(1), pp.13–21.

Del Río, J. a et al., 1997. A role for Cajal-Retzius cells and reelin in the development of hippocampal connections. *Nature*, 385, pp.70–74.

Roessler, E. et al., 1996. Mutations in the human Sonic Hedgehog gene cause holoprosencephaly. *Nat.Genet.*, 14, pp.357–360.

Rubin, A.N. et al., 2010. The germinal zones of the basal ganglia but not the septum generate GABAergic interneurons for the cortex. *The Journal of neuroscience : the official journal of the Society for Neuroscience*, 30(36), pp.12050–62.

Sahara, S. et al., 2007. Sp8 exhibits reciprocal induction with Fgf8 but has an opposing effect on anterior-posterior cortical area patterning. *Neural development*, 2, p.10.

Sahay, A., Wilson, D.A. & Hen, R., 2011. Pattern separation: a common function for new neurons in hippocampus and olfactory bulb. *Neuron*, 70(4), pp.582–8.

Savaskan, N.E. et al., 2002. Impaired postnatal development of hippocampal neurons and axon projections in the Emx2-/- mutants. *Journal of Neurochemistry*, 83(5), pp.1196–1207.

Schlessinger, A.R., Cowan, W.M. & Gottlieb, D.I., 1975. An autoradiographic study of the time of origin and the pattern of granule cell migration in the dentate gyrus of the rat. *The Journal of comparative neurology*, 159(2), pp.149–75.

Seki, T. et al., 2014. Distinctive population of Gfap-expressing neural progenitors arising around the dentate notch migrate and form the granule cell layer in the developing hippocampus. *Journal of Comparative Neurology*, 522(2), pp.261–283.

Shimazu, K. et al., 2006. NT-3 facilitates hippocampal plasticity and learning and memory by regulating neurogenesis. *Learning & memory (Cold Spring Harbor, N.Y.)*, 13(3), pp.307–15.

Shimogori, T. et al., 2004. Embryonic signaling centers expressing BMP,

WNT and FGF proteins interact to pattern the cerebral cortex. *Development (Cambridge, England)*, 131(22), pp.5639–5647.

Shinozaki, K. et al., 2004. Emx1 and Emx2 cooperate in initial phase of archipallium development. *Mechanisms of Development*, 121(5), pp.475–489.

Simeone, a et al., 1992. Two vertebrate homeobox genes related to the Drosophila empty spiracles gene are expressed in the embryonic cerebral cortex. *The EMBO journal*, 11(7), pp.2541–2550.

Soriano, E., Cobas, A., Fairen, A., 1986. Asynchronism in the neurogenesis of GABAergic and non-GABAergic neurons in the mouse hippocampus. *Brain Res*, 395, pp.88–92.

Soriano, E. & Frotscher, M., 1989. A GABAergic axo-axonic cell in the fascia dentata controls the main excitatory hippocampal pathway. *Brain Research*, 503(1), pp.170–174.

Soriano, E. & Frotscher, M., 1993. GABAergic innervation of the rat fascia dentata: a novel type of interneuron in the granule cell layer with extensive axonal arborization in the molecular layer. *The Journal of comparative neurology*, 334(3), pp.385–396.

Soriano, E. & Frotscher, M., 1994. Mossy cells of the rat fascia dentata are glutamate-immunoreactive. *Hippocampus*, 4(1), pp.65–69.

Soriano E, Cobas A, F.A., 1989a. Neurogenesis of glutamic acid decarboxylase immunoreactive cells in the hippocampus of the mouse. I. Regio superior and regio inferior. *J Comp Neurol*, 281, pp.586–602.

Soriano E, Cobas A, F.A., 1989b. Neurogenesis of glutamic acid decarboxylase immunoreactive cells in the hippocampus of the mouse. II. Area dentata. *J Comp Neurol*, 281, pp.603–611.

Spalding, K.L. et al., 2013. Dynamics of hippocampal neurogenesis in adult humans. *Cell*, 153(6), pp.1219–27.

Stanfield, B.B. & Cowan, W.M., 1979. The development of the hippocampus and dentate gyrus in normal and reeler mice. *The Journal of comparative neurology*, 185(3), pp.423–59.

Suda, Y., Hossain, Z.M., Kobayashi, C., Hatano, O., Yoshida, M., Matsuo, I. and Aizawa, S., 2001. Emx2 directs the development of diencephalon in cooperation with Otx2. *Development*, 128, pp.2433–2450.

Sur, M. & Rubenstein, J., 2005. Patterning and Plasticity of the Cerebral Cortex. *Science*, 310(215), pp.805–810.

Takiguchi-Hayashi, K. et al., 2004. Generation of reelin-positive marginal zone cells from the caudomedial wall of telencephalic vesicles. *The Journal of neuroscience : the official journal of the Society for Neuroscience*, 24(9), pp.2286–2295.

Tole, S. et al., 2000. Emx2 is required for growth of the hippocampus but not for hippocampal field specification. *The Journal of neuroscience : the official journal of the Society for Neuroscience*, 20(7), pp.2618–2625.

Tole, S. & Grove, E. a, 2001. Detailed field pattern is intrinsic to the embryonic mouse hippocampus early in neurogenesis. *The Journal of neuroscience : the official journal of the Society for Neuroscience*, 21(5), pp.1580–1589.

Tricoire, L. et al., 2011. A blueprint for the spatiotemporal origins of mouse hippocampal interneuron diversity. *The Journal of neuroscience : the official journal of the Society for Neuroscience*, 31(30), pp.10948–70.

Urbán, N. & Guillemot, F., 2014. Neurogenesis in the embryonic and adult brain: same regulators, different roles. *Frontiers in cellular neuroscience*, 8(November), p.396.

Varela-Nallar, L. & Inestrosa, N.C., 2013. Wnt signaling in the regulation of adult hippocampal neurogenesis. *Frontiers in cellular neuroscience*, 7, p.100.

Ventura, R.E. & Goldman, J.E., 2007. Dorsal radial glia generate olfactory bulb interneurons in the postnatal murine brain. *The Journal of neuroscience : the official journal of the Society for Neuroscience*, 27(16), pp.4297–302.

Wang, B., Lufkin, T. & Rubenstein, J.L.R., 2011. Dlx6 regulates molecular properties of the striatum and central nucleus of the amygdala. *Journal of Comparative Neurology*, 519(12), pp.2320–2334.

Wichterle, H. et al., 2001. In utero fate mapping reveals distinct migratory pathways and fates of neurons born in the mammalian basal forebrain. *Development (Cambridge, England)*, 128(19), pp.3759–71.

Wilson, S.W. & Rubenstein, J.L.R., 2000. Induction and Dorsoventral Patterning of the Telencephalon. *Signals*, 28, pp.641–651.

Wray, S. et al., 1994. A subset of peripherin positive olfactory axons delineates the luteinizing hormone releasing hormone neuronal migratory pathway in developing mouse. *Developmental biology*, 166(1), pp.349–54.

Yoshida, M. et al., 1996. Effects of coculture with the septum on the expression of long-term potentiation in organotypic hippocampal slice cultures. *Neuroscience research*, 26(4), pp.377–85.

Yoshida, M. et al., 1997. Emx1 and Emx2 functions in development of dorsal telencephalon. *Development (Cambridge, England)*, 124(1), pp.101–111.

Yoshida, M. et al., 2006. Massive loss of Cajal-Retzius cells does not disrupt neocortical layer order. *Development*, 133, pp.537–545.

Young, K.M. et al., 2007. Subventricular zone stem cells are heterogeneous with respect to their embryonic origins and neurogenic fates in the adult olfactory bulb. *The Journal of neuroscience : the official journal of the Society for Neuroscience*, 27(31), pp.8286–96.

Yozu, M., Tabata, H. & Nakajima, K., 2005. The caudal migratory stream: a novel migratory stream of interneurons derived from the caudal ganglionic eminence in the developing mouse forebrain. *The Journal of neuroscience : the official journal of the Society for Neuroscience*, 25(31), pp.7268–7277.

Zhang, L. et al., 2011. The Wnt/β-catenin signaling pathway in the adult neurogenesis. *The European journal of neuroscience*, 33(1), pp.1–8.

Zhao, C. et al., 2008. Mechanisms and Functional Implications of Adult Neurogenesis. *Cell*, 132(4), pp.645–660.

Zhao, M. et al., 2007. Fibroblast growth factor receptor-1 is required for long-term potentiation, memory consolidation, and neurogenesis. *Biological psychiatry*, 62(5), pp.381–90.

Zhao, T. et al., 2006. Emx2 in the developing hippocampal fissure region. *The European journal of neuroscience*, 23(11), pp.2895–907.

Zhao, Y., 1999. Control of Hippocampal Morphogenesis and Neuronal Differentiation by the LIM Homeobox Gene Lhx5. *Science*, 284(5417), pp.1155–1158.

Zhou, C.-J., Zhao, C. & Pleasure, S.J., 2004. Wnt signaling mutants have decreased dentate granule cell production and radial glial scaffolding abnormalities. *The Journal of neuroscience : the official journal of the Society for Neuroscience*, 24(1), pp.121–6.

ANNEX

Article

The Ventral Hippocampus Is the Embryonic Origin for Adult Neural Stem Cells in the Dentate Gyrus

Guangnan Li,[1,][*] Li Fang,[2] Gloria Fernández,[1] and Samuel J. Pleasure[1,][*]
[1]Department of Neurology, Programs in Neuroscience and Developmental Stem Cell Biology, Institute for Regenerative Medicine, University of California, San Francisco, CA 94158, USA
[2]Epitomics, an Abcam Company, 863 Mitten Road, Suite 103, Burlingame, CA 94010, USA
*Correspondence: grant.li@ucsf.edu (G.L.), sam.pleasure@ucsf.edu (S.J.P.)
http://dx.doi.org/10.1016/j.neuron.2013.03.019

SUMMARY

Adult neurogenesis represents a unique form of plasticity in the dentate gyrus requiring the presence of long-lived neural stem cells (LL-NSCs). However, the embryonic origin of these LL-NSCs remains unclear. The prevailing model assumes that the dentate neuroepithelium throughout the longitudinal axis of the hippocampus generates both the LL-NSCs and embryonically produced granule neurons. Here we show that the NSCs initially originate from the ventral hippocampus during late gestation and then relocate into the dorsal hippocampus. The descendants of these cells are the source for the LL-NSCs in the subgranular zone (SGZ). Furthermore, we show that the origin of these cells and their maintenance in the dentate are controlled by distinct sources of Sonic Hedgehog (Shh). The revelation of the complexity of both the embryonic origin of hippocampal LL-NSCs and the sources of Shh has important implications for the functions of LL-NSCs in the adult hippocampus.

INTRODUCTION

There are two sites of adult neurogenesis in the rodent CNS: the cortical subventricular zone (SVZ) and the dentate subgranular zone (SGZ) in the hippocampal formation. In the dentate gyrus (DG), adult neurogenesis refines network functions by constant addition of new neurons to the granule cell layer (GCL) (Clelland et al., 2009; Li and Pleasure, 2010; Sahay et al., 2011). However, little is known about the developmental program controlling the formation of the neurogenic niche where neurogenesis is sustained in the DG (Altman and Das, 1967). Compared to the SVZ, the most pronounced feature of DG niche development is the complete dissociation of the long-lived neural stem cells (LL-NSCs) in the SGZ from the embryonic germinative zone (Altman and Bayer, 1990a; Li et al., 2009).

Previous studies presumed that the LL-NSCs in the SGZ arise from the neuroepithelium adjacent to the cortical hem during embryonic development of the hippocampus (Li and Pleasure, 2005), either directly translocating from the VZ to the dentate

primordium (Eckenhoff and Rakic, 1984) or indirectly relocating from the migratory stream formed during late gestation (Altman and Bayer, 1990a). This model is somewhat supported by the analysis of mutants defective either in cortical hem development or in the reception of key signals from the cortical hem. The cortical hem is a hippocampal organizer enriched in signaling molecules (such as Wnts and Bmps) that patterns the hippocampal neuroepithelium into functionally distinct subfields (Mangale et al., 2008), including the primordium of the DG. The loss of the transcription factor Lef1, a mediator of the canonical Wnt signaling pathway, results in the underproduction of granule cells perinatally (Galceran et al., 2000; Zhou et al., 2004) and complete loss of the SGZ postnatally (Li et al., 2008). Meanwhile, ectopic upregulation of canonical Wnt signaling in the hippocampal neuroepithelium is sufficient to promote granule cell fate (Machon et al., 2007). These studies provide evidence that Wnt activity is critical for promoting granule cell fate prenatally. However, direct evidence supporting that SGZ LL-NSCs originate from the equivalent septotemporal level of the dentate neuroepithelium is still missing.

Recently, it has become clear that the Hedgehog (Hh) signaling pathway is prominently involved in SGZ development. The ablation of Smo, the obligatory receptor for Hh signaling (Machold et al., 2003), or the impairment of primary cilia, an organelle essential for Hh signaling (Breunig et al., 2008; Han et al., 2008), leads to SGZ deficiency but apparently still allows production of granule neurons at embryonic stages. Fate-mapping analysis also reveals that embryonic dentate NSCs are Hh responsive during late gestation before they populate their permanent niche in the dentate and that quiescent SGZ NSCs are still Hh responsive throughout adulthood (Ahn and Joyner, 2005; Encinas et al., 2011). What is not clear from these studies is whether precursors in the embryonic dentate VZ are the Hh-responding cells and how the Hh-responding NSCs interact with the Hh-producing cells during relocation.

In this study, we set out to determine how Hh signaling controls the formation of the dentate SGZ by investigating when and where NSCs perceive Hh ligands before ultimately settling in the SGZ and, more importantly, to explore the germinative origins of LL-NSCs. We find that SGZ formation requires an extracortical source of Hh during late embryonic stages. More intriguingly, the ventral hippocampus is the main cellular source for the SGZ. Long-term fate-mapping analysis further confirms that the prenatal Hh-responding cells restricted in the amygdalo-hippocampal region contribute to the LL-NSCs of the

SGZ. In contrast to long-held assumptions in the literature, these observations lead to a model that the LL-NSCs from the ventral hippocampus migrate along the longitudinal axis of the hippocampus from temporal to septal poles before settling. Subsequently, local neuronal sources of Shh maintain these LL-NSCs in the SGZ postnatally and throughout adulthood. The results of our study support the idea that the adult dentate gyrus is a mosaic structure. The embryonically produced DGCs from equivalent anatomic levels of the dentate in the septotemporal plane are supplemented by the DGCs whose progenitors originate from the most caudotemporal region of the ventral hippocampus. This raises new questions about the nature of the granule neuron heterogeneity and the regulation of neurogenesis.

RESULTS

Hh-Responsive Cells Are Concentrated in the Ventral Hippocampal Neuroepithelium during Late Gestation

Previous studies reported that during the last week of gestation in rodents, a migratory stream from the dentate neuroepithelium adjacent to the cortical hem courses through the fimbriodentate junction (FDJ) and either assumes a subpial route or fans out into the hilus (Altman and Bayer, 1990a; Li et al., 2009). Prospective NSCs destined for the SGZ are believed to derive from this migratory stream (Altman and Bayer, 1990a) or directly translocate from the dentate primordium (Eckenhoff and Rakic, 1984). Taking into consideration the findings that NSCs responding to Hh can be labeled during late gestation (Ahn and Joyner, 2005; Li et al., 2009) and that Hh-signaling is required to establish SGZ progenitors (Han et al., 2008; Machold et al., 2003), we reasoned that upon perceiving Hh in the dentate VZ or along the migratory stream, precursors are induced or specified to become dentate NSCs. To test this hypothesis, we decided to begin with the Hh-responding line Gli1-nLacZ (Bai et al., 2002) to study the static distribution of Hh-responding cells at the perinatal ages when the prospective SGZ NSCs can be traced by the tamoxifen-inducible line Gli1-CreERT2 (Ahn and Joyner, 2005; Li et al., 2009).

The rodent hippocampus is situated at the mediotemporal edge of the neocortex and straddles the thalamus along its septotemporal axis. Dorsal to the thalamus is the dorsal hippocampus, whereas ventral to the thalamus is the ventral hippocampus. Sagittal sections at different mediolateral levels (shown as schemas in Figures 1A and 1E) allow us to comprehensively examine the distribution of Gli1-nLacZ+ cells throughout the developing hippocampus, including both the dorsal and ventral arms.

To our surprise, at E17.5 Gli1-nLacZ+ cells were basically absent from the dorsal dentate primordium (arrowheads in Figures 1B′ and 1C′). By contrast, Gli1-nLacZ expression occupied the whole VZ of the ventral hippocampus at the far end of the temporal pole (arrowhead in Figure 1B″), about half at the midlevel (arrowhead in Figure 1C″), but only about one-third at the transitional level (arrowhead in Figure 1D′). At the most temporal level, Gli1-nLacZ+ cells were noticeably distributed from VZ to the forming DG (arrow in Figure 1B″).

By postnatal day 0 (P0), Gli1-nLacZ remained absent from the dorsal dentate primordium (arrowheads in Figures 1F′ and 1G′), and only sparse Gli1-nLacZ+ cells were detectable in the dorsal DG (arrows in Figures 1F′ and 1G′). However, Gli1-nLacZ expression now covered the whole VZ of the ventral hippocampus at all levels (arrowheads in Figures 1F″, 1G″, and 1H′). Gli1-nLacZ+ cells were observed in the ventral-forming DG at the more lateral/septal level (arrows in Figure 1G″). At the transitional level, Gli1-nLacZ+ cells were distributed from the ventral to the dorsal arm around the fimbria (arrows in Figure 1H′). The perinatal distribution of Hh-responding cells in the hippocampus prompted us to investigate whether the descendants of these perinatal Hh-responding cells, when most of them are still restricted in the ventral hippocampus by birth, give rise to the NSCs that settle in the SGZ at all septotemporal levels.

Postnatal Fate-Mapping Analysis of Cells Responding to Hh at Prenatal and Perinatal Ages

In our previous study, we showed that some derivatives of the Hh-responding cells labeled at E17.5 constituted the postnatal radial glia in the SGZ of the DG (Li et al., 2009). In light of our finding that Gli1-nLacZ+ cells mostly populated the VZ of the ventral hippocampus at this age, we wished to know how these cells contribute to the dentate gyrus at all septotemporal levels. To address these questions, we turned to fate-mapping analysis using the Gli1-CreERT2 line (Ahn and Joyner, 2004) crossed to the cre reporter line Ai14 (Rosa-CAG-LSL-tdTomato-WPRE) (Madisen et al., 2010). After independent tamoxifen injections at E15.5, E17.5, or P0, the distribution of recombined cells was examined at P15 (Figures 2A–2I). If the recombined cells generate the NSCs eventually located in the SGZ, we would expect that radial NSCs and clusters of granule cells (the progeny of the NSCs) would be labeled by tdTomato (tdT) expression by this age.

When tamoxifen was injected at E15.5, a small number of tdT+ clusters were found in the suprapyramidal blade of the ventral DG (arrowhead in Figure 2A), whereas very few isolated tdT+ cells were seen in the transitional ventral DG (arrow in Figure 2B) and in the dorsal DG (arrows in Figure 2C). When tamoxifen was injected at E17.5, tdT+ clusters were found in the DG at all the septotemporal levels (Figures 2D–2F). At the current dosage of tamoxifen (3 mg/40 g animal), 69% ± 4% of the Blbp+ cells displaying radial orientation in the SGZ were also tdT+ at P15 (Figures S1B, S1B′, and S1C, available online), whereas 61% ± 6% of the Sox2+ cells were also tdT+ (Figure S1A, S1A′, and S1C). The pattern of tdT+ clusters labeled at E15.5 showed minimal overlap with those labeled at E17.5, indicating that the effect of tamoxifen was transient and diminished by 48 hr. When tamoxifen was injected at P0, tdT+ clusters were found in the inner aspect of the GCL in the ventral DG (arrowheads in Figures 2G and 2H, the arrow in Figure 2H indicated the boundary between ventral and dorsal DG). Meanwhile, tdT+ clusters continued to heavily make up the dorsal DG at all levels (Figure 2I). Therefore, the Hh-responding cells in the ventral hippocampus start to make a large contribution to the ventral DG around E15.5 and to the dorsal DG around E17.5.

Progeny of Hh-Responding Cells from the Temporal Pole Arrive in the Dentate Septal Pole ahead of the Appearance of Local Hh-Responding Cells

Static analysis showed that Gli1-nLacZ+ cells were initially concentrated in the ventral hippocampus and then later
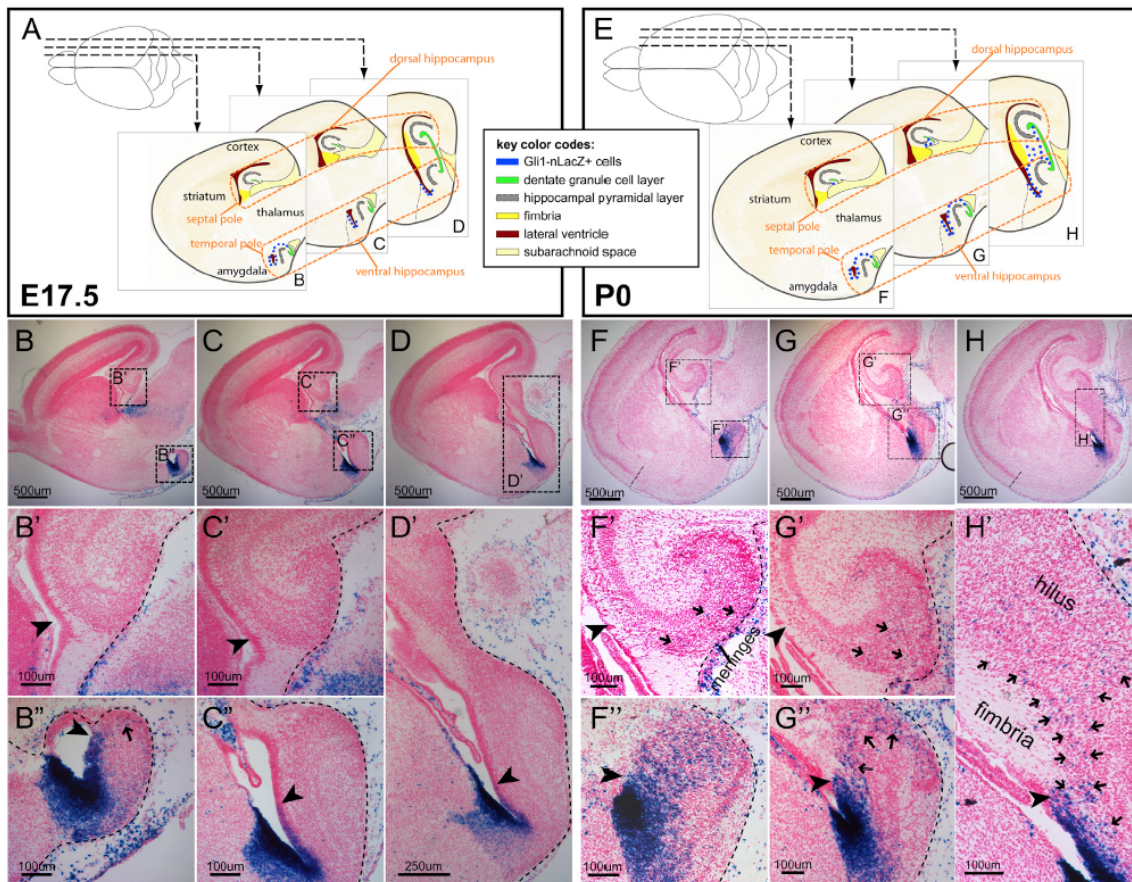
Figure 1. Perinatal Distribution of Gli1-nLacZ Hh-Responding Cells in the Hippocampus

(A) Schemas of Gli1-nLacZ distribution at E17.5 are shown at the three levels of the sagittal sections.

(B–D') From medial to lateral, three levels of sagittal sections for Gli1-nLacZ staining at E17.5 are shown. At E17.5, Gli1-nLacZ expression occupies the whole ventricular zone (VZ) of the ventral hippocampus at the far end of the temporal pole (B″, arrowhead), half at the midlevel (C″, arrowhead), but only one-third at the transitional level (D', arrowhead). A stream of Gli1-nLacZ+ cells from VZ to the dentate pole are noticeable at the end of the temporal pole (B″, arrow). Gli1-nLacZ+ cells are clearly absent in the dorsal dentate primordium (B' and C', arrowheads).

(E) Schemas of Gli1-nLacZ distribution at P0 are shown at the three levels of the sagittal sections.

(F–H') From medial to lateral, three levels of sagittal sections for Gli1-nLacZ staining at P0 are shown. At P0, Gli1-nLacZ expression covers the whole VZ of the ventral hippocampus at all levels (F″, G″, and H', arrowheads). By contrast, Gli1-nLacZ remains absent from the dentate primordium in the dorsal hippocampus (F' and G', arrowheads). At the transitional level, Gli1-nLacZ+ cells spread from ventral to dorsal (H', arrows). Sparse Gli1-nLacZ+ cells are also detected in the dorsal DG, displaying a gradient with the lowest in the septal pole (F', G', and H', arrows).

appeared in the developing DG in a temporal (high)-to-septal (low) gradient. We define these two populations as early Hh-responding cells in the VZ of ventral hippocampus and late Hh-responding cells in the local DG, respectively. The expression of Gli1-nLacZ in the late Hh-responding cells might be due either to the retention of the LacZ protein after they leave their origin or to actively responding to local Shh after they reach the forming DG. We wished to determine the spatial relationship of the progeny of early Hh-responding cells relative to the late Hh-responding cells in the developing DG at birth. To address this, we examined the progeny of the Hh-responding cells

marked by tamoxifen injection at E17.5 after crossing the Gli1-CreERT2 line with Ai14 in the mice also carrying Gli1-nLacZ to identify late Hh-responding cells at the same time points and anatomic levels. At P0, we examined the expression of both tdT and LacZ using alternate sagittal sections covering all septo-temporal dentate levels (the complete data set is in Figure S1D). X-gal staining rather than antibody staining was used to maximize the detection sensitivity for LacZ. Interestingly, at more temporal levels, tdT+ cells (Figure 2M) had a wider distribution than Gli1-nLacZ+ cells (Figure 2J). At more septal levels, tdT+ cells were still present (arrows in Figures 2N, 2N', 2O, and 2O'),

143

whereas nLacZ+ cells were scarce (Figure 2K) or completely absent (Figure 2L) from the dentate plate, despite the presence of nLacZ+ cells in the meninges labeled by Laminin (presumed to be meningeal fibroblasts) (Figure 2M). These results demonstrated that progeny marked at E17.5 with the Gli1-CreERT2 line can reach more septal levels before late Hh-responding cells are established locally at the same septotemporal levels in the developing DG.

The Descendants of the Hh-Responding Cells from the Ventral Hippocampal VZ Display a Continuous Stream into the Dorsal DG

The above data inspired us to determine the spatial connection between the progeny of the Hh-responding cells and the ventral hippocampal VZ. To do this, we initially analyzed the distribution of tdT+ cells 1 day after tamoxifen induction at E16.5 (Figures 3A–3F). We confirmed that heavy recombination indeed occurred in the VZ of temporal hippocampus (oval in Figure 3B) but was completely absent from the VZ of the dorsal dentate (arrowhead in Figure 3C). From temporal to septal hippocampus (arrows in Figures 3B, 3E, 3F, and 3C), the gradient distribution of tdT+ closely mimicked the pattern of Gli1-nLacZ+ cells at the similar age (Figures 1B and 1C).

Then, we analyzed the representative sagittal levels (Figures 3G–3I) and the serial sagittal sections (Figure S2) for the distribution of tdT+ cells at P0 with tamoxifen induction at E17.5. The tdT+ cells formed a continuous stream (arrows in Figure 3G′) from the VZ at the temporal pole of the ventral hippocampus (white oval in Figure 3G′) to the forming ventral dentate GCL, which showed close apposition to the meninges at the ventral fimbriodentate junction (vFDJ) (Figures 3G and 3G′). Of note, the tdT+ cells seen in the mantle of the amygdalo-hippocampal region could have arisen from the amygdalo-hippocampal VZ (oval in Figure 3G′). At the mediolateral level where the dorsal and ventral dentate gyri joined each other (green oval in Figures 3H and 3H′), a large number of tdT+ cells were apparent. The higher cell density in this region probably indicated ongoing local proliferation. In the dorsal hippocampus, most tdT+ cells localized in the dorsal fimbriodentate junction (dFDJ) (green oval in Figures 3I and 3I′), and some of them were distributed further into the hilus at the same longitudinal levels (Figure 3I′). The presence of the tdT+ cells near the upper blade indicated that there might be de novo induction of Hh-responding cells (Figure 3I′). Quite strikingly, the tdT+ cells at the dFDJ had little connection to the dorsal dentate neuroepithelium at any level and this cell population probably represented the "intrinsic component" first described by Altman and Bayer (1990a). All these data taken together reinforce our model (Figure 3J) that the progeny of the Hh-responding cells from the ventral hippocampus VZ feed into the dentate gyrus during late gestation in the temporoseptal direction (red arrow in Figure 3J), initially staying in the vFDJ/dFDJ close to the meninges and then radiating into the hilus before the SGZ forms.

Hh-Responding Cells in the Hippocampus of Hh-Signaling Mutants

What is the anatomic Shh source for the Hh-responding cells in the VZ of the ventral hippocampus? Previous studies suggested that Shh from the subpallial septum might regulate NSCs in the adult DG through the long-range axonal targeting via the septo-hippocampal pathway (Lai et al., 2003). However, it is not clear whether Shh from the septum would regulate the developing DG, particularly at these ages when the septohippocampal projection is not yet fully developed (Supèr and Soriano, 1994). In order to pinpoint the Hh-producing cells that interact with the dentate precursors, we compared the distribution of the Hh-responding cells around birth between Emx1cre-Shh and Emx1cre-Smo conditional mutants. If other Hh members (Dhh or Ihh) within the Emx1 domain or Hh sources (Shh or other members) outside the Emx1 domain (essentially the dorsal forebrain) were required for the development of the DG, Hh-responding cells would be expected to be unaffected in the Emx1cre-Shh cKO.

By crossing Emx1cre to the cre reporter Rosa-Yfp, we confirmed that at P1 Emx1-cre showed recombination in the ventral hippocampus (Figure 4B), including its VZ (Figures S3B and S3B′). By P1, Gli1-nLacZ+ cells were found in the dorsal DG of the wild-type control (Figure 4C) but were mostly absent from the Emx1-Shh cKO at the same anatomical level (Figure 4E). When one copy of the Gli1-nLacZ was present, Gli1-nLacZ+ cells were completely abolished throughout the DG along the whole longitudinal axis in both Emx1-Shh and Emx1-Smo cKOs (Figures 4E–4H). However, the Gli1-nLacZ+ cells in the VZ of the ventral hippocampus were entirely missing only in Emx1-Smo mutants (arrowheads in Figure 4H′), not Emx1-Shh mutants (arrowheads in Figure 4F′), even though they were not as abundant as in the control (arrowheads in Figure 4D′). In the Emx1-Shh cKO, Gli1-nLacZ+ cells (likely due to the slow turnover of nLacZ) were also detected in a region slightly away from the VZ of the ventral hippocampus (arrows in Figure 4F′), as in the control (arrows in Figure 4D′).

It has been reported that Gli1-nLacZ expression is affected by the functional copy number of Shh (Garcia et al., 2010). We reasoned that different copy numbers of Shh and Gli1-nLacZ would give us further insights into the formation of Gli1-nLacZ+ cell stream from the VZ of the ventral hippocampus and the de novo induction of Hh-responding cells in the forming DG. To facilitate the analysis, the developing dorsal dentate can be divided into upper and lower portions by a line connecting the tip of the CA3 field and the apex of the dentate pole. In relation to the $Gli1^{Z/+};Shh^{F/F}$ animals (Figures S3D, S3D′, S3E, and S3E′), when one copy of the Shh flox allele was replaced with an Shh null allele in the $Gli1^{Z/+};Shh^{F/-}$ animals, the number of Gli1-nLacZ+ cells in the dorsal dentate was dramatically reduced in both portions (Figures S3F and S3F′), the Gli1-nLacZ expression showed a decreased level in the VZ of the ventral hippocampus, and the stream of the Gli1-nLacZ+ cells emanating from the VZ was also reduced (Figures S3G and S3G′). Interestingly, all of these phenotypes could be restored in the $Gli1^{Z/Z};Shh^{F/F}$ animals when an extra copy of Gli1-nLacZ was present (Figures S3H, S3H′, S3I, and S3I′). However, when the remaining Shh flox allele was floxed out in the Emx1 domain in the $Emx1^{cre/+};Gli1^{Z/Z};Shh^{F/-}$ animals, most of the Gli1-nLacZ+ cells were abolished in the upper portion of the dorsal dentate, whereas residual Gli1-nLacZ+ cells were still present at the entrance of the hilus in the lower portion (Figures S3J
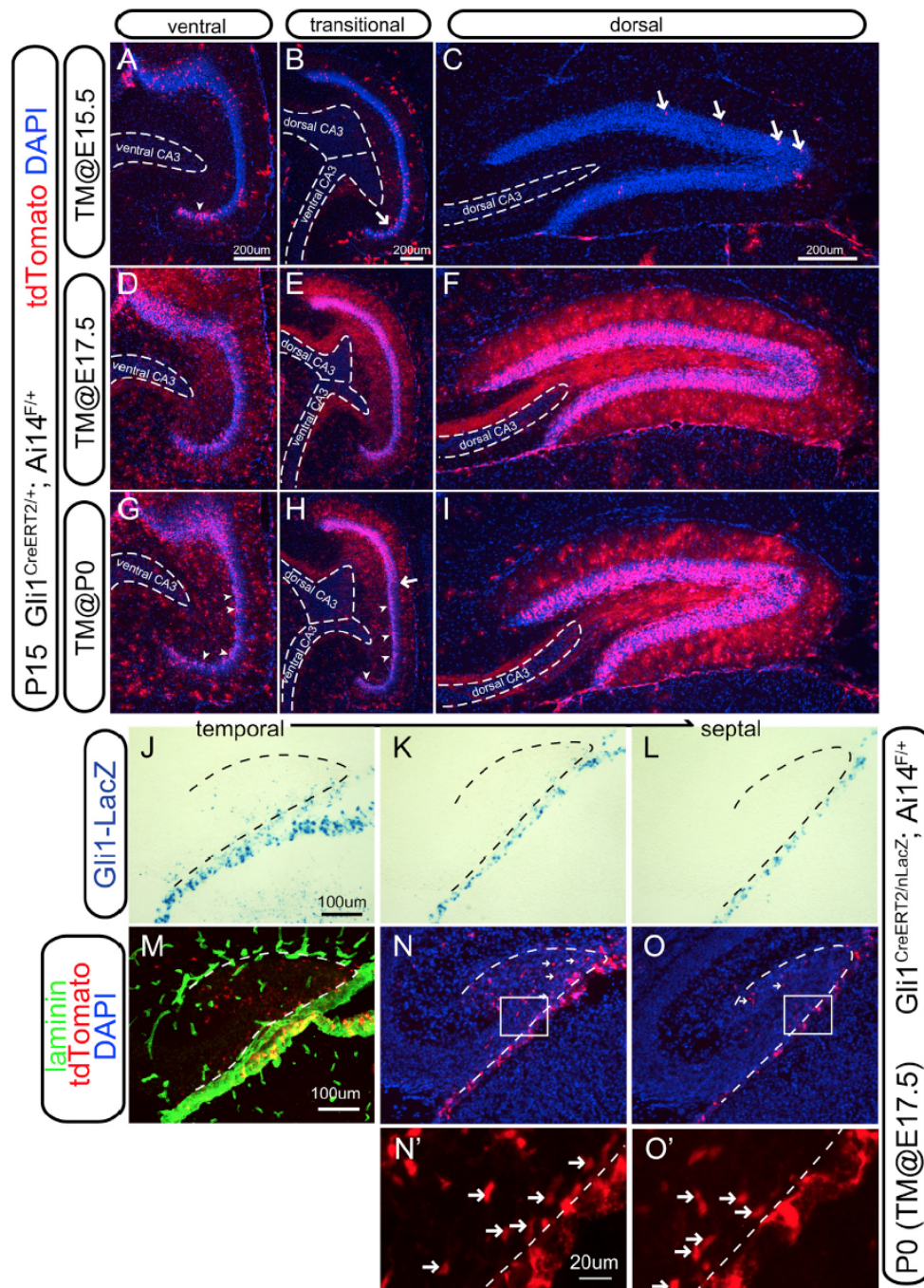
144

Figure 2. Fate-Mapping Analysis of Hh-Responding Cells by Gli1-CreERT2 with Prenatal or Perinatal Tamoxifen Injections

(A–I) The distribution of tdT+ cells in the dentate gyrus was examined at P15 in mice carrying both Gli1-CreERT2 and Cre reporter Ai14 after tamoxifen (TM) injection at E15.5 (A–C), E17.5 (D–F), and P0 (G–I), of which the ventral (A, D, and G), transitional (B, E, and H), and dorsal (C, F, and I) aspects are shown, respectively.

(legend continued on next page)
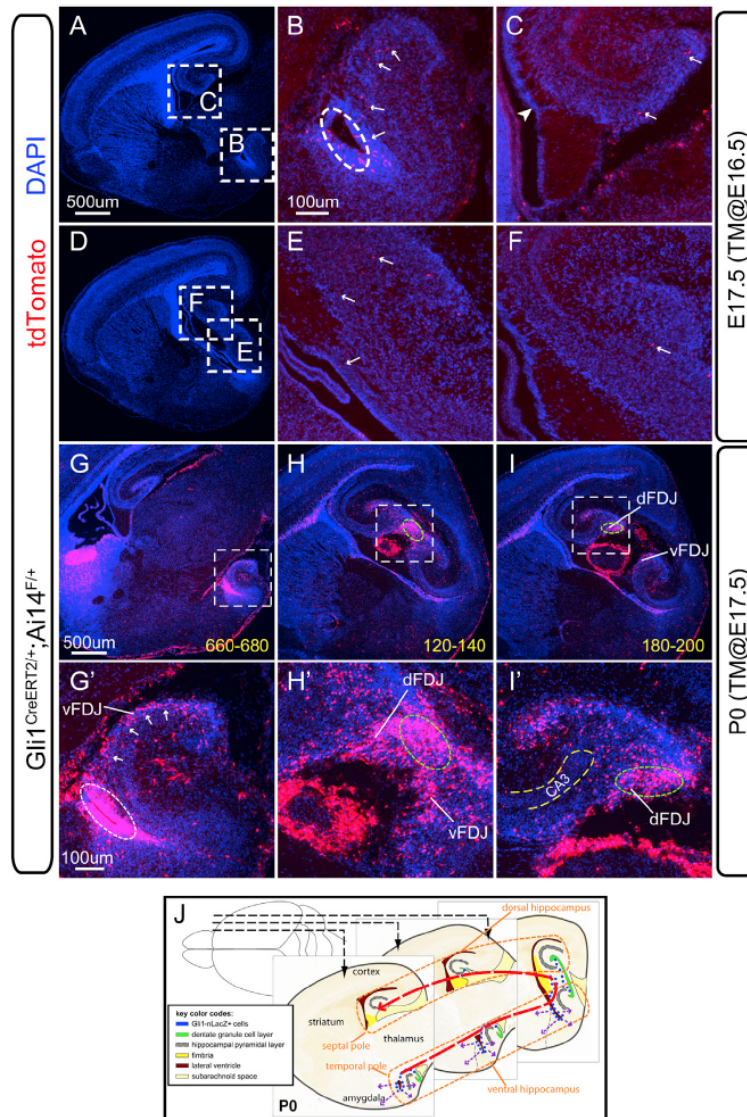
Figure 3. The Short-Term Distribution for the Progeny of Hh-Responding Cells Derived from the Ventral Hippocampus

(A–F) The distribution of tdT+ cells in the $Gli1^{CreERT2/+}$;$Ai14^{F/+}$ animals are shown 1 day after tamoxifen (TM) induction at E16.5. The two representative sagittal levels (A and D) are used for analysis. Boxed areas are shown at the higher magnification in (B), (C), (E), and (F). From the temporal pole to the septal pole, the tdT+ cells (arrows in B, C, E, and F) display a gradient distribution.

(G–I') The distribution of tdT+ cells in the $Gli1^{CreERT2/+}$;$Ai14^{F/+}$ animals are shown 2 days after tamoxifen (TM) induction at E17.5. The three representative sagittal sections are chosen to highlight the main features of the tdT+ cells from the newborns (P0), whereas a series of sections from every 60 μm are shown in Figure S2. The progeny of Hh-responding cells are identified by tdT expression. Throughout the whole hippocampus, the VZ of the temporal hippocampus is the most heavily labeled by tdT (white oval in G'). There is a remarkable cell stream in the vFDJ regions (arrows in G'). The tdT+ cells are continuous from the vFDJ into the dFDJ at the transitional level (green oval in H and H') and taper off in the dorsal hippocampus toward the septal pole (green oval in I and I'). The thickness distance as micron from the first section (in the Figure S2) is shown at the bottom-right corners in (G), (H), and (I). dFDJ, dorsal fimbriodentate junction; vFDJ, ventral fimbriodentate junction.

(J) The schema shows that the temporal-to-septal distribution (red arrow) of the progeny of the Hh-responding cells originated from the VZ of the ventral hippocampus at the perinatal age. In addition, the VZ of the amygdalo-hippocampal region also gives rise to other cells in different directions (purple arrows).

Shh floxed allele were removed from the pallial neuronal lineage (Goebbels et al., 2006) (Figures S3L, S3L', S3M, and S3M') but not the ventral hippocampal VZ (Figures S3C and S3C'). Therefore, Shh from the neuronal cells within the Emx1 domain contributes to the de novo Hh-responding activity seen locally in the DG, whereas Hh from outside the Emx1 domain is responsible for the Hh-responding activity in the VZ of the ventral hippocampus in the $Emx1^{cre/+}$;$Gli1^{Z/Z}$;$Shh^{F/-}$ animals.

This somewhat unexpected finding led us to ask whether Shh was the only Hh family member responsible for the

and S3J'), which appeared to be continuous with the Gli1-nLacZ+ cell stream from the VZ of the ventral hippocampus (Figures S3K and S3K'). The Gli1-nLacZ distribution pattern in the $Emx1^{cre/+}$;$Gli1^{Z/Z}$;$Shh^{F/-}$ animals was phenocopied in the $Neurod6^{cre/+}$;$Gli1^{Z/+}$;$Shh^{F/F}$ animals when two copies of the

(J–O') Mice carrying Gli1CreERT2, Gli1-nLacZ, and Ai14 were analyzed at P0 after tamoxifen injection at E17.5. At P0, the representative sagittal sections of the dorsal DG from temporal (J) to septal (L) levels are shown for Gli1-nLacZ distribution. In the meantime, the distributions of tdT+ cells representing the progeny of the recombined cells are shown with the next sections corresponding to (J) and (K). The complete set of the alternative sections for the Gli1-nLacZ and tdT+ cells are shown in the Figure S1. Basement membrane of the meninges and blood vessels are labeled by Laminin expression (M). Of note, tdT+ cells are detectable at the septal level (arrows in N and O), where Gli1-nLacZ expression is absent in the dentate field (K and L). Boxed areas in (N) and (O) are shown at higher magnification in (N') and (O'), the arrows in which highlight the presence of tdT+ cells at the entrance of the hilus.

Figure 4. Perinatal Distribution of Gli1-nLacZ in Various Shh Signaling Conditional Mutants

(A) The schemas are illustrated for the sagittal sections from the P1 animals shown in (B)–(M).

(B) With the cre reporter Rosa-Yfp, Emx1-cre shows recombination in the ventral hippocampus.

(C, D, and D′) In the control, Gli1-nLacZ+ cells are detected in the hilus of both dorsal (C) and ventral (D) DG, and particularly in the VZ of the ventral hippocampus (arrowheads in D′). Gli1-nLacZ+ cells are obvious in the region away from the VZ (arrows in D′).

(E, F, and F′) In the Emx1-Shh conditional knockout, Gli1-nLacZ+ cells are absent from the hilus of both dorsal and ventral DG (E and F) but still present in the VZ of the ventral hippocampus (F′). Gli1-nLacZ+ cells are still evident in the region away from the VZ (arrows in F′).

(G, H, and H′) In the Emx1-Smo conditional knockout, Gli1-nLacZ+ cells are absent in the dorsal (G) and ventral (H and arrowheads in H′) hippocampus, without affecting their distribution in the VZ of the amygdala (H and H′).

(I, J, and J′) In the NesCre-Shh conditional knockout, Gli1-nLacZ activity is completely abolished in the hippocampus (I and J) and the VZ of the amygdalo-hippocampal region (J′).

(K–M) A domain of Shh-producing cells is located in the amygdala. At P0, cumulative fate mapping with the Shh-gfpcre and Ai14 lines shows a tdT+ domain in the amygdala (arrow in K). The fate-mapping analysis with Shh-CreERT2 and Ai14 upon tamoxifen injection at E17.5 shows a subset of tdT+ cells at P1 in the amygdala as in (K). They are colabeled with Nr2f2 (arrows in M) but not overlapped with the Otp+ cells (L).

VZ (Figures 4J and 4J′) of the ventral hippocampus. The CA fields in the ventral hippocampus also showed a distorted appearance due to the development of hydrocephalus and/or patterning defects in the NesCre-Shh conditional mutant (Figure 4J and data not shown). Therefore, we conclude that Shh is the sole ligand required for Hh-responding cells in the ventral hippocampus but that Shh is produced by both a local source for the forming DG and an extracortical source for the VZ of the ventral hippocampus.

Crossing Shh-Gfpcre mice with Ai14 allowing cumulative fate mapping for Shh-expressing cells revealed that a domain of tdT+ cells was localized within the amygdala, close to the ventral hippo-

Hh-responding activity in the amygdalo-hippocampal region. We used the CNS-specific cre (NesCre) to conditionally remove Shh. The NesCre-Shh conditional mutants showed complete absence of Hh-responding cells in both DG (Figure 4I) and the

campus (arrow in Figure 4K). By crossing the tamoxifen-inducible Shh-CreERT2 line with Ai14, a subset of tdT+ were found in the same amygdalar domain when the expression was examined at P1 after tamoxifen injection at E17.5 (Figure 4L),

suggesting that amygdalar Shh was actively expressed at E17.5. This is in line with the Shh mRNA expression pattern in the Allen Brain Atlas Database (http://developingmouse.brain-map.org/data/search/gene/index.html?term=shh). These tdT+ cells coexpressed the transcription factor Nr2f2 (displaying high level of expression in the amygdala) (arrows in Figure 4M) but were excluded from the Otp domain (Figure 4L). The timing and location of the Shh expression in the amygdala suggested that it is a likely Shh source regulating the Hh-responding cells in the ventral hippocampus.

Shh-Signaling Conditional Mutants Support a Complex Anatomical Origin for Dentate Stem Cells
The analysis above showed that all the Hh-responding activity was abolished in both the hilar region and the VZ of the ventral hippocampus in the Emx1-Smo cKOs, whereas in the Emx1-Shh cKOs, Hh-responding activity was eliminated only in the hilar region but was still present in the VZ of the ventral hippocampus. We wished to further examine the migratory streams of the developing DG in the Emx1-Shh cKOs and Emx1-Smo cKOs with the generic proliferation marker Ki67 (Figures 5A–5G) and neurogenic precursor marker Tbr2 (Figures 5H–5N).

The removal of the obligatory Hh coreceptor Smo from the pallial region by Emx1-cre resulted in a severe reduction of Ki67+ cell density by 75% ± 2% in the hilar region at the transitional level of the DG (arrows in Figure 5B) in relation to the control (arrows in Figure 5A). However, the removal of Shh by the same cre driver only led to a moderate proliferation decrease by 22% ± 5% (arrows in Figure 5C). Noticeably, compared to the control (arrowheads in Figure 5A), Ki67+ cells at the entrance of hilus from the ventral hippocampus were more affected in the Emx1-Smo cKO (arrowheads in Figure 5B) than the Emx1-Shh cKO (arrowheads in Figure 5C). Similarly, Ki67+ and Tbr2+ cells in the dorsal FDJ were significantly diminished by 71% ± 2% and 63% ± 3%, respectively, in the Emx1-Smo cKO (arrows in Figures 5E and 5I) but only slightly decreased by 19% ± 5% and 3% ± 5%, respectively, in the Emx1-Shh cKO (arrows in Figures 5F and 5J), as compared to the control (arrows in Figures 5D and 5H). In contrast, the dorsal SVZ of the dentate was minimally affected in both Emx1-Smo and Emx1-Shh cKOs, as judged by Ki67 and Tbr2 (arrowheads in Figures 5D–5F and 5H–5J, respectively). Tbr2+ cells in the migratory stream of the ventral hippocampus were also reduced by 55% ± 3% in the Emx1-Smo cKO but had little change (104% ± 3% over the control) in the Emx1-Shh cKO (arrows in Figures 5K–5M). All these data strengthen the model that progeny of the Hh-responding cells from the VZ of the ventral hippocampus serve as the critical source for the cells migrating into the dorsal DG and an Shh source outside the Emx1 domain essentially controls the size of this stream, whereas the role of local Shh source in the DG is dispensable for this process.

Shh Sources for the Postnatal Dentate Gyrus
The cumulative fate-mapping analysis with the Shh-gfpcre line (Harfe et al., 2004) showed complex dynamics of distribution for the Shh-lineage in the developing DG. Some of the cells derived from the Shh lineage were oligodendrocyte progenitors in the prenatal and perinatal DG (Figures S4A–S4C). However,

conditional mutant mice deleting Shh from the oligodendrocyte lineage with Olig2-cre (Schüller et al., 2008) had very little alteration to the Hh-responding cells in the DG as examined at P7 (Figure S4D). The Shh-lineage was fate mapped postnatally to the hilar mossy cells, as defined by Calretinin+ staining in the dorsal DG (Figures 6A, 6A′, and 6A″) but not the ventral DG (Figures 6B, 6B′, and 6B″). Mossy cells derived from the Shh lineage projected to the inner molecular layer of the DG (Figures 6A and 6A″). In addition, neurons in the medial entorhinal cortex (MEC) (Figures S4E–S4G), which project to the middle molecular layer of the DG (Figures 6A″ and 6B″), were also part of the Shh lineage.

In order to evaluate the contribution of neuronal (mossy cells and/or MEC) Shh to the Hh-responding activity in the postnatal DG, the distribution of Gli1-nLacZ+ cells was examined at P7 in the mutant mice in which Shh was conditionally removed from the neocortical and hippocampal neurons by Neurod6-cre (Goebbels et al., 2006). Compared to the control (Figures 6C and 6F), the loss of Hh-responding activity in the hilus of Neurod6-Shh cKO (Figures 6E and 6H) was almost as effective as Emx1-Shh cKO (Figures 6D and 6G). Therefore, the neuronal Shh is the key source responsible for the Hh-responding activity locally in the DG.

The Role of the Local Shh in SGZ Formation and Maintenance
Our data favor the model that ventral hippocampus-derived NSCs contribute to the NSCs in the SGZ. However, if the local Shh plays a critical role in the formation of the SGZ, its absence would result in severe SGZ deficiency. To test this, we looked into SGZ formation at P15 by removing either Smo or Shh from the hippocampus with Emx1-cre and compared their phenotypes for SGZ formation. In relation to the control (Figure 7A), there was a complete lack of the radial glia marker Blbp in the SGZ of Emx1-Smo cKO (Figure 7B) but only a mild decrease of the Blbp cell density by 28% ± 4% in the SGZ of Emx1-Shh cKO (Figures 7C and 7I) and 18% ± 3% in Neurod6-Shh cKO (Figures 7D and 7I). Consistently, the radial glial scaffolding in the DG, visualized by Gfap staining, was severely affected in the Emx1-Smo cKO but relatively intact in the Emx1-Shh cKO and Neurod6-Shh cKO (Figures S5A–S5D and S5A′–S5D′). In addition, we examined the length of the two blades of the dentate gyrus among these mutants. In comparison with the control, the length of the upper and lower blades were 61% ± 1% and 24% ± 1% in the Emx1-Smo cKO, whereas they were 81% ± 5% and 76% ± 3% in the Emx1-Shh cKO and 102% ± 4% and 98% ± 3% in the Neurod6-Shh cKO (Figure S5E). Compared to the complete absence of proliferation in the SGZ of Emx1-Smo cKO (Figure 7F, Figures S5G and S5G′), there was a relatively milder proliferation defect in the Emx1-Shh cKOs and Neurod6-Shh cKOs as judged by Ki67 (a decease by 35% ± 3% and 27% ± 2%, respectively, Figures 7G, 7H, and 7J, in relation to the control) and Tbr2 (a decrease by 60% ± 7% and 38% ± 4%, respectively, Figures S5F–S5I and S5J, in relation to the control). Consequently, the thickness of the GCL was affected among the different genotypes: about eight cells in the control, four cells in Emx1-Smo cKO, and six cells in Emx1-Shh cKO or Neurod6-Shh cKO (Figures S5F′–S5I′). The
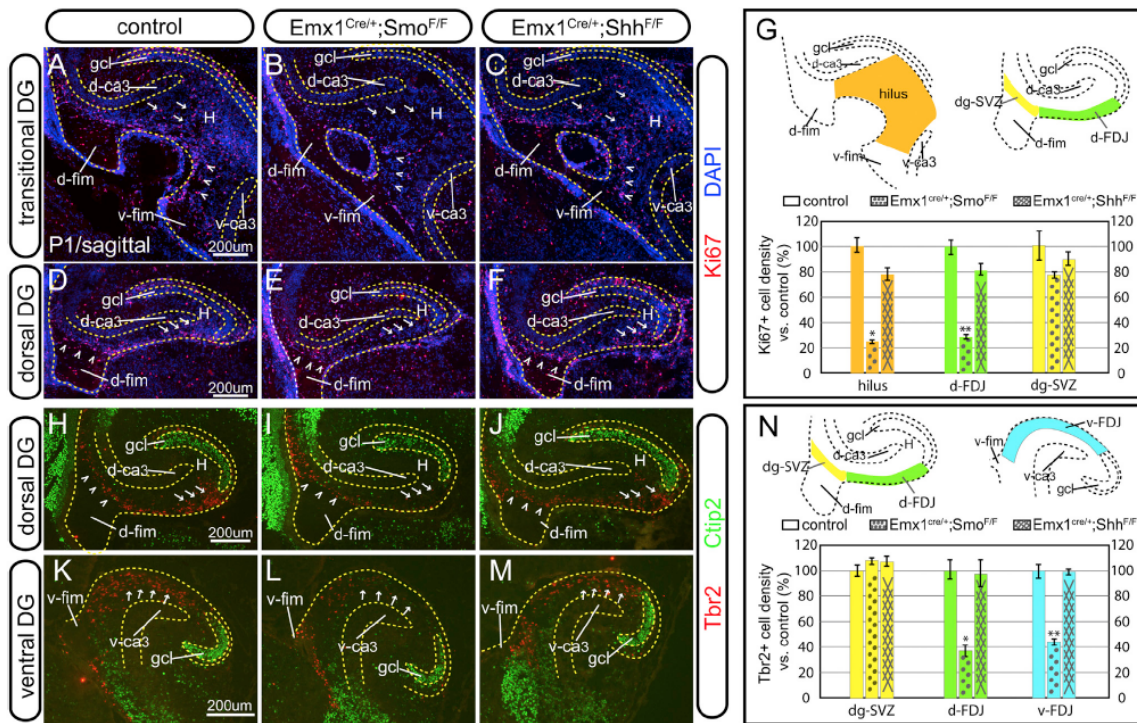
Figure 5. The Dentate Migratory Streams in the Shh Signaling Conditional Mutants

(A–F) Ki67+ proliferative cells at P1 are shown at the transitional level (A–C) and in the dorsal DG (D–F) for the control (A and D), Emx1-Smo cKO (B and E), and Emx1-Shh cKO (C and F), respectively. Compared to the control, Ki67+ proliferating cells in both the hilar region (arrows in A–C) and the hilar entrance from the ventral hippocampus (arrowheads in A–C) are severely compromised in the Emx1-Smo cKO but only mildly affected in the Emx1-Shh cKO. In the dorsal hippocampus, they show comparative number of Ki67+ cells at the SVZ of the dentate primordium (arrowheads in D–F). However, compared to the control (arrows in D), Ki67+ cells in the dFDJ are greatly diminished in the Emx1-Smo cKO (arrows in E) but only slightly reduced in the Emx1-Shh cKO (arrows in F).

(G) Quantification is shown for the density of Ki67+ cells in various regions from the control, Emx1-Smo cKO, and Emx1-Shh cKO. Compared to the control (100% ± 6% and 100% ± 6%), the Ki67+ cell densities found in the hilus (orange) and d-FDJ (green) are only 25% ± 2% (n = 5, p < 0.001) and 29% ± 2% (n = 5, p < 0.001) for the Emx1-Smo cKO, whereas they are 78% ± 5% (n = 5, p < 0.05) and 81% ± 5% (n = 5, p < 0.05) for the Emx1-Shh cKO. In the dg-SVZ (yellow), the Ki67+ cell densities in the Emx1-Smo cKOs and Emx1-Shh cKOs are 77% ± 3% (n = 5, p = 0.13) and 89% ± 6% (n = 5, p = 0.42) as much as the controls (100% ± 12%).

(H–M) Tbr2+ neurogenic cells at P1 are shown in the dorsal DG (H–J) and the ventral DG (K–M) for the control (H and K), Emx1-Smo cKO (I and L), and Emx1-Shh cKO (J and M), respectively. Similar to the Ki67 pattern, they show comparative number of Tbr2+ cells at the SVZ of the dentate primordium (arrowheads in H–J). However, compared to the control (arrows in H), Tbr2+ cells in the dFDJ are greatly diminished in the Emx1-Smo cKO (arrows in I) but only slightly reduced in the Emx1-Shh cKO (arrows in J). In relation to the control (arrows in K), Tbr2+ cells in the vFDJ are greatly diminished in the Emx1-Smo cKO (arrows in L) but only slightly reduced in the Emx1-Shh cKO (arrows in M).

(N) Quantification is shown for the density of Tbr2+ cells in various regions from the control, Emx1-Smo cKO, and Emx1-Shh cKO. In the dg-SVZ (yellow), Tbr2+ cell densities are comparable among the three genotypes: 100% ± 5% for the control, 108% ± 3% for the Emx1-Smo cKO (n = 5, p = 0.39), and 107% ± 4% for Emx1-Shh cKO (n = 5, p = 0.58). However, compared to the control (100% ± 8% and 100% ± 6%), the Tbr2+ cell densities found in the d-FDJ (green) and v-FDJ (cyan) are 37% ± 3% (n = 5, p < 0.001) and 45% ± 3% (n = 5, p < 0.001) for the Emx1-Smo cKO, whereas they are 97% ± 5% (n = 5, p = 0.6) and 104% ± 3% (n = 5, p = 0.14) for the Emx1-Shh cKO.

Data are shown as mean ± SEM and p values for the indicated sample sizes are returned by Student's t test for two-tailed distribution with unequal variance. dg-SVZ, subventricular zone of dentate gyrus; gcl, granule cell layer; d-ca3, dorsal CA3; v-ca3, ventral CA3; H, hilus; d-FDJ, dorsal fimbriodentate junction; v-FDJ, ventral fimbriodentate junction; d-fim, dorsal fimbria; v-fim, ventral fimbria.

divergent phenotypes in SGZ formation between Emx1-Smo and Emx1-Shh (or Neurod6-Shh) cKOs further validate the model that the Hh-responding cells retained in the ventral hippocampus of the Emx1-Shh cKO or Neurod6-Shh cKO (but completely absent from the Emx1-Smo cKO) are responsible for the initial formation of the SGZ, whereas Shh from the Emx1 domain is relatively dispensable for this in light of the only slightly compromised SGZ in its absence.

As we showed previously that de novo local Hh-responding activity was mostly abolished in the Neurod6-Shh cKO (Figures 6E and 6H, and Figures S3L and S3L'), we asked in the same genetic background whether Hh-responding cells from the ventral

149
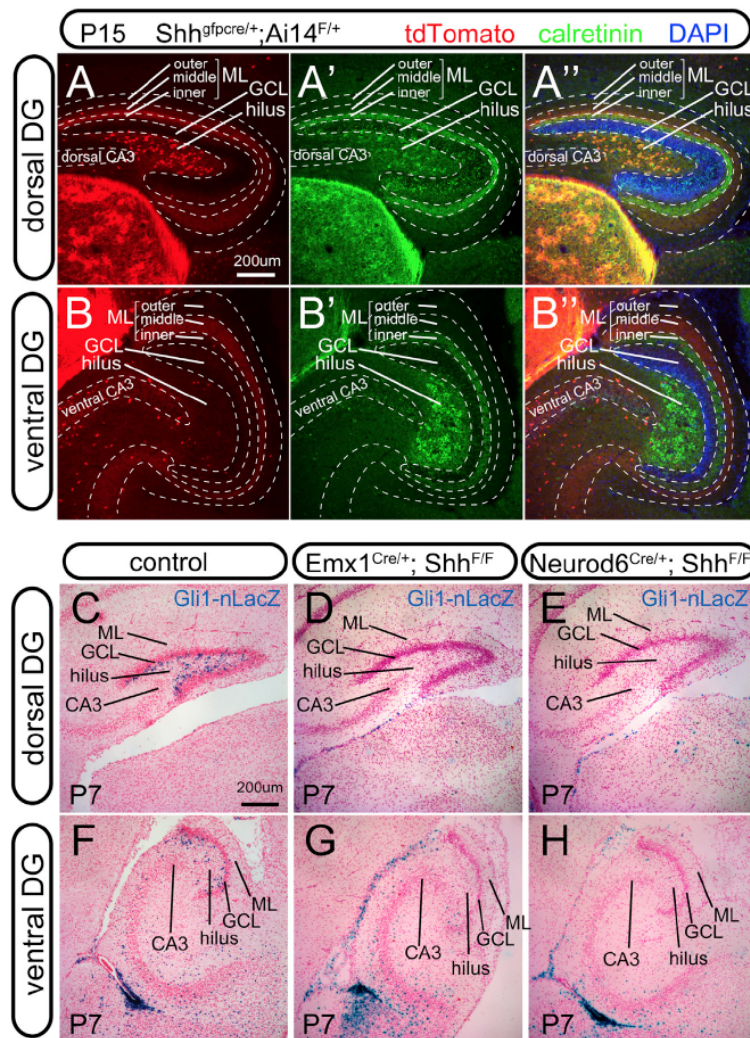
Figure 6. The Shh Sources for the Postnatal DG

(A–B″) At P15, cumulative fate mapping of the Shh-producing cells with the Shh-gfpcre and Ai14 lines is shown in the dorsal and ventral DG (A and B, respectively). In the dorsal dentate gyrus, tdT expression is colocalized with hilar mossy cell marker Calretinin (A′ and A″). In the dorsal and ventral dentate gyrus, tdT expression is also detected in the midmolecular layer (A″, B′, and B″), where the neurons of the medial entorhinal cortex project their fibers.

(C–H) At P7, Gli1-nLacZ+ cells are present in the hilus of both dorsal and ventral DG in the control (C and F) but completely abolished in the Emx1-Shh cKO (D and G) and Neurod6-Shh cKO (E and H). GCL, granule cell layer; ML, molecular layer; SGZ, subgranular zone.

scendants of Hh-responding cells in the ventral hippocampus still contribute to the GCL and a few of them also take up residence in the SGZ, whereas in the presence of local Shh, more descendants can be retained in the SGZ, supporting the idea that the local Shh serves to maintain NSCs in the SGZ.

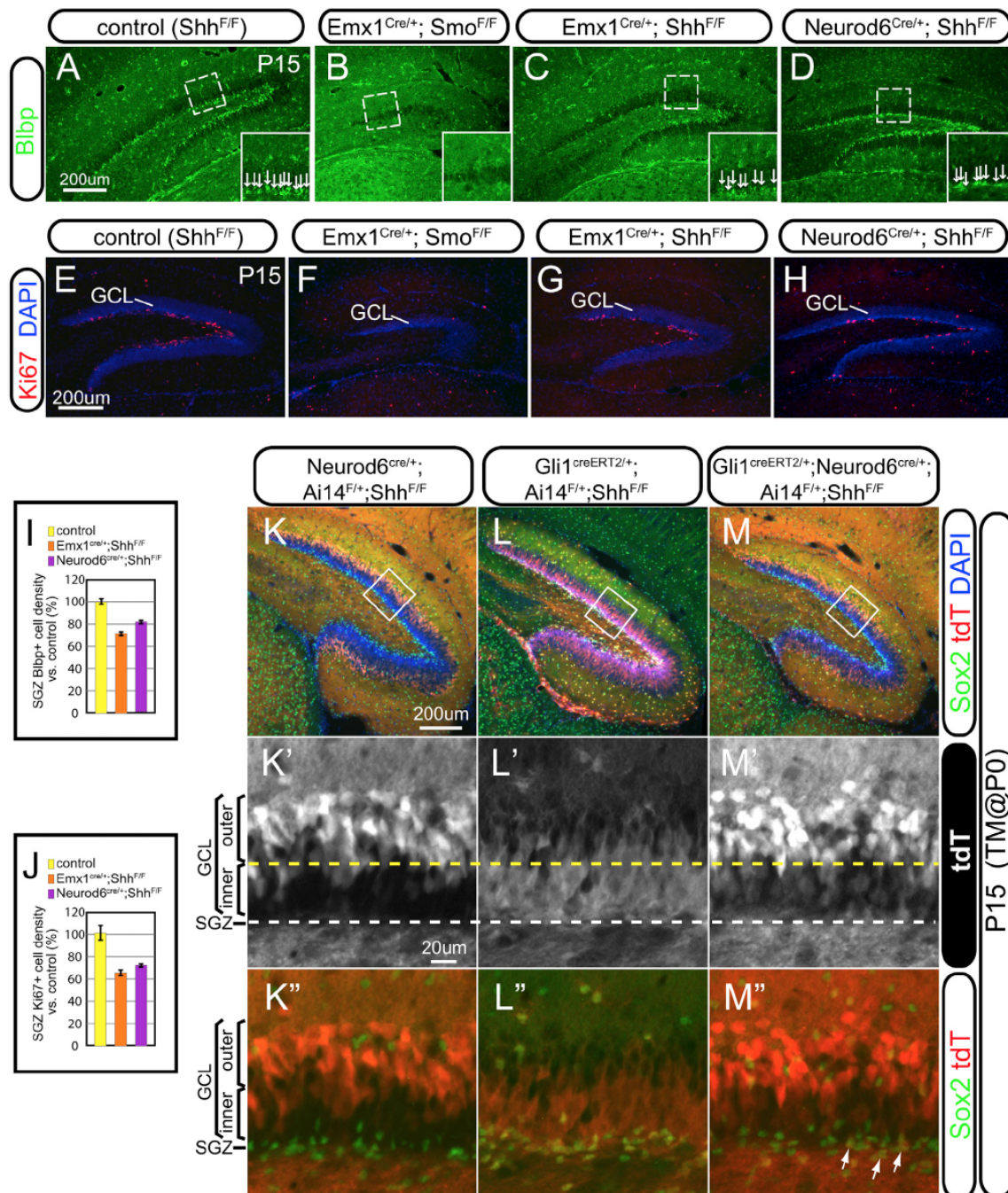**The Descendants of the Prenatal Hh-Responding Cells Contribute to the LL-NSCs in the SGZ**

The long-term fate of the descendants derived from the prenatal Hh-responding cells has not been determined yet. By crossing the Gli1-CreERT2 line with the cre reporter Ai14, we could evaluate the tdT-expressing cells over a long time after tamoxifen injection at E17.5. In order to increase neurogenesis in aging animals (van Praag et al., 2000), we also subjected them to environment enrichment (EE) for 2 months and then examined the SGZ when they reached 1 year of age (Figure 8A). A number of radially oriented tdT+ cells still retained the expression of the radial glia marker Blbp (arrows in Figures 8B and 8C). More importantly, some of the tdT+ cells also expressed the immature neuronal marker Dcx (arrows in Figures 8D and 8E). Therefore, some of the descendents derived from the prenatal Hh-responding cells maintain the characteristics of NSCs and they are still neurogenic even in aged animals.

DISCUSSION

Since the discovery of neurogenesis in the adult rodent hippocampus (Altman and Das, 1967), the central question of where and how the LL-NSCs relocate to the SGZ of the DG has remained unresolved. Identification of the embryonic origin of the LL-NSCs is the first and perhaps the most important step

hippocampus can contribute to dorsal dentate development, in particular, SGZ formation, by genetic fate-mapping analysis with the Gli1-CreERT2 line. For that purpose, we examined animals by P15 with tamoxifen injection at birth using Ai14 as the cre reporter. We confirmed that Neurod6-cre showed recombination activity mostly in the outer GCL with little in the inner GCL (Figures 7K and 7K′) but not in the SGZ at all (Figure 7K″) (Goebbels et al., 2006). In Gli1$^{creERT2/+}$;Ai14$^{F/+}$;Shh$^{F/F}$ animals, tdT+ cells occupied both the inner GCL and SGZ, as indicated by colabeling with the stem cell marker Sox2 (Figures 7L, 7L′, and 7L″). Strikingly, in Gli1$^{creERT2/+}$;Neurod6$^{cre/+}$;Ai14$^{F/+}$;Shh$^{F/F}$ animals, tdT+ cells not only populated the outer GCL but also the inner GCL (Figures 7M and 7M′), with a few coexpressing Sox2 in the SGZ (arrows in the Figure 7M″). These data taken together indicate that even in the absence of local Shh in the forming DG, de-

**Figure 7. The Formation of the SGZ in the Emx1-Smo, Emx1-Shh, and Neurod6-Shh cKOs**

(A–D) SGZ formation is assessed with the radia glial marker Blbp in the control (A), Emx1-Smo cKO (B), Emx1-Shh cKO (C), and Neurod6-Shh (D). There is a complete lack of Blbp+ cells in the SGZ of Emx1-Smo cKO (B) but only a moderate decrease in the Emx1-Shh cKO (C) and Neurod6-Shh cKO (D). The arrangement of Blbp+ cells in the SGZ is shown at the higher magnification in the insets.

(legend continued on next page)

Neuron
Dentate Stem Cell Origin
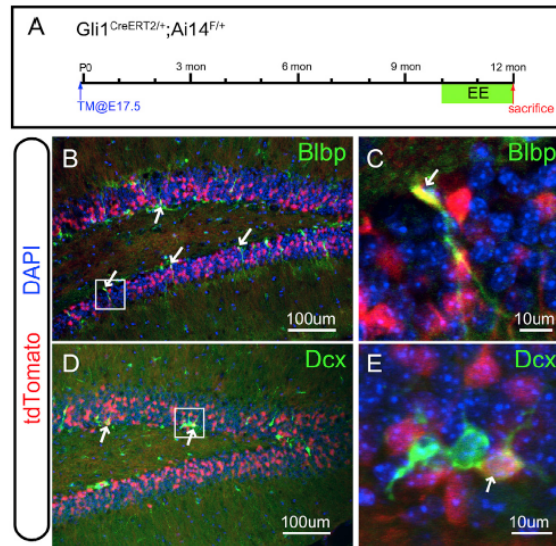
Figure 8. The Long-Term Fate Mapping of the Prenatal Hh-Responding Cells in the Dentate Gyrus
(A) The schema shows the strategy for the long-term fate mapping of the prenatal Hh-responding cells in the dentate gyrus. By crossing the Gli1CreERT2 line with the Ai14 line, the cell fate of the Hh-responding cells labeled by tamoxifen injection at E17.5 is examined in the 1-year-old animals after environment enrichment (EE) for 2 months (green box).
(B and C) Some tdT+ cells are marked by the neural stem cell marker Blbp in the SGZ (arrows in B) in the 1-year-old animals. The boxed area in (B) is shown at the higher magnification in (C).
(D and E) Some tdT+ cells are also labeled by the immature neuronal marker Dcx (arrows in D) in the 1-year-old animals. The boxed area in (D) is also shown at the higher magnification in (E).

toward a thorough understanding of this complex developmental process. It has been assumed in the literature that the resident NSCs in the SGZ come from the dentate primordium/VZ at the equivalent longitudinal level (Altman and Bayer, 1990a; Eckenhoff and Rakic, 1984; Li and Pleasure, 2005). In this study, we provide evidence that NSCs from the ventral hippocampus contribute to the development of the SGZ throughout the longitudinal axis of the hippocampus. Moreover, the analysis of the interaction between Hh-responding and Hh-producing cells in the perinatal and postnatal DG not only lends extra support for

this model but also reveals the distinct roles of Shh from the different sources in SGZ formation and maintenance.

The Ventral Hippocampus Contributes to the Neural Stem Cells in the Subgranular Zone
How to keep track of the long-term behaviors of the embryonic NSCs is the main challenge in studying the embryonic origins of adult LL-NSCs. First of all, the markers (such as Nestin, Gfap, Blbp, Glast, etc.) commonly used to label embryonic NSCs may not reliably predict their future fates, since embryonic NSCs can lose their "stemness" due to proliferation/differentiation during development; second, it is still hard to predict cell fates by simply referring to their initial anatomical locations, since there is a drastic reorganization during the development of the dentate gyrus; third, the relatively long developmental process to establish the SGZ makes time-lapse imaging techniques impractical. In light of these technical considerations, inducible genetic fate-mapping tools are the most powerful way to address this issue (Joyner and Zervas, 2006). Examining the genetically tagged progeny of embryonic NSCs opens up the possibility of following the temporal lineage allocation and teasing out the temporal contribution of embryonic NSCs of distinct origins to adult hippocampal LL-NSCs in the SGZ.

Our static analysis of the developing hippocampus showed the predominant localization of Gli1-nLacZ+ Hh-responding cells in the VZ of the amygdalo-hipppocampal area during late gestation and a gradient of Gli1-nLacZ+ cells in the temporo-septal direction at perinatal ages, providing the first hint that embryonic NSCs in the ventral hippocampus may be the potential source for the LL-NSCs in the SGZ of the dorsal DG. This notion is further strengthened by our fate-mapping analysis. At E17.5, most Hh-responding cells were still restricted to the ventral hippocampus, the progeny of which could be genetically marked with the Gli1-CreERT2 upon tamoxifen induction; these cells were later found in the postnatal SGZ at all septotemporal levels. De novo Hh-responding cells also gradually appeared locally in the hilus of the dorsal hippocampus postnatally; however, the progeny of the Hh-responding cells derived from the ventral hippocampus appeared at more septal levels along the longitudinal axis in the dorsal DG before the local Hh-responding cells were detected. The functional significance of the ventral hippocampus-derived NSCs is further established by the regional manipulations of Shh signaling. In addition to confirming that Hh-signaling is essential for the development of the NSCs in the SGZ (Han et al., 2008; Machold et al., 2003), the SGZ

(E–H) Proliferative Ki67+ cells in the SGZ are shown for the control (E), Emx1-Smo cKO (F), Emx1-Shh cKO (G), and Neurod6-Shh (H). Ki67+ cells are completely abolished in the Emx1-Smo cKO (F) but only mildly affected in the Emx1-Shh cKO (K) and Neurod6-Shh cKO (H).
(I) Quantification of Blbp+ cell densities in the SGZ is made for the control, Emx1-Shh cKO, and Neurod6-Shh cKO. It is 72% ± 4% (n = 5, p < 0.01) in the Emx1-Shh cKOs and 82% ± 3% (n = 5, p < 0.01) in the Neurod6-Shh cKOs, as compared to the controls (100% ± 6%).
(J) Quantification of Ki67+ cell densities in the SGZ is made for the control, Emx1-Shh cKO, and Neurod6-Shh cKO. It is only 65% ± 3% (n = 5, p < 0.01) in the Emx1-Shh cKOs and 73% ± 2% (n = 5, p < 0.01) in the Neurod6-Shh cKOs, as compared to the controls (100% ± 7%).
(K–M″) Fate-mapping analysis in the absence of local Shh in the DG. Animals are examined by P15 with tamoxifen injection at birth using Ai14 as the cre reporter. In Neurod6$^{cre/+}$;Ai14$^{F/+}$;Shh$^{F/F}$ animals (K), tdT+ cells are mostly restricted in the outer GCL (K′) but absent from the SGZ as indicated by the lack of colabeling with Sox2, the marker for NSCs (K″). In Gli1$^{creERT2/+}$;Ai14$^{F/+}$;Shh$^{F/F}$ animals (L), tdT+ cells are present mostly in the inner GCL (L′) and SGZ (L″). By contrast, in Gli1$^{creERT2/+}$;Neurod6$^{cre/+}$;Ai14$^{F/+}$;Shh$^{F/F}$ animals (M), despite the lack of local Shh in the dentate, tdT+ cells are present in both inner GCL (M′) and SGZ (arrows in M″), in addition to the outer GCL.
Data are shown as mean ± SEM and p values for the indicated sample sizes are calculated by Student's t test for two-tailed distribution with unequal variance. GCL, granule cell layer; SGZ, subgranular zone.

deficiency in the Emx1-Smo cKOs directly supports the notion that SGZ NSCs arise exclusively from the Emx1 domain. When Shh was removed from the entire Emx1 domain, local Hh-responding cells in the DG were abolished in the whole hippocampus, whereas the Hh-responding cells in the VZ of the ventral hippocampus were relatively unaffected. Thus, the relative intactness of the SGZ in the dorsal hippocampus of Emx1-Shh cKOs can only be accounted for by the Hh-responding cells retained in the ventral hippocampus, which appear sufficient to serve as the source for the NSCs of the SGZ in the dorsal hippocampus. Indeed, genetic fate-mapping analysis with Gli1-CreERT2 line in the Neurod6-Shh cKO background demonstrated that descendants of the Hh-responding cells from the perinatal age can contribute to the inner granule cell layer and NSCs in the SGZ by P15 even in the absence of the de novo local Hh-responding activity in the DG. We conclude from these different lines of genetic evidence that embryonic NSCs from the ventral hippocampus contribute to the LL-NSCs in the DG throughout the longitudinal axis of the hippocampus.

The functional significance of this "mosaic" organization of the dentate gyrus with regards to the distinct involvement of the dorsal and ventral dentate in spatial learning versus emotional processing is quite interesting to consider. At this point, our data do not allow hard conclusions to be drawn regarding the nature of this developmental relationship; however, our elucidation of the developmental origin for the LL-NSC in the dentate is important. In the future, using selective reagents that target ventrally derived LL-NSC selectively should allow novel insights into the circuit and functional relationship between these two divisions of the dentate.

Shh Sources for the Perinatal and Postnatal Dentate Gyrus

Previous studies suggested that an Shh source from the septum via the septohippocampal projection regulates both SGZ establishment (Machold et al., 2003) and maintenance (Lai et al., 2003). Our analysis of Hh-responding cells with Gli1-nLacZ line in the Emx1-Shh cKO background shows that Shh from pallial sources is exclusively responsible for all the Hh-responding activity in the hippocampus throughout the septotemporal axis, except the VZ of the ventral hippocampus. The findings in this study argue against the direct contribution of Shh from the septum. Shh was also suggested to be a target gene of Sox2 in the DG NSCs, and thus NSCs are proposed to be the Shh source for the feedback regulation (Favaro et al., 2009). However, our cumulative fate-mapping analysis with the Shh-gfpcre does not seem to mark any NSCs in the DG and, more importantly, removal of Shh from the differentiated neuronal lineage by Neurod6-cre is sufficient to abolish literally all the Hh-responding activity in the DG, supporting the idea that Shh involved in the regulation of adult SGZ mainly comes from neurons rather than other local cell types (either astrocytes or progenitors).

Relationship between the Mediolateral and Temporoseptal Migratory Streams during Dentate Development

Previous studies revealed the successive development of germinative matrices at different locations during the formation of the DG (Altman and Bayer, 1990a, 1990b). Around the beginning of the third week of gestation in mice, the primary matrix is noticeable at the VZ of the dentate primordium, whereas the secondary matrix develops in the SVZ of the dentate primordium throughout the third week of gestation (Li et al., 2009). At perinatal ages, the secondary matrix dissolves into two components (Altman and Bayer, 1990a): the extrinsic component extends subpially and forms the transient neurogenic niche that gives rise to the outer shell of the GCL (Li et al., 2009), whereas the intrinsic component invades the hilus and gives rise to the tertiary matrix (Altman and Bayer, 1990a). During the second postnatal week, the tertiary matrix progressively gives way to the SGZ (Altman and Bayer, 1990a; Li et al., 2009). In addition to this well-recognized stream originating from the VZ of the dentate at the equivalent longitudinal level, which migrates in the mediolateral direction, in this study we provide evidence for the presence of another stream, originating from the VZ of the ventral hippocampus and spreading in the temporoseptal direction (red arrow in Figure 3J). These two different streams appear to converge at the entrance of the hilus in close proximity to the pial meninges. In the Emx1-Smo cKO, the extrinsic component (the subpial component) is only moderately affected, whereas the intrinsic component is severely compromised, supporting the idea that the mediolateral migratory stream is Hh independent and mainly contributes to development of the outer shell of the suprapyramidal blade, while the temporoseptal migratory stream originating from the ventral hippocampus is Hh dependent and mostly contributes to the development of the tertiary matrix, the inner shell of the DG and the prospective SGZ.

Previous work using minimal aggregation chimeras indicated that the outer portion of the dentate granule cell layer had a developmentally divergent origin from the bulk of the granule neurons residing in the inner portion of the granule cell layer, which are believed to arise from SGZ progenitors (Martin et al., 2002). In this assay, it is difficult to dissect when and where the chimeric LacZ aggregates came from at the anatomical level. Our genetic fate-mapping analysis using the Gli1-CreERT2 line with tamoxifen induction shows that the inner and outer portions of the dentate have distinct but somewhat overlapping temporal origins between embryonic days 15.5 (E15.5) and P0. As well, our identification of the ventral source of the LL-NSCs further supplies an anatomic distinction between the births of embryonically produced DGC at widespread septotemporal levels, while providing evidence for a distinct anatomic origin for the SGZ NSCs.

In summary, we have provided evidence linking the developmental origin of the LL-NSCs in the adult dentate gyrus to the germinative VZ in the ventral hippocampus. We believe that this finding will lead to a new framework to understand the general paradigms for retaining the LL-NSCs in the different anatomical structures in the adult brain.

EXPERIMENTAL PROCEDURES

Animals

The following mouse lines were obtained from Jackson Laboratory: Gli1-nLacZ (stock 008211), Gli1-CreERT2 (stock 007913), Ai14 (stock 007914), Rosa-Yfp (stock 006148), Emx1-cre (stock 05628), Nes-Cre (stock 003771),

153

Shh-gfpcre (stock 005622), Shh-CreERT2 (stock 005623), Shh$^{flox/flox}$ (stock 004293), and Smo$^{flox/flox}$ (stock 004526). Olig2-cre was kindly provided by Dr. D. Rowitch (UCSF) and Neurod6-Cre by Dr. S. Goebbels and Dr. K.A. Nave (Max Planck). The day of vaginal plug was considered E0.5. Mouse colonies were maintained at UCSF in accordance with National Institutes of Health and UCSF guidelines.

Environment Enrichment

For environment enrichment, six to ten mice were housed in the One Cage 2100 system, which is almost triple the size of the regular cage. The cages were also equipped with igloos, tunnels, running wheels, and various toys.

Tamoxifen Induction

Tamoxifen (T5648, Sigma) was dissolved in corn oil (C8267, Sigma) at 20 mg/ml. Pregnant females were administrated intraperitoneally (i.p.) with 3 mg of tamoxifen per 40 g animal. Neonates were injected subcutaneously with 50 μl of tamoxifen stock solution.

LacZ Staining

Animals for LacZ staining were perfused with 2% paraformaldehyde (PFA) and the dissected brains were postfixed with 2% PFA for 2 hr at 4°C. Tissues were cryoprotected in 30% sucrose, embedded in OCT, and then kept at −80°C for long-term storage. Perinatal tissues were sectioned at 20 μm and P7 tissues at 16 μm. X-gal staining was developed at 37°C overnight in the staining solution (5 mM $K_3Fe(CN)_6$, 5 mM $K_4Fe(CN)_6$, 5 mM EGTA, 0.01% deoxycholate, 0.02% NP40, 2 mM $MgCl_2$, and 1 mg/ml X-gal). Sections were postfixed with 10% formalin at room temperature overnight. Slides were then counterstained with nuclear-fast red (H-3403, Vector Laboratories) at room temperature for 10 min before proceeding for dehydration (70%, 95%, 100% ethanol, xylene twice) and coverslipping with Mount-Quick (Ted Pella).

Immunohistochemistry

Animals were perfused with 1 × PBS followed by 4% PFA. Dissected brains were postfixed in 4% PFA overnight. They were then cryoprotected in 30% sucrose until they sank. Brain tissues were embedded in OCT and kept at −80°C. Brain sections made on a cryostat at 12 μm were directly collected on slides for perinatal tissues or cut at 30 μm for P15 or older tissues as floating sections in 1 × PBS and mounted onto slides after staining. Sections were stained with the following primary antibodies overnight at 4°C in blocking buffer: 10% lamb serum, 0.3% Triton X-100, 0.05% NaN_3 in 1 × PBS; they were then rinsed in wash buffer (0.3% Triton X-100 in 1 × PBS) three times. They were further stained with the Alexa Fluor-conjugated secondary antibodies (Invitrogen) in the same blocking buffer for 2 hr at room temperature and counter stained with DAPI for 0.5 hr. Primary antibodies were used as follows: rat anti-GFP (1:1,000; Nacalai Tesque), rat anti-Ctip2 (1:1,000; Abcam), rabbit anti-Blbp (1:1,000; Chemicon), rabbit anti-Calretinin (1:1,000; Chemicon), rabbit anti-Ki67 (1:500, monoclonal antibody; Neomarker), rabbit anti-Tbr2 (1:1,000; gift from Dr. R. Hevner, University of Washington), rabbit anti-Gfap (1:1,000; Dako), rabbit anti-Laminin (1:500; Sigma-Aldrich), rabbit anti-Otp (1:1,000; gift from Dr. F. Vaccarino, Yale University), guinea pig anti-Sox10 (1:1,000; gift from Dr. M. Wegner, Institut für Biochemie), rabbit anti-Olig2 (1:1,000; gift from Dr. D. Rowitch, UCSF), rabbit anti-Dcx (1:500; Abcam), and rabbit anti-Sox2 (1:1,000; Epitomics).

Image Analysis and Quantification

Images were acquired using a Nikon E600 microscope equipped with a cooled charge-coupled device camera (QCapture Pro; QImaging). For colocalization analysis, confocal images were taken with LSM 510 meta two-photon microscope (Carl Zeiss). Brain sections of the similar anatomical levels from five brains for controls or mutants were chosen for quantification. The densities of indicated cell types in each region were quantified and shown as percentage of the mean ± SEM for n given samples over the controls. Data were analyzed using two-tailed Student's t test with unequal variance. Any p value less than 0.05 was considered significant.

SUPPLEMENTAL INFORMATION

Supplemental Information includes six figures and can be found with this article online at http://dx.doi.org/10.1016/j.neuron.2013.03.019.

REFERENCES

Ahn, S., and Joyner, A.L. (2004). Dynamic changes in the response of cells to positive hedgehog signaling during mouse limb patterning. Cell *118*, 505–516.

Ahn, S., and Joyner, A.L. (2005). In vivo analysis of quiescent adult neural stem cells responding to Sonic hedgehog. Nature *437*, 894–897.

Altman, J., and Bayer, S.A. (1990a). Migration and distribution of two populations of hippocampal granule cell precursors during the perinatal and postnatal periods. J. Comp. Neurol. *301*, 365–381.

Altman, J., and Bayer, S.A. (1990b). Mosaic organization of the hippocampal neuroepithelium and the multiple germinal sources of dentate granule cells. J. Comp. Neurol. *301*, 325–342.

Altman, J., and Das, G.D. (1967). Postnatal neurogenesis in the guinea-pig. Nature *214*, 1098–1101.

Bai, C.B., Auerbach, W., Lee, J.S., Stephen, D., and Joyner, A.L. (2002). Gli2, but not Gli1, is required for initial Shh signaling and ectopic activation of the Shh pathway. Development *129*, 4753–4761.

Breunig, J.J., Sarkisian, M.R., Arellano, J.I., Morozov, Y.M., Ayoub, A.E., Sojitra, S., Wang, B., Flavell, R.A., Rakic, P., and Town, T. (2008). Primary cilia regulate hippocampal neurogenesis by mediating sonic hedgehog signaling. Proc. Natl. Acad. Sci. USA *105*, 13127–13132.

Clelland, C.D., Choi, M., Romberg, C., Clemenson, G.D., Jr., Fragniere, A., Tyers, P., Jessberger, S., Saksida, L.M., Barker, R.A., Gage, F.H., and Bussey, T.J. (2009). A functional role for adult hippocampal neurogenesis in spatial pattern separation. Science *325*, 210–213.

Eckenhoff, M.F., and Rakic, P. (1984). Radial organization of the hippocampal dentate gyrus: a Golgi, ultrastructural, and immunocytochemical analysis in the developing rhesus monkey. J. Comp. Neurol. *223*, 1–21.

Encinas, J.M., Michurina, T.V., Peunova, N., Park, J.H., Tordo, J., Peterson, D.A., Fishell, G., Koulakov, A., and Enikolopov, G. (2011). Division-coupled astrocytic differentiation and age-related depletion of neural stem cells in the adult hippocampus. Cell Stem Cell *8*, 566–579.

Favaro, R., Valotta, M., Ferri, A.L., Latorre, E., Mariani, J., Giachino, C., Lancini, C., Tosetti, V., Ottolenghi, S., Taylor, V., et al. (2009). Hippocampal development and neural stem cell maintenance require Sox2-dependent regulation of Shh. Nat. Neurosci. *12*, 1248–1256.

Galceran, J., Miyashita-Lin, E.M., Devaney, E., Rubenstein, J.L., and Grosschedl, R. (2000). Hippocampus development and generation of dentate gyrus granule cells is regulated by LEF1. Development *127*, 469–482.

Garcia, A.D., Petrova, R., Eng, L., and Joyner, A.L. (2010). Sonic hedgehog regulates discrete populations of astrocytes in the adult mouse forebrain. J. Neurosci. *30*, 13597–13608.

Goebbels, S., Bormuth, I., Bode, U., Hermanson, O., Schwab, M.H., and Nave, K.A. (2006). Genetic targeting of principal neurons in neocortex and hippocampus of NEX-Cre mice. Genesis *44*, 611–621.

Han, Y.G., Spassky, N., Romaguera-Ros, M., Garcia-Verdugo, J.M., Aguilar, A., Schneider-Maunoury, S., and Alvarez-Buylla, A. (2008). Hedgehog signaling and primary cilia are required for the formation of adult neural stem cells. Nat. Neurosci. *11*, 277–284.

Harfe, B.D., Scherz, P.J., Nissim, S., Tian, H., McMahon, A.P., and Tabin, C.J. (2004). Evidence for an expansion-based temporal Shh gradient in specifying vertebrate digit identities. Cell *118*, 517–528.

Joyner, A.L., and Zervas, M. (2006). Genetic inducible fate mapping in mouse: establishing genetic lineages and defining genetic neuroanatomy in the nervous system. Dev. Dyn. *235*, 2376–2385.

Lai, K., Kaspar, B.K., Gage, F.H., and Schaffer, D.V. (2003). Sonic hedgehog regulates adult neural progenitor proliferation in vitro and in vivo. Nat. Neurosci. *6*, 21–27.

Li, G., and Pleasure, S.J. (2005). Morphogenesis of the dentate gyrus: what we are learning from mouse mutants. Dev. Neurosci. *27*, 93–99.

Li, G., and Pleasure, S.J. (2010). Ongoing interplay between the neural network and neurogenesis in the adult hippocampus. Curr. Opin. Neurobiol. *20*, 126–133.

Li, G., Berger, O., Han, S.M., Paredes, M., Wu, N.C., and Pleasure, S.J. (2008). Hilar mossy cells share developmental influences with dentate granule neurons. Dev. Neurosci. *30*, 255–261.

Li, G., Kataoka, H., Coughlin, S.R., and Pleasure, S.J. (2009). Identification of a transient subpial neurogenic zone in the developing dentate gyrus and its regulation by Cxcl12 and reelin signaling. Development *136*, 327–335.

Machold, R., Hayashi, S., Rutlin, M., Muzumdar, M.D., Nery, S., Corbin, J.G., Gritli-Linde, A., Dellovade, T., Porter, J.A., Rubin, L.L., et al. (2003). Sonic hedgehog is required for progenitor cell maintenance in telencephalic stem cell niches. Neuron *39*, 937–950.

Machon, O., Backman, M., Machonova, O., Kozmik, Z., Vacik, T., Andersen, L., and Krauss, S. (2007). A dynamic gradient of Wnt signaling controls initia-

tion of neurogenesis in the mammalian cortex and cellular specification in the hippocampus. Dev. Biol. *311*, 223–237.

Madisen, L., Zwingman, T.A., Sunkin, S.M., Oh, S.W., Zariwala, H.A., Gu, H., Ng, L.L., Palmiter, R.D., Hawrylycz, M.J., Jones, A.R., et al. (2010). A robust and high-throughput Cre reporting and characterization system for the whole mouse brain. Nat. Neurosci. *13*, 133–140.

Mangale, V.S., Hirokawa, K.E., Satyaki, P.R., Gokulchandran, N., Chikbire, S., Subramanian, L., Shetty, A.S., Martynoga, B., Paul, J., Mai, M.V., et al. (2008). Lhx2 selector activity specifies cortical identity and suppresses hippocampal organizer fate. Science *319*, 304–309.

Martin, L.A., Tan, S.S., and Goldowitz, D. (2002). Clonal architecture of the mouse hippocampus. J. Neurosci. *22*, 3520–3530.

Sahay, A., Scobie, K.N., Hill, A.S., O'Carroll, C.M., Kheirbek, M.A., Burghardt, N.S., Fenton, A.A., Dranovsky, A., and Hen, R. (2011). Increasing adult hippocampal neurogenesis is sufficient to improve pattern separation. Nature *472*, 466–470.

Schüller, U., Heine, V.M., Mao, J., Kho, A.T., Dillon, A.K., Han, Y.G., Huillard, E., Sun, T., Ligon, A.H., Qian, Y., et al. (2008). Acquisition of granule neuron precursor identity is a critical determinant of progenitor cell competence to form Shh-induced medulloblastoma. Cancer Cell *14*, 123–134.

Supèr, H., and Soriano, E. (1994). The organization of the embryonic and early postnatal murine hippocampus. II. Development of entorhinal, commissural, and septal connections studied with the lipophilic tracer Dil. J. Comp. Neurol. *344*, 101–120.

van Praag, H., Kempermann, G., and Gage, F.H. (2000). Neural consequences of environmental enrichment. Nat. Rev. Neurosci. *1*, 191–198.

Zhou, C.J., Zhao, C., and Pleasure, S.J. (2004). Wnt signaling mutants have decreased dentate granule cell production and radial glial scaffolding abnormalities. J. Neurosci. *24*, 121–126.

155